Final Report
Airborne Geophysical Survey, Fort Ord, California

January 29-February 17, 2005

September 30, 2005

Prepared for

Fort Ord BRAC Office
Presidio of Monterey, Monterey County, CA

and the

U.S. Army Engineer Research and Development Center
Vicksburg, MS

Prepared by

Battelle-Oak Ridge
and
Oak Ridge National Laboratory

Executive Summary

In early 2005, an airborne geophysical survey was conducted at Fort Ord near Monterrey, CA for the Fort Ord BRAC Office and the U. S. Army Engineer Research and Development Center (ERDC). The objective of this airborne geophysical survey was to acquire, process, and analyze geophysical data for high densities of anomalies that may be related to targets and/or ranges likely to be highly contaminated with surface and subsurface OE items and artifacts. The main survey consisted of a 1281 hectares (ha) (equivalent to 3166 acres (ac)) magnetic survey using a transect survey method on alternating lines (providing an effective coverage of 2562 ha (6332 ac)). A 72 ha (178 ac) electromagnetic survey was conducted within the main area and was flown at full coverage (high density). In addition, a supplemental 41 ha (101 ac) magnetic survey was flown at the MRS-16 area at full coverage at the request of the Fort Ord BRAC Office. A well-established and documented geophysical prove-out site containing inert ordnance items was used as calibration targets for this survey. The data acquired during this survey will assist the Fort Ord BRAC Office and their contractors in a variety of characterization, screening-level, and removal activities associated with determination of the extent of potential UXO-related contamination at the site.

The magnetic survey data analysis was based on calibration measurements acquired at three different altitudes (2m, 4m, and 5.5m) at the prove-out site within the main survey area. This calibration site contained a suite of ordnance items, emplaced by BRAC personnel, as well as pipes, serving as UXO simulants, emplaced on the surface by Battelle personnel. The analytic signal map at 2m flight height indicates that targets larger than 90mm diameter can be detected with a high degree of certainty. However, this altitude was only rarely achieved during the actual survey (1%). The median height on the main survey block was 3.5m. At 4m altitude, only the pipes, presumed clusters, and the largest of the single targets are clearly visible. Data at this altitude and lower represent 61% of the total survey block. At 5.5m altitude, the pipes and the largest of the clusters are still visible, but discrete objects cannot be reliably and consistently detected. Data at 5.5m altitude and below represent 88% of the total survey block. This supports the decision to use a 5m altitude cut-off threshold for detection of clusters of ordnance and debris within the main survey area. Eighty-three percent of the main survey block was surveyed at flight heights lower than the 5m cutoff. Maps with a 4m cut-off were produced to represent a higher level of sensitivity.

From the analytic signal map, various linear features were observed that are associated with roads, tracks, pipelines or other cultural features. The most obvious of these is the interpreted pipeline across the northern portion of the survey block. Additional linear features, corresponding to analytic signal anomalies which trace topographic ridge and trough lines, may be geologic in origin or associated with collections of debris that have settled in local depressions. Large contiguous blocks (two or more lines) of high amplitude response (>2nT/m) were selected and outlined with polygons. The boundaries of these polygons should not be taken as physical target boundaries. Other polygons, around blocks of medium amplitude response (>0.5nT/m), may be associated with clusters of debris. Numerous other moderate amplitude responses exist within the survey area, but these are likely more geologic in origin.

In contrast to the primary survey block, the survey height in the MRS-16 area was too great to discriminate individual objects (median height 6.4m). Clusters of objects may also be masked at this altitude. Infrastructure such as fences and roads are the most likely source of the observable anomalies.

The ORAGS-TEM system shows even more altitude dependence than the magnetic system. This is particularly apparent in EM Block A, where taller vegetation forced higher survey altitudes (3-5 m above ground level) in the southwest half of the area. On this side of the survey block there are virtually no anomalies. On the northeast side, where survey heights were generally at or below 2 m above ground level, electromagnetic anomalies are abundant. Sources appear to be both clusters of UXO and individual items.

This survey was successful in delineating areas of greater and lesser ordnance contamination over roughly 2562 ha of land at Fort Ord. Detection of single isolated items, however, cannot be achieved with these data due to the size of potential ordnance items, the survey height, and the transect method employed. Therefore the data are NOT suitable for declaring an area free of contamination, as some ordnance types at this location fall below the detection threshold of the system, and only a portion of other ordnance types will be detected. Further, areas of rough topography or tall vegetation forced increased flight height (>5m) in some locations (as in the MRS-16 area), rendering 16% of the data unsuitable for detection of the targets of interest. These factors are consistent with the goal of the project, which was to approximate concentrations of ordnance in those portions of Fort Ord where suitable data could be acquired.

Table of Contents

List of Acronyms

AGL	Above Ground Level
ASCII	American Standard Code for Information Interchange
ASL	Above Sea Level
BRAC	Base Realignment and Closure
CASP	California State Plane
DEM	Digital Elevation map
EM	Electromagnetic
EMI	Electromagnetic Induction
EOD	Explosives Ordnance Disposal
EPA	U.S. Environmental Protection Agency
ERDC	U.S. Army Corps of Engineers, Environmental Research & Development Center, Vicksburg MS
FFT	Fast Fourier Transform
GIS	Geographic Information System
GPS, DGPS, RT-DGPS	(Real Time- (Differential)) Global Positioning System
HAE	Height above ellipsoid
HGL	Height above ground level
IGRF	International Geomagnetic Reference Field
LiDAR	Light Detection and Ranging
MEC	Munitions and Explosives of Concern
MR	Munitions Response
NAD83	North American Datum 1983
OB/OD	Open burning/open detonation
OE	Ordnance and Explosives
ORAGS	Oak Ridge Airborne Geophysical System
ORAGS-TEM	ORAGS Time-domain Electromagnetic
ORNL	Oak Ridge National Laboratory
QA/QC	Quality Assurance/Quality Control
TEM	Transient Electromagnetic
TIF, GeoTIF	(Geographically referenced) Tagged Information File
UTM	Universal Transverse Mercator
UXO	Unexploded Ordnance

List of Figures

List of Tables

1. Introduction

This report describes the methodology and results of a low-altitude helicopter geophysical survey carried out jointly by Battelle and Oak Ridge National Laboratory (ORNL) and for the purpose of detecting and mapping both surface and buried unexploded ordnance (UXO) in a 2562 ha portion of the Impact Area at Fort Ord in Monterey, California. This survey also provided the opportunity to examine the utility of helicopter-borne magnetic and electromagnetic (EM) systems for assessing ordnance-related soil and groundwater contamination.

1.1. Background

The project involved the application of the state-of-the-art Oak Ridge Airborne Geophysical System (ORAGS) airborne magnetometer and time-domain EM systems developed and deployed by staff at Oak Ridge National Laboratory (ORNL) at a number of sites, including Sierra Army Depot in California, the Badlands Bombing Range in South Dakota, Ft. Detrick in Maryland, Nomans Land Island in Massachusetts, New Boston Air Force Station in New Hampshire, Camp Wellfleet in Massachusetts, and Shumaker Naval Ammunition Depot in Arkansas. During the course of this project, several ORNL project staff moved from ORNL to Battelle, where they continued to work on this project. At the time of the writing of this report, all project staff had successfully moved from ORNL to Battelle, thereby completing the commercialization of the technology from a government laboratory (ORNL) to a private sector firm (Battelle).

Data, survey results, and all associated information obtained during the course of the project were made available to the U.S. Army Engineer Research and Development Center (ERDC) and the Fort Ord Base Realignment and Closure (BRAC) Office for use by various project team members including Explosive Ordnance Disposal (EOD) technicians and contractors.

1.2. Project Site Description

Information in this section was taken from the Fort Ord Cleanup website maintained by MACTEC Engineering and Consulting, Inc.: http://www.fortordcleanup.com/foprimer/.

Fort Ord is near Monterey Bay in Monterey County, California, approximately 80 miles south of San Francisco. The base consists of about 28,000 acres near the cities of Seaside, Sand City, Monterey, Del Rey Oaks, and Marina. Laguna Seca Recreation Area and Toro Regional Park border Fort Ord to the south and southeast, respectively. Land use east of Fort Ord is primarily agricultural.

In 1917, the US Army bought the present day East Garrison and nearby lands on the east side of Fort Ord to use as a maneuver and training ground for field artillery and cavalry troops stationed at the Presidio of Monterey. Before the Army's use of the property, the area was agricultural, as is much of the surrounding land today. No permanent improvements were made until the late 1930s, when administrative buildings, barracks, mess halls, tent pads, and a sewage treatment plant were constructed. From 1947 to 1975, Fort Ord was a basic training center. After 1975, the 7th Infantry Division occupied Fort Ord. Light infantry troops operated without heavy tanks,

armor, or artillery. Fort Ord was selected in 1991 for decommissioning, but troop reassignment was not completed until 1994 when the post formally closed. Although Army personnel still operate parts of the base, no active Army division is stationed at Fort Ord.

The area's climate is characterized by warm, dry summers and cool, rainy winters. The Pacific Ocean is the principal influence on the climate at Fort Ord. Daily ambient air temperatures typically range from 5° to 20°C, but temperatures in the low 40s have occurred. Fog is common in the morning throughout the year. Winds are generally from the west. The average annual rainfall of 35cm occurs almost entirely between November and April. Because the predominant soil is permeable sand, runoff is limited and streamflow only occurs intermittently and within the very steep canyons in the eastern portion of Fort Ord.

Figure 1.1: A portion of the Fort Ord Impact Area

Fort Ord is located on California's central coast, a biologically diverse and unique region. The range and combination of climactic, topographic, and soil conditions at Fort Ord support many biological communities. Various plant communities identified at the Fort Ord sites include coast live oak woodland, central maritime chaparral, central coastal scrub, vegetatively stabilized dune, northern foredune grassland, landscaped, valley needlegrass grassland, seasonally wet grassland, vernal pool, upland ruderal, and wet ruderal. Central maritime chaparral is the most extensive natural community at Fort Ord, occupying approximately 5060ha in the south-central portion of the base. Oak woodlands are widespread at Fort Ord and occupy the next largest area, about 2020ha. Grasslands, primarily in the southeastern and northern portions of the base, occupy approximately 1800ha.

Elevations at Fort Ord range from approximately 275m above mean sea level near Impossible Ridge, on the east side of the base, to sea level at the beach. The predominant topography of the area reflects morphology typical of the dune sand deposits that underlie the western and northern portions of the base. In these areas, the ground surface slopes gently west and northwest, draining toward Monterey Bay. The topography in the southeastern third of the base is notably different from the rest of the base. This area has relatively well-defined, eastward-flowing drainage channels within narrow, moderately to steeply sloping canyons. Runoff is into the Salinas Valley.

Fort Ord is within the Coast Ranges Geomorphic Province. The region consists of northwest-trending mountain ranges, broad basins, and elongated valleys generally paralleling the major geologic structures. In the Coast Ranges, older, consolidated rocks are characteristically exposed in the mountains but are buried beneath younger, unconsolidated alluvial fan and fluvial sediments in the valleys and lowlands.

The geology of Fort Ord generally reflects older, consolidated rock that is exposed at the surface near the southern base boundary and becomes buried under a northward-thickening sequence of poorly consolidated deposits to the north. Fort Ord and the adjacent areas are underlain, from depth to ground surface, by one or more of the following older, consolidated units:

- Mesozoic granite and metamorphic rocks
- Miocene marine sedimentary rocks of the Monterey Formation
- Upper Miocene to lower Pliocene marine sandstone of the Santa Margarita Formation (and possibly the Pancho Rico and/or Purisima Formations). Locally, these units are overlain and obscured by geologically younger sediments, including:
- Plio-Pleistocene alluvial fan, lake, and fluvial deposits of the Paso Robles Formation
- Pleistocene eolian and fluvial sands of the Aromas Sand
- Pleistocene to Holocene valley fill deposits consisting of poorly consolidated gravel, sand, silt, and clay

A system of sand dunes lies between Highway 1 and the shoreline. The western edge of the dunes has an abrupt drop of 10 to 20m, and the dunes reach an elevation of 43m above mean sea level on the gentler, eastern slopes. The dunes provide a buffer zone that isolates the Beach Trainfire Ranges from the shoreline to the west. In some areas, spent ammunition had accumulated on the dune slopes as the result of years of range operation. Numerous former target ranges, ammunition storage facilities, and two inactive sewage treatment facilities lie east of the dunes.

Undeveloped land in the inland portions of Fort Ord included infantry training areas and open areas used for livestock grazing and recreational activities such as hunting, fishing, and camping. A large portion of this undeveloped land is occupied by the Impact Area (formerly called the Multi-Range Area). This area was used for advanced military training operations.

An area known as the Impact Area is located in the south-central portion of Fort Ord and is designated a Munitions Response (MR) site. Lands within the boundaries of the Impact Area are expected to have the highest density of Munitions and Explosives of Concern (MEC) with

specific target areas having the highest densities. Types of MEC found at Fort Ord include artillery projectiles, rockets, hand grenades, land mines, pyrotechnics, bombs, demolition materials and other items. Known MR sites are posted with warning signs and are off-limits to unauthorized people.

1.3. Airborne Magnetometer System

ORNL developed the airborne magnetometer system (shown in Figure 1.2) that was used for data acquisition at Fort Ord. This system, known as the Oak Ridge Airborne Geophysical System-Arrowhead, is now operated by Battelle. It provides a substantial increase in detection capability compared to previous airborne systems (Aerodat HM-3 and ORNL Hammerhead) because of a new boom architecture designed to position more magnetic sensors at low-noise locations, a significantly higher sampling frequency, and a unique aircraft orientation system.

Figure 1.2: ORAGS-Arrowhead system in operation at Fort Ord.

Four magnetometers at 1.7meter line spacing are located in the forward V-shaped boom (Figure 1.3), and two magnetometers are located in each of the lateral booms (8 total magnetometers). The “Arrowhead” system is mounted on a Bell 206 Long Ranger helicopter and flown as low to the earth’s surface as safety permits (average 3.5m at Fort Ord) in pre-programmed traverses over the survey areas. Survey speeds were approximately 20m/s. Flight lines were spaced 25m apart (providing nominal 50% coverage with a 12m swath of sensors spaced 1.7m apart) with data recorded at 120 Hz. Base station magnetic readings were recorded in order to monitor diurnal magnetic activity. This diurnal magnetic activity is removed from the data as part of the data processing. Airborne magnetic data are acquired during daylight hours only.

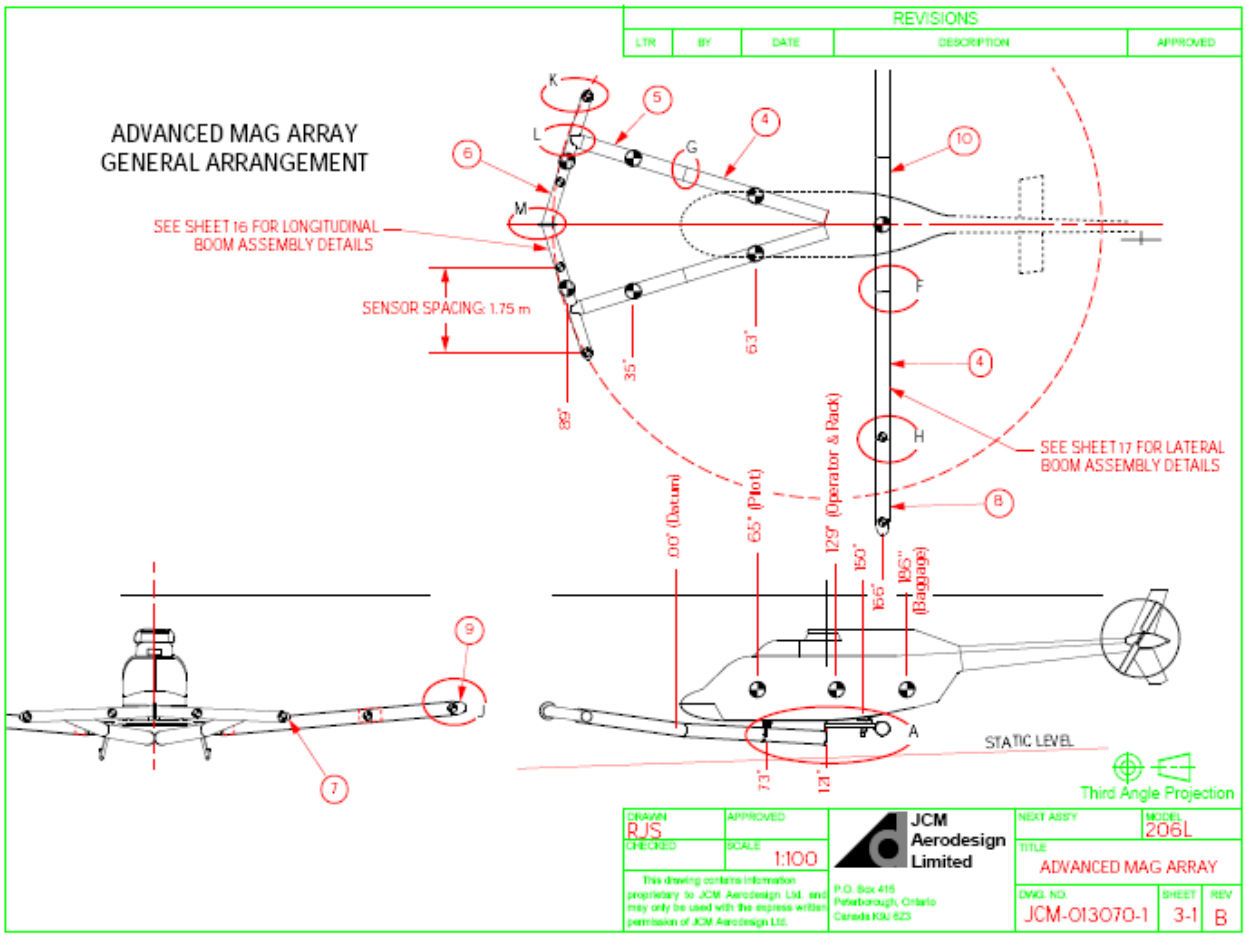

Figure 1.3: General system layout for ORAGS-Arrowhead.

The orientation system is based on four Global Positioning System (GPS) antennas. A fluxgate magnetometer is mounted in the forward assembly to compensate for the magnetic signature of the aircraft. A laser altimeter is mounted beneath the helicopter, at approximately the same altitude as the sensors to monitor sensor height above the ground. Data are recorded digitally on the ORAGS™ console (Figure 1.4) inside the helicopter in a binary format. The magnetometers are sampled at a 1200 Hz sample rate and desampled to 120Hz to allow sufficient bandwidth to eliminate helicopter rotor noise.

Figure 1.4: ORAGS-Arrowhead console as installed in the Bell B206L helicopter.

1.4. Airborne Electromagnetic System

In addition to the ORAGS-Arrowhead system, ORNL also has recently completed performance evaluation of the airborne electromagnetic system that provided supporting data over a portion of the larger magnetic survey area at Fort Ord. The Oak Ridge Airborne Geophysical System-Time-domain Electromagnetic (ORAGS-TEM) system is a boom-mounted electromagnetic induction system that mounts on rigid Kevlar and carbon fiber booms attached to the underside of a Bell 206L Long Ranger helicopter (shown in Figure 1.5). As with the Arrowhead system, the rigid boom architecture enables the helicopter to fly closer to the ground, thus increasing system resolution, while also enabling precise control of receiver positions which allows more accurate determination of UXO locations.

For the Fort Ord survey, the transmitter coil was arranged in a rectangular two-lobed geometric configuration, as shown in Figure 1.6. A current is established in the loop, then rapidly switched off, inducing a secondary magnetic field in the earth, the decay of which is measured in the receiver coils. In this configuration, a transmitter cable is supported by a 12 m x 3 m rectangular, composite frame. The turnoff time for the lobed configuration is approximately 160 μs. The receiver system will consist of two large single turn loops having dimensions of about 2.7 m x 2.7 m as shown in Figure 1.6.

Figure 1.5: ORAGS-TEM airborne electromagnetic induction system similar to that used at Fort Ord.

Figure 1.6: ORAGS-TEM system in flight. The red square line shows the large receiver coil position, and the black line represents the rectangular two-lobed transmitter coil layout.

1.5. Site-Specific Effects on Boom-Mounted Helicopter Systems

Each survey site presents a unique set of conditions that can affect the performance and results of the boom-mounted helicopter systems. Variations in vegetation height forces changes in survey altitudes, and small individual ordnance items are less detectable as survey height increases. The presence of cultural features, such as buildings, above-ground phone and power lines, and fences can also force higher survey altitudes, or totally exclude some areas from being surveyed. Weather conditions, in particular wind patterns, can cause attitudinal variations in helicopter systems, and these variations often will appear as low frequency variations in the electromagnetic or magnetic response with respect to targets of interest. Topographic changes can produce similar low frequency effects as the helicopter's altitude above ground level changes. Variations in the magnetic susceptibility of underlying soil or rock can also produce anomalies. Usually these are low amplitude, long wavelength anomalies that are easily distinguishable from UXO anomalies, but at some sites localized magnetic soils or individual magnetic boulders can produce magnetic anomalies that are virtually indistinguishable from UXO anomalies, both in amplitude and wavelength. With respect to EM systems, long wavelength anomalies may be produced by variations in soil or rock conductivity, but these anomalies typically have very low amplitudes. Geological conditions can only rarely produce EM anomalies that mimic UXO anomalies in both amplitude and wavelength. With the exception of some metallic ore deposits and localized zones of high magnetic susceptibility, geological structures are usually less conductive than metals by several orders of magnitude (Telford, 1990). Larger UXO tends to produce narrow, high amplitude anomalies that decay slowly in comparison to geological anomalies. Conductive, two-dimensional geological structures can produce high amplitudes and slow decay, but in map view anomalies will appear elongate, unlike those produced by UXO. Compact geological features that may produce anomalies of the same wavelength as UXO also typically will produce much lower anomaly amplitudes because of their low conductivities relative to steel or aluminum. An exception occurs in areas where magnetic boulders or compact pockets of highly magnetically susceptible soils occur. The transient EM responses from these magnetic geological occurrences may be largely indistinguishable from that of smaller UXO anomalies (Billings et al., 2003).

2. Mission Objectives

The objective of this airborne geophysical survey was to acquire, process, and analyze geophysical data for high densities of anomalies that may be related to targets and/or ranges likely to be highly contaminated with surface and subsurface OE items and artifacts within the area illustrated in Figure 3.1. The main survey consisted of a 1281 ha magnetic survey using the transect survey method on alternating lines (providing an effective coverage of 2562 ha). The 72 ha electromagnetic survey is located within the main Impact Area and was surveyed at full coverage (high-density). In addition, a supplemental 41 ha site, known as the MRS-16 area, was flown with the magnetic system at full coverage at the request of the Fort Ord BRAC Office. A well-established and documented geophysical prove-out site containing inert ordnance items was used as calibration for this survey. The data acquired during this survey will assist the Fort Ord BRAC Office, and their contractors in a variety of characterization, screening-level, and removal activities associated with determination of the extent of potential UXO-related contamination at the site.

It is important to recognize that the airborne data are NOT suitable for declaring an area FREE of contamination, because some ordnance types at Fort Ord fall below the detection threshold of the system, and only a percentage of other ordnance types will be detected. Furthermore, the transect method employed at Fort Ord reduces the 2562 ha of effective coverage to 50% actually surveyed in detail. Rough topography and tall vegetation increased flight height and reduced the coverage to 42% which has any potential for detecting large single pieces of ordnance. Clusters of ordnance, however, represent a legitimate target for this technology and methodology over the entire 2562 ha, allowing for interpolation between lines and across gaps caused by increased flight height. Thus the goal of the project to identify locations of high anomaly densities that may be indicative of potential former target locations and/or ranges that are likely to be highly contaminated with UXO has been successfully met.

3. Survey Parameters and Procedures

The airborne survey was completed during the 20 day period (on-site) between January 29, 2005 and February 17, 2005. Surveying included total field magnetic and time-domain electromagnetic components. All surveying was flown at as low an altitude as possible, in keeping with topography, vegetation and safety considerations. The magnetometer array was flown at 25m line spacing. With a 12m swath width, the survey of the Impact Area block provided an actual coverage of about 50%. The electromagnetic system, with two receiver coils separated laterally by 10 m center-to-center, was flown with an interleaved line spacing of 5 m to achieve essentially 100% coverage over two blocks within the area covered by the ORAGS-Arrowhead system.

Aircraft ground speed was maintained at approximately 10-15 m/s (20-35 mph). The survey aircraft was a Bell 206L helicopter. Operations were based at Monterey Peninsula Airport (MRY). The GPS base station was established at a known NASA monument at location NAD83 120° 34' 29.85951" West, 40° 22' 35.23890" North, NAVD 88 1263.725 meters. The magnetic diurnal base station was established in a magnetically quiet region at the airport.

A comprehensive Operational Emergency Response Plan was developed and issued previously to address issues related to flight operations, safety, and emergency response. This plan was incorporated into an overall Mission Plan developed to manage field survey operations.

The survey crew included Les Beard, David Bell, William Doll, Jeff Gamey, and Jacob Sheehan from ORNL and Battelle, and Jeff Fullerton, Marcus Watson and Derrick Wilkinson from National Helicopters Inc., Toronto, Canada.

3.1. Instrumentation

Both the ORAGS-Arrowhead airborne magnetic system and the ORAGS-TEM airborne electromagnetic system were deployed at Fort Ord. A real-time differential GPS was used for navigation based on OmniStar satellite differential corrections. This provided the pilot with navigation information with a dynamic accuracy of 1m. Differential corrections for data positioning were enabled by using a Novatel DL4 Differential Global Positioning System base station for post-processing. A laser altimeter was used to monitor terrain clearance in-flight. The laser altimeter provided accuracy to 5cm over the normal operational range. Ground-based magnetometer and GPS base stations were operated at the base of operations (Monterey Peninsula Airport) for positioning and magnetometer diurnal calibration purposes. A Gem Instruments GSM-19 magnetometer, recording background magnetic field at 3s intervals was used as the magnetic base station.

3.2. Survey Areas

The acquisition area for this project totaled 2603 ha, including the geophysical prove-out area. Survey boundary coordinates for the magnetic survey area were provided by BRAC personnel, as illustrated in Figure 3.1. Survey boundaries for the electromagnetic survey were provided by ERDC personnel. The main magnetic survey area of 2562 ha was flown in a "transect" mode

(every-other line, or 50% density), at the lowest achievable altitude (that is both safe and attainable) based on the targets of interest (size, depth) and terrain (safety). The 41 ha MRS-16 area was flown at full coverage at the request of the BRAC office. In addition, the survey conducted over the geophysical prove-out area (located within the main magnetic survey area) included a variety of altitudes ranging from 2m to 5.5m in order to develop quantitative measures of sensor performance for the targets of interest. The 72 ha electromagnetic survey area is located within the main area and was flown at full density.

3.3. Magnetic Data Acquisition

The ORAGS–Arrowhead data were desampled in the signal processing stage to a 120 Hz recording rate using a finite impulse response (FIR) anti-alias filter. All other raw data were interpolated to a 120 Hz rate. This results in a down-line sample density of approximately 15cm at typical survey speeds. Data were converted to an ASCII format and imported into a Geosoft format database for processing. With the exception of the differential GPS post-processing and the calculation of compensation coefficients, all data processing was conducted using the Geosoft software suite.

3.4. Electromagnetic Data Acquisition

Electromagnetic data were acquired using the ORAGS-TEM system with the transmitter in dual lobed mode, as shown in Figure 1.6, and two single turn 2.7-m x 2.7-m receiver loops affixed to the underside of the boom assembly and coincident with the two transmitter loops. The choice of large single loop receivers over smaller receivers was based on the superior performance of the large loop receivers in field trials at Badland Bombing Range for 2-3 m survey heights (Beard et al., 2004). The centers of the receiver coils were 10-m apart. Lines were flown with nominal 5-m line spacing to achieve effective 100 percent coverage. High sample rates are required to measure the EM decay signal. One decay signal is stored for each transmitted pulse. The rate at which pulses are transmitted is known as the base frequency. The transient EM decays were acquired at a rate of 10, 800 samples per second with a transmitter base frequency of 90 Hz. The decays were separated into six response decay bins. Bins 1-6 are arranges as follows: bin 1/sample 1, bin 2/samples 2-3, bin 3/samples 4-7, bin 4/samples 8-15, bin 5/samples 16-23, bin 6/samples 24-25. Sample N is the TEM response measured 92.5xN microseconds after the end of the transmitter turnoff ramp. Decays were averaged over the bin samples and recorded in the database. The 90 Hz base frequency was chosen, based on data collected at Badlands Bombing Range, to deliver a strong response from ordnance (ORNL, 2003). GPS and laser altimeter data were sampled at 30 Hz. All binned transient EM data were down-sampled to 30 Hz, and converted to ASCII format. The ASCII data were imported into a Geosoft database for processing. As with the magnetic data, the differential GPS were post-processed outside Geosoft, but otherwise, all other data were processed using Geosoft.

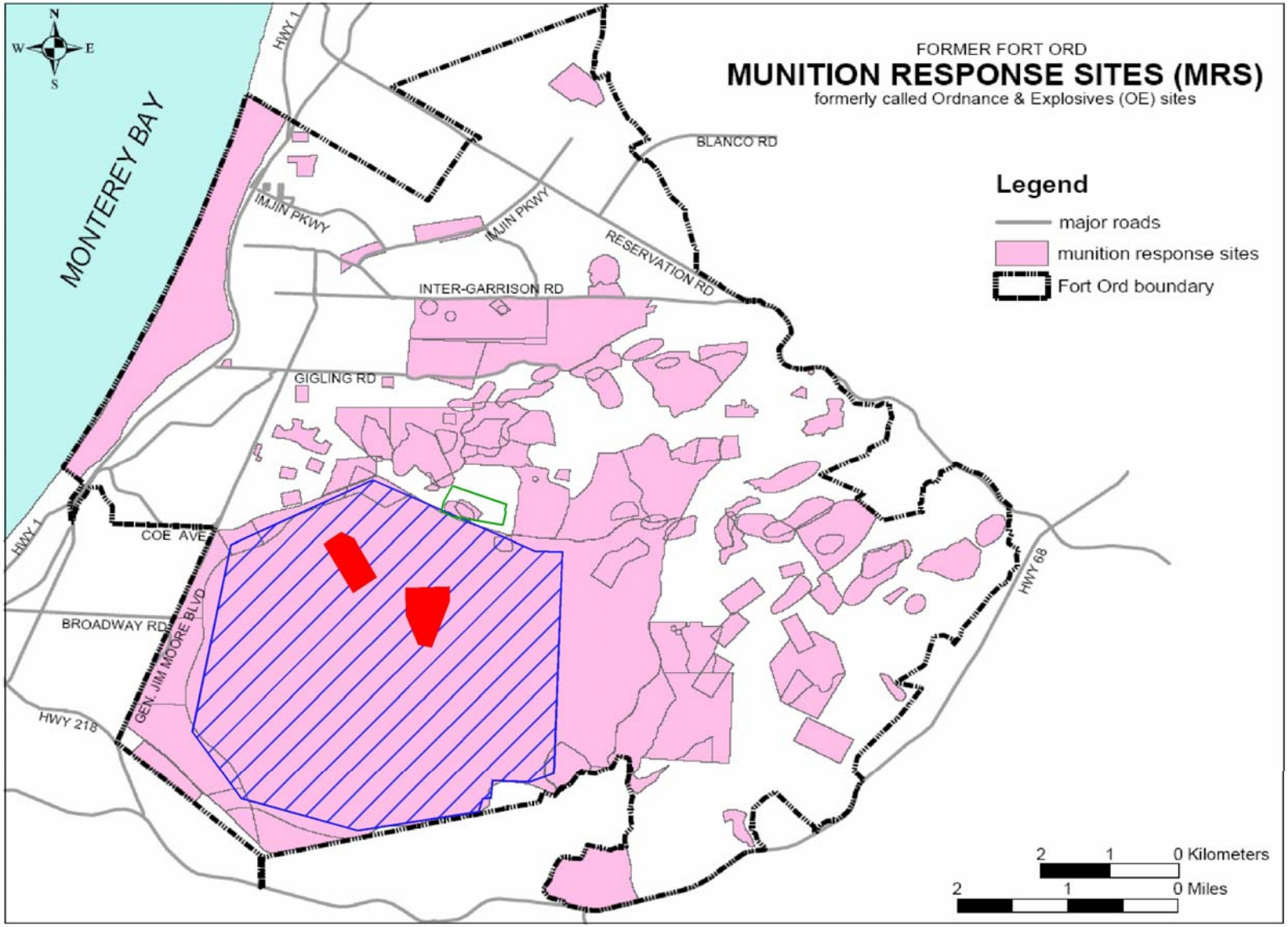

Figure 3.1: Fort Ord survey areas. Magnetometer survey is indicated by the blue hatched region, and the EM survey is indicated by the red blocks. The MRS-16 survey area is outlined in green.

3.5. Positioning

With both the magnetic and electromagnetic systems, the pilot was guided during flight by an on-board navigation system that used satellite-fed DGPS positions. This provided sufficient accuracy for data collection (approximately 1m), but was inadequate for final data positioning. To increase the accuracy of the final data positioning, a base station GPS was established at a monument on Fort Ord (GSFC-7421) at location NAD83 36° 35' 21.71529" North 121° 46' 19.67986" West NAVD 88 284.5 meters. Raw data were collected in the aircraft and on the ground for differential corrections. These were applied in post-processing to provide 2cm accuracy in the antenna positioning (based on the software's quality assurance parameters). The final latitude and longitude data were projected onto an orthogonal grid using the North American Datum 1983 (NAD 83) UTM Zone 10N, meters. After processing, data were re-projected onto NAD83 California State Plane (CASP) Zone 4 in US survey feet for a presentation consistent with the system used by the majority of surveyors at Fort Ord. All map products therefore are presented in units of US survey feet.

The location of the true base station monument was confused by a nearly-identical, undocumented monument in a more visible location. This discrepancy was detected during the first QC check of the calibration grid and was rectified. The location of the undocumented monument was determined by a Fort Ord civil survey crew and the positioning data for that day were re-processed. Subsequent flights used the true base station monument.

The location of each magnetometer sensor was calculated using the GPS antenna location and the aircraft orientation, as measured by the Ashtech Attitude Determination Unit at a 2Hz sample rate (ADU2). This system comprises four GPS antennae spread across the boom array and linked to a single processor that outputs pitch, roll and azimuth. These data are combined with the physical geometry of the array to calculate the position and relative height of each magnetometer sensor.

Vertical positioning was monitored by laser altimeter with an accuracy of 2cm. These data showed intermittent reflections from the top of the foliage canopy (Figure 3.2). They were processed to remove this effect to within 10cm. Vertical positioning was also monitored by the GPS, which provides sensor height above the ellipsoid (HAE). A digital elevation map (DEM) was compiled using HAE and laser altimeter data, and was subsequently incorporated into the altitude calculations for each sensor. The DEM was compared to existing LiDAR (Light Detection and Ranging) data to confirm the relative accuracy of the processing. The DEM was based on the GPS altitude which showed inherently less absolute accuracy than the LiDAR, but represents a more complete data set with sufficient relative accuracy for measuring slope changes beneath the helicopter swath. Thus the GPS-based DEM was sufficient for instrument altitude calculations (height above ground level), but should not be used for absolute topographic measurements (height above sea level).

These calculations reduce the absolute accuracy of the magnetometer sensor locations. The final accuracy of the sensor positions is estimated to be approximately 1m horizontally based on the calibration grid results, and 15cm vertically based on the range of the final altimeter data.

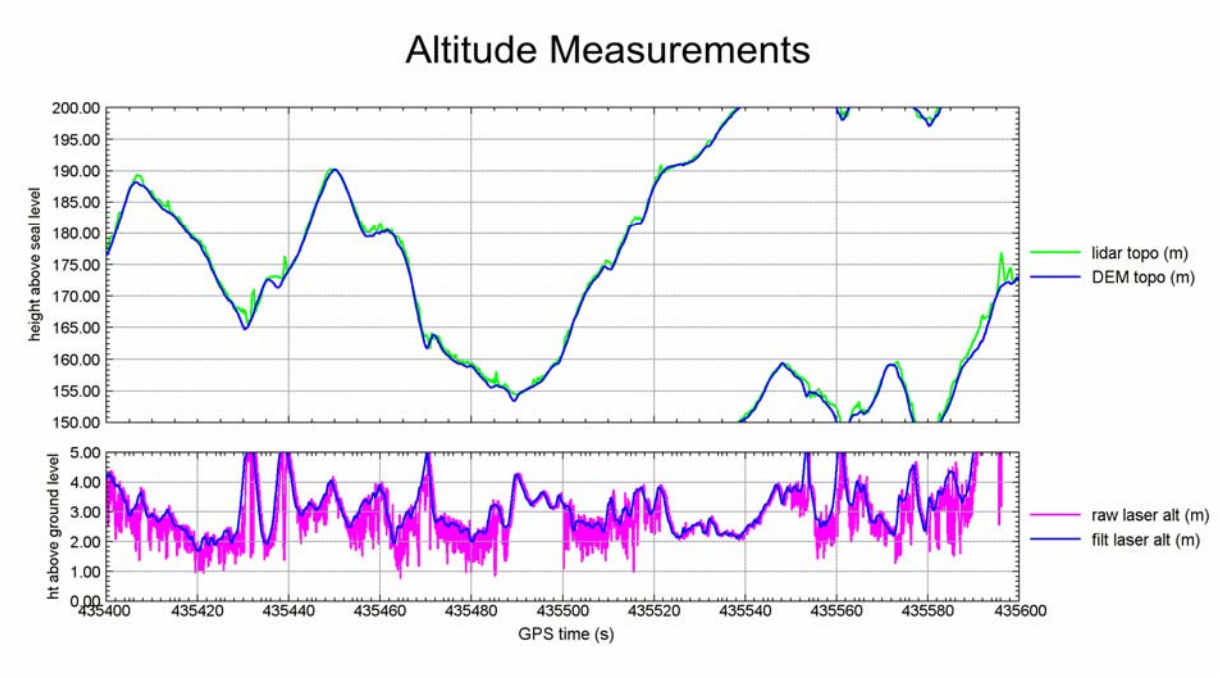

Figure 3.2: Sample altitude profiles for heights ASL and AGL. (top) LiDAR and GPS-based DEM topographic profiles. (bottom) Raw and processed laser altimeter data showing vegetation penetration.

4. Magnetic Data Processing

The magnetic data were processed in several stages. This included correction for time lags, removal of sensor dropouts, compensation for dynamic helicopter effects, removal of diurnal variation, correction for sensor heading error, array balancing, and removal of helicopter rotor noise. The calculation of the vertical magnetic gradient and the magnetic analytic signal (total gradient) were derived from the total field magnetic data. Anomaly density maps were also derived from the analytic signal peaks. For presentation purposes, the vertical gradient and analytic signal data were divided into high and low altitude maps to avoid misinterpretation of the data. The total field data show both high and low altitude data and the anomaly density data are derived only from the low altitude data.

4.1. Quality Control

The data were examined in the field to ensure sufficient data quality for final processing. Each of the processing steps listed above were evaluated and tested. The adequacy of the compensation data, heading corrections, time lags, orientation calibration, overall performance and noise levels, and data format compatibility were all confirmed during data processing. During survey operations, flight line locations were plotted to verify full coverage of the area. Missing lines or areas where data were not captured were rejected and reacquired. Data were also examined for high noise levels, data drop outs, unacceptable diurnal activity or other unacceptable conditions. Lines deemed to be unacceptable were re-flown during the acquisition stage. Occasional lines deviated from a straight flight path due to local topography. In instances where the pilot intentionally slid sideways down the hill in order to maintain uniform sensor clearance, the sensor altitude was given priority over uniform coverage unless adjacent swaths actually crossed. In total, four lines were rejected and reflown for coverage and quality issues that were not caught by the pilot and operator while in the field.

4.2. Time Lag Correction

There is a lag between the time the sensor makes a measurement and when it is time-stamped and recorded. This applies to both the magnetometer and the GPS. Accurate positioning requires a correction for this lag. Time lags between the magnetometers, fluxgate and GPS signals were measured by a proprietary ORAGS utility. This utility sends a single EM pulse that is visible in the data streams of all three instruments. This lag was corrected in all data streams before processing.

4.3. Sensor Drop-outs

Cesium vapor magnetometers have a preferred orientation to the Earth's magnetic field. As a result of the motion of the aircraft, the sensor dead zones will occasionally align with the Earth's field. In this event, the readings drop out, usually from a local average of over 53,000 nT to 0 nT. This usually occurs only during turns between lines, and rarely during on-line surveying (<1sec of data loss per day). All dropouts were removed manually during processing.

4.4. Aircraft Compensation

The presence of the helicopter in close proximity to the sensors causes considerable deviation in the readings, which requires compensation. The orientation of the aircraft with respect to the sensors and the motion of the aircraft through the earth's magnetic field are contributing factors. A calibration flight is flown to record the information necessary to remove these effects. The maneuver consists of flying a box-shaped flight path at high altitude to gain information in each of the cardinal directions. During this procedure, the pitch, roll and yaw of the aircraft are varied. This provides a complete picture of the effects of the aircraft at all headings in all orientations. The entire maneuver was conducted twice for comparison. The information was used to calculate coefficients for a 19-term polynomial for each sensor. The fluxgate data were used as the baseline reference channel for orientation. The polynomial is applied post flight to the raw data, and the results are referred to as the compensated data.

4.5. Rotor Noise

The aircraft rotor spins at a constant rate of about 400rpm. This introduces noise to the magnetic readings at a frequency of approximately 6.6 Hz. Harmonics at multiples of this base are also observable, but have much smaller amplitudes. This frequency is usually higher than the spatial frequency created by near-surface metallic objects and is removed with a frequency filter.

4.6. Heading Corrections

Cesium vapor magnetometers are susceptible to heading errors. The result is that one sensor will give different readings when rotated about a stationary point. This error is usually less than 0.2 nT. Heading corrections are applied to adjust readings for this effect.

4.7. Array Balancing

These sensors also show a lower degree of absolute accuracy than they do relative accuracy. Different sensors in identical situations will measure the same relative change, but they may differ as to whether the change was from 50,000 to 50,001 or from 50,100 to 50,101. After individual sensors are heading corrected to a uniform background reading, the background readings of each sensor are corrected or balanced to one another across the entire array.

4.8. Magnetic Diurnal Variations

The earth's magnetic field can vary by hundreds of nT over the course of a day. This means that measurements made in the air include a randomly drifting background level. A base station sensor was established to monitor and record this variation every three seconds. The time stamps on the airborne and ground units were synchronized to GPS time. The diurnal activity recorded at the base station was extremely quiet. In general, diurnal variations were less than 5 nT per hour. Processing included defaulting repeated values, linearly interpolating between the remaining points and applying a 10 second low-pass filter (equivalent to 3 points of raw data). The processed data are subtracted directly from the airborne data on a point-by-point basis.

4.9. Total Magnetic Field

After the application of the previously-cited geophysical corrections, the end result is the Total Magnetic Field Intensity, or Total Field. These data are interpolated onto a regular grid at 0.5m intervals (pixel size) using a minimum curvature technique with an extrapolated footprint of 1.5m (extension beyond the last data point). This forms the basis of the gridded data maps.

The total field data represent the Earth's magnetic field at approximately 3.5m above the ground surface (average survey height). It responds to all magnetic sources to a depth equivalent to the area of the survey (i.e. several km). Many of these sources are irrelevant to the scope of this project. It is therefore beneficial to remove effects that are caused by features at a much larger scale or greater depth than those of interest. In particular, the N-S trend in all large area surveys can extend the dynamic range so that smaller anomalies do not span more than one color in the presentation palette. The regional magnetic field can be determined in several ways, and in general consists of anomalies that have much longer wavelengths than the features of interest. The regional response was removed using a 1-D minimum curvature method, B-Spline. The map that results from the subtraction of the regional magnetic field from the total magnetic field is called the residual magnetic map.

This residual technique was applied to the data at Fort Ord, but was only presented in the original field maps for QC purposes. The variations in altitude across the area called into question the appropriate cut-off for the residual calculation. Thresholds appropriate for lower altitude data will necessarily exclude the broader anomalies observed at higher altitudes, and broader thresholds begin to introduce low frequency noise into the residual, deriving from magnetic variations in the soils or from roll of the helicopter. It was therefore determined to calculate and present the vertical gradient and analytic signal from the total field rather than the residual field.

4.10. Vertical Magnetic Gradient

The vertical magnetic gradient is calculated from the total field data using an FFT function. This process reduces geologic influence and sharpens near-surface features. Typically, geologic blocks are reduced to contact points and discrete targets are reduced to dipolar responses. Visually, this product is similar to the residual total field, but is less subjective in the selection of processing parameters.

These data were masked based on the gridded altimeter data so that null responses due to high altitude would not be confused with null responses due to lack of near-surface debris. Both high and low altitude data are presented in map form, with thumbnails of the low altitude data provided in the text of this report. A cut-off of 5m was chosen based on examination of the data, particularly in the ODDS test grid (see section 6.1) and the area of Range 43&48. The range area was known to be almost uniformly covered with debris and had a suitably wide range of survey heights from very low to very high. Assuming a uniform distribution, the loss of signal can be correlated to the altitude to determine a suitable cut-off threshold. Within this data set, some discrete anomalies were still observable at 6m altitude, but the number and amplitude of anomalies dropped significantly before this point.

The calibration grid was flown at three nominal altitudes (2m, 4m, 5.5m). Although this test grid was not representative of the high density clusters that were the objective of this survey, it was clear that even these collections of discrete objects were still detectable as a group at 5m altitude. Supplementary maps with a 4m altitude cut-off were also produced to represent the highest sensitivity sections of the data set.

4.11. Analytic Signal

The analytic signal is calculated from the gridded total field data as the square root of the sum of the squares of three orthogonal magnetic gradients. It represents the maximum rate of change of the magnetic field in three-dimensional space – a measure of how much the readings would change by moving a small amount in the direction of maximum change.

There are several advantages to using the analytic signal. It is generally easier to interpret than total field or vertical gradient data for small object detection because it has a simple positive response above a zero background. The amplitude of the response depends on the strength of the magnetic anomaly. In comparison, total field and vertical gradient maps typically display a dipolar response to small, compact sources (having both a positive and negative deviation from the background). The actual source location is at a point between the two peaks that is dependent upon the magnetic latitude of the site and the properties of the source itself. Analytic signal is essentially symmetric about the target, is always a positive value and is less dependent on magnetic latitude. More generally, the analytic signal highlights the corners of source objects, but for small targets at the latitude of this survey, these corners converge into a single peak almost directly over the target.

The dominant noise source in analytic signal is line-to-line inconsistencies in the gridded data which impact the gradients. These may be caused by heading error, sensor balancing, altitude variation or uncompensated aircraft effects. The minimum anomaly threshold was set above the analytic signal noise floor at 0.5nT/m for single peaks. This represents the 2.5:1 signal-noise ratio based on a measured noise floor of 0.2nT/m.

4.12. Altitude Calculations

As described above, the laser altimeter data detected reflections from both the ground and the upper canopy of the vegetation. These were processed to remove the effect of the foliage canopy as much as possible to an accuracy of approximately 10cm. It should be noted, however, that this does not necessarily imply full penetration was achieved at all points. These data were then combined with the GPS height above ellipsoid (HAE) data to produce a digital elevation map (DEM). The results compared well with the LiDAR data provided by Fort Ord. The GPS HAE measurement has sufficient accuracy to correct the sensor altitudes for local variations in topographic slope beneath the helicopter, but has inherently less absolute accuracy than the LiDAR. The DEM should therefore not be used for detailed topographic studies.

The laser DEM was then scanned into the database at each sensor location (rather than at the laser altimeter position). This provided sensor height above the ground which included both orientation effects (pitch, roll, azimuth) and topography effects (slope of the ground under the helicopter). The resulting altitude map shows these effects as changes across the array. For example, a progressive altitude change from side-side across a swath indicates that the helicopter flew parallel to the slope. Where the helicopter flew directly up (or down) a slope the effect shows higher (or lower) altitudes on the lateral sensors. This is the altitude parameter that was used to mask the grids into high and low certainty areas.

The median altitude for the main survey block was 3.5m. The rough topography and erratic vegetation induced more variation in survey altitude than is ideal. To avoid misleading future analysts, the data were divided into low and high altitude (high and low sensitivity) maps. A histogram of the altitude data is presented in Figure 4.1. An analysis of the analytic signal data from the calibration grid (section 6.1) indicated that small, discrete anomalies dropped below the noise threshold between 5m and 6m altitude. As a result, an altitude threshold of 5m was chosen as the cut-off. This placed 83% of the data in the high-confidence category. Supplementary maps with a 4m cut-off (66% of the data) were produced to show only the highest sensitivity data.

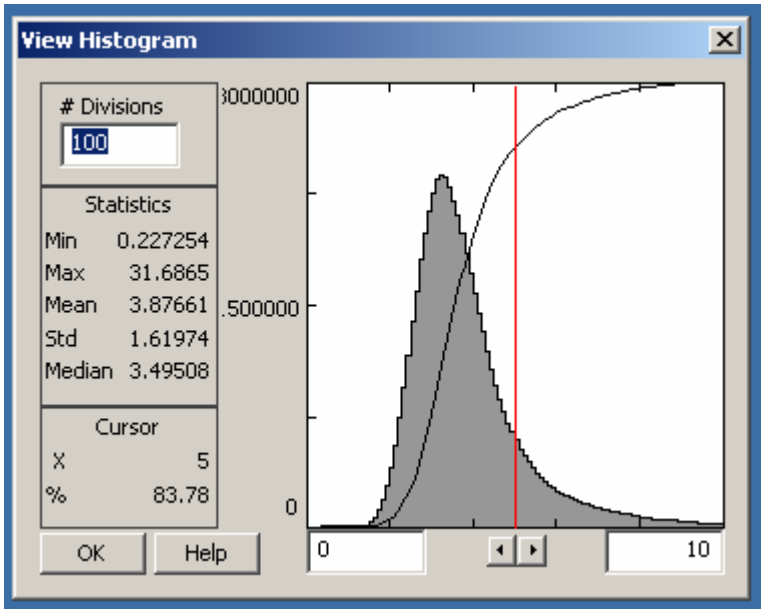

Figure 4.1: Histogram and related statistics of altimeter data for all sensors after correction for orientation and topography.

4.13. Altitude Implications for Magnetic Fields

The sensitivity of magnetic surveys is dependent upon the distance between the sensors and the object that is to be detected. Figure 4.2 shows the change in amplitude of a residual magnetic field anomaly produced by a ferrous object for varying sensor altitudes. The absolute amplitudes shown are scalable to the target in question and are roughly 50x higher than the typical ordnance at Fort Ord. In this model, all of the magnetization is induced by the earth's magnetic field. In most targets, particularly in scrap and metallic debris, additional signal amplitude will be contributed by permanent magnetization effects.

The anomalies are computed for local magnetic inclination and declination. The profiles are along a north-south line and the vertical distances between sensor and target are 2, 4, 8, and 16 m. Similar reductions in amplitude with increasing sensor height also occur in the analytic signal response. More complicated anomaly shapes, often cumulative in amplitude, are caused by target shape effects or overlapping anomalies from multiple natural or man-made sources. Such is the case with closely-spaced sources such as those found in the clusters and range targets which are the objective of the Fort Ord survey.

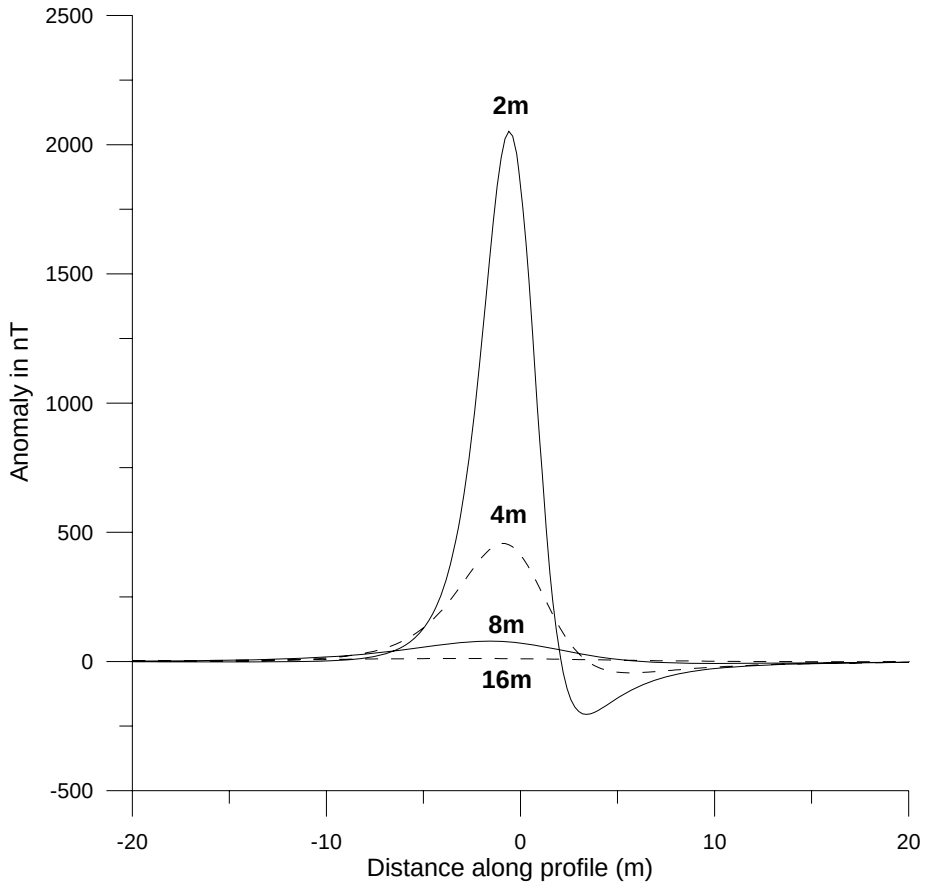

Figure 4.2: Falloff in magnetic anomaly amplitude with increased sensor height above a ferrous target.

The effect of altitude on magnetic response amplitude is generally identical to the effect of burial depth. It is the separation between the sensor and the source that is the defining factor, regardless of whether that space is filled with air or (non-magnetic) soil. Figure 4.3 illustrates maximum detection depths for a variety of ordnance types under normal flight conditions. If the flight height must be adjusted upwards from the nominal 1.5m altitude shown, then the maximum detection depth will show a corresponding reduction.

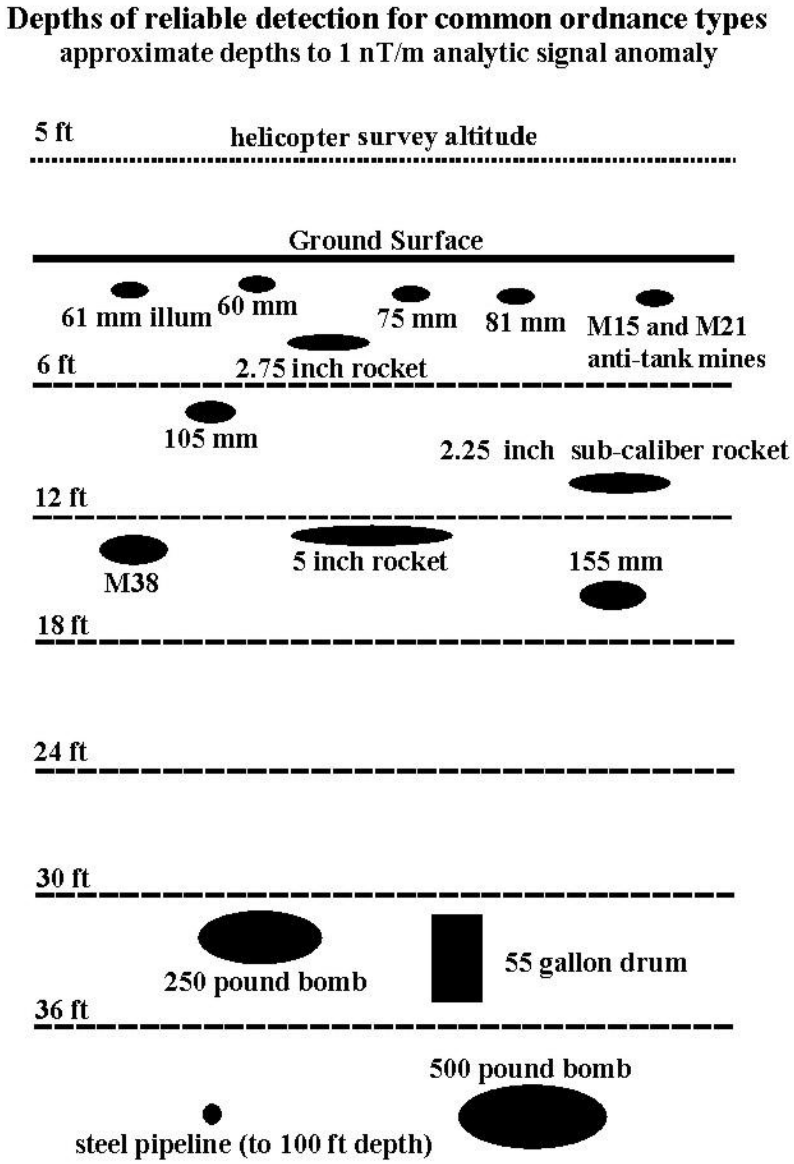

Figure 4.3: Maximum detection depths for typical ordnance types at a nominal 1.5m survey altitude.

4.14. Anomaly Density

Airborne magnetic anomalies were picked automatically from the gridded analytic signal data using a minimum threshold of 0.5nT/m. Peak selection was limited to grid points which exceeded all of their neighbors. This reduced the number of peaks selected over long, linear features such as pipelines and fences. This selection was further reduced by masking out all those where the sensor altitude was over 5m. Because it was assumed that the presence of metallic frag and other debris was indicative of UXO potential, no other discrimination techniques were applied for this survey objective.

Anomaly density was calculated by counting the number of airborne anomalies in each 25m x 25m data window and dividing by the percentage of the window covered by magnetic data below 5m altitude. On average, each survey swath is 12m wide with 25m line spacing. For every 25m window, the average coverage should be about 50%. This is increased slightly by the small extrapolation at the edges of each swath, but is reduced where the survey altitude is above 5m. If the coverage decreased below 10% no density was calculated. The number of anomalies per window was scaled to units of airborne anomalies per hectare (x16).

The density of airborne anomalies was compared to corresponding ground anomaly densities acquired by Parsons Engineering. This was done by simply dividing the airborne- and ground-based anomaly density grids. The area of comparison was quite small and the ratio of ground to airborne densities was irregular and inconclusive, ranging from 2:1 to 9:1. An average of 5:1 would represent a reasonable scaling factor between the two survey modes, but is only accurate to a factor of two. It should be noted that the ground survey will detect much smaller targets regardless of the anomaly density, so that any comparison between the two can never be more than qualitative.

It must be recognized that if the ODDS test grid is indicative of the ordnance types and densities over the rest of the Fort Ord site, the airborne magnetometer system is not sufficiently sensitive to detect all discrete ordnance items that may be present. This in fact was not the objective of the survey as demonstrated by the 50% coverage flight plan. For altitudes at and below the 5m threshold, however, it is sufficiently sensitive to detect the clusters or ordnance and debris that are the targets of this survey. This too was demonstrated at the ODDS test grid because even with the low density of targets there, they combined to for recognizable clusters. Areas with low density counts (below that in the test grid) however are not necessarily clear of ordnance. The density measurements presented here are only approximations based on magnetic anomalies. There may be a considerable difference between the number of magnetic anomalies and a count of actual UXO items.

5. Electromagnetic Data Processing

The QA/QC and time lag stages of electromagnetic data processing are similar to those for the magnetic data. However, sensor dropouts are not an issue with active source EM data, nor are compensation, heading or diurnal corrections necessary. Single loop receivers on the port and starboard side of the helicopter were of identical dimension and mounting, and so the sensors were in this sense balanced.

5.1. Quality Control

The data were examined in the field to ensure sufficient data quality for final processing. Each of the processing steps listed above were evaluated and tested. The adequacy of time lags, noise levels, and data format compatibility were all confirmed during data processing. During survey operations, flight line locations were plotted to verify full coverage of the area. Missing lines or areas where data were not captured were rejected and reacquired. Data were also examined for high noise levels, or other unacceptable conditions. Lines deemed to be unacceptable were re-flown during the acquisition stage.

5.2. Rotor and Blade Noise

The aircraft rotor spins at a constant rate of approximately 400 rpm and the blades have twice this frequency. This introduces noise to the electromagnetic readings at frequencies of approximately 6.6 and 13.2 Hz. Harmonics at multiples of this base are also observable, but are much smaller. These frequencies are usually higher than the spatial frequency created by near surface metallic objects and is removed with a frequency filter.

5.3. EM Response Leveling

EM leveling involves application of methodologies to correct for drift, or offsets between adjacent flight lines in order to generate a corrected map product that accurately represents resistivity (ohm-m or mS/m) or response to buried metals (mV). The electromagnetic (millivolt) response of the receiver coils can be affected by a number of factors such that the base level of the measurement is non-zero even in an entirely non-conductive environment. To correct for this shift and drift, we flew high altitude excursions 50-100 m AGL after every few survey lines. From the high altitude background excursions, we were able to construct background curves for each flight which we removed from the binned EM responses. This method is required for conductivity estimation. However, the maps produced using this method retained small offsets between lines, causing them to have a striped or corrugated appearance, so we abandoned this method and used an alternative leveling approach in which we estimated the background EM field using multiple B-spline iterations on a given flight, then subtracted the background field response. This produced better quality maps from a visual perspective for anomaly detection than did the use of high altitude excursions.

6. Ordnance and Resistivity Calibration Sites

Two calibration sites were used to support the airborne survey. The primary site was used to assess sensitivity of the magnetic system to ordnance. In addition to this, a second site was established for ground-truthing the electromagnetic system for resistivity calculations. Both sites are described in this section.

6.1. Magnetic Data: Ordnance Calibration Site

The ordnance calibration grid data are analyzed in two sections. The first is the daily QC flights over a line of three pipes simulating 2.75" rockets established by Battelle to verify positioning and system performance. This line was flown in two directions (N-bound, S-bound) each day. Results are presented in Appendix A.

This procedure successfully identified a problem with the base station GPS location coordinates which was immediately resolved as described in Section 3.5. In the January 29 (1-29) plots it will be noted that only two targets are visible. This is because the set of double pipes was oriented in such a way that the permanent magnetization of one almost completely cancelled that of the other. Analysis of the data shows that positioning accuracy and repeatability is within 1m.

The second part of the ordnance calibration grid was the ODDS test grid. Magnetic and electromagnetic data were acquired over the geophysical prove-out area to develop and determine "signatures" of ordnance and ordnance-related items, clusters, and groupings that form the objectives of the airborne survey. In addition, these data were used during the interpretation of the airborne data to aid in quality control and classification of anomalies of interest for further investigation.

The location and contents of the geophysical prove-out area were provided to ORNL and Battelle staff by Parsons Engineering and the Corps of Engineers. This site is broken into four blocks. Target information was provided for only two of these blocks. The content of the other two blocks remained unknown to our team, but it was understood that the density of targets was considerably higher in these blocks. To our knowledge, a "cluster" of UXO has never been adequately defined. For this survey, we define this to be a collection of ordnance or debris with sufficient spatial density such that their combined magnetic moments meet or exceed the moments of individual targets in the ODDS test grid. Because these emplaced items were meant to be detectable as discrete items with a ground-based system, and because the density of debris on known ranges greatly exceeds this level, this should be viewed as a conservative definition.

This site was flown at three different heights with the magnetometer system in order to estimate the detection capabilities of the system over the typical range of flight altitudes. Altitude and analytic signal maps for the magnetic data are shown in Figures 6.1 through 6.6. The median height achieved for these three passes was 2.0m, 3.9m, and 5.5m. We note that the sensor altitude on each swath is higher on the east side of each swath due to the local topography. Targets larger than 90mm in diameter are plotted as circles on each map. Targets smaller than 90mm that registered as a distinct peak in the 2m analytic signal map are plotted as plus signs. The 2.75" pipes are shown as crossed circles.

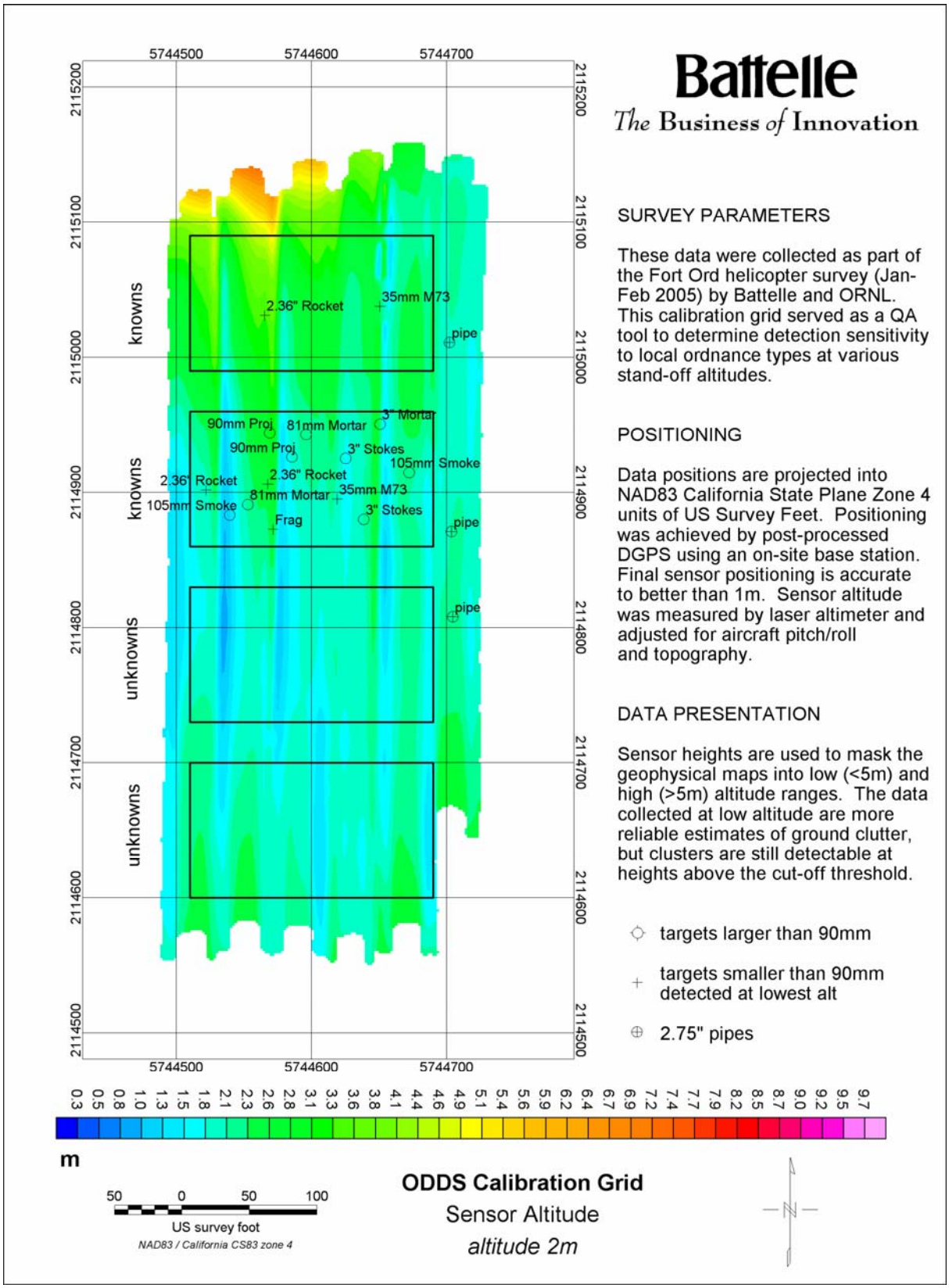

Figure 6.1: Altitude for nominal 2m survey at the ordnance calibration site.

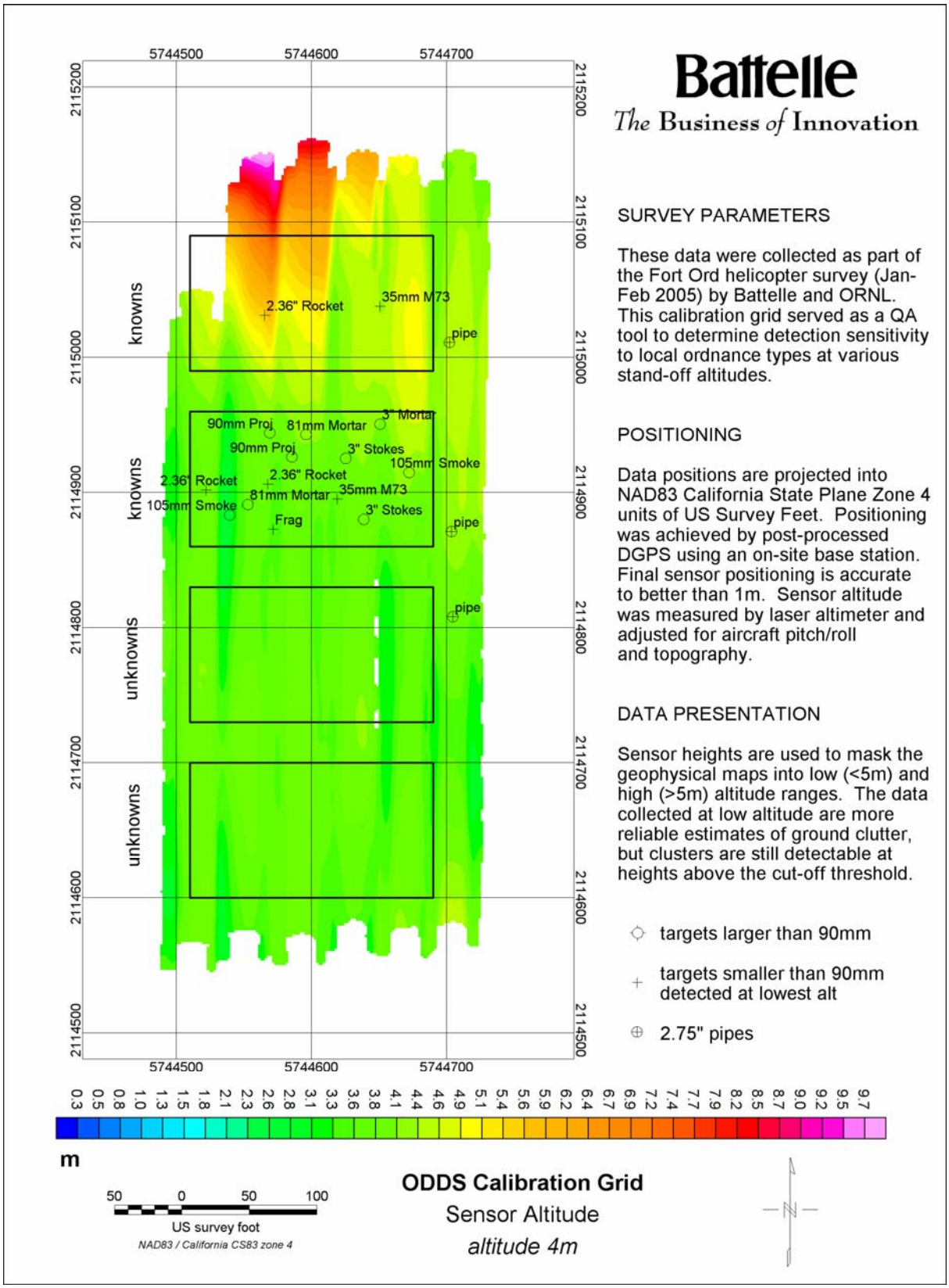

Figure 6.2: Altitude for nominal 4m survey at the ordnance calibration site.

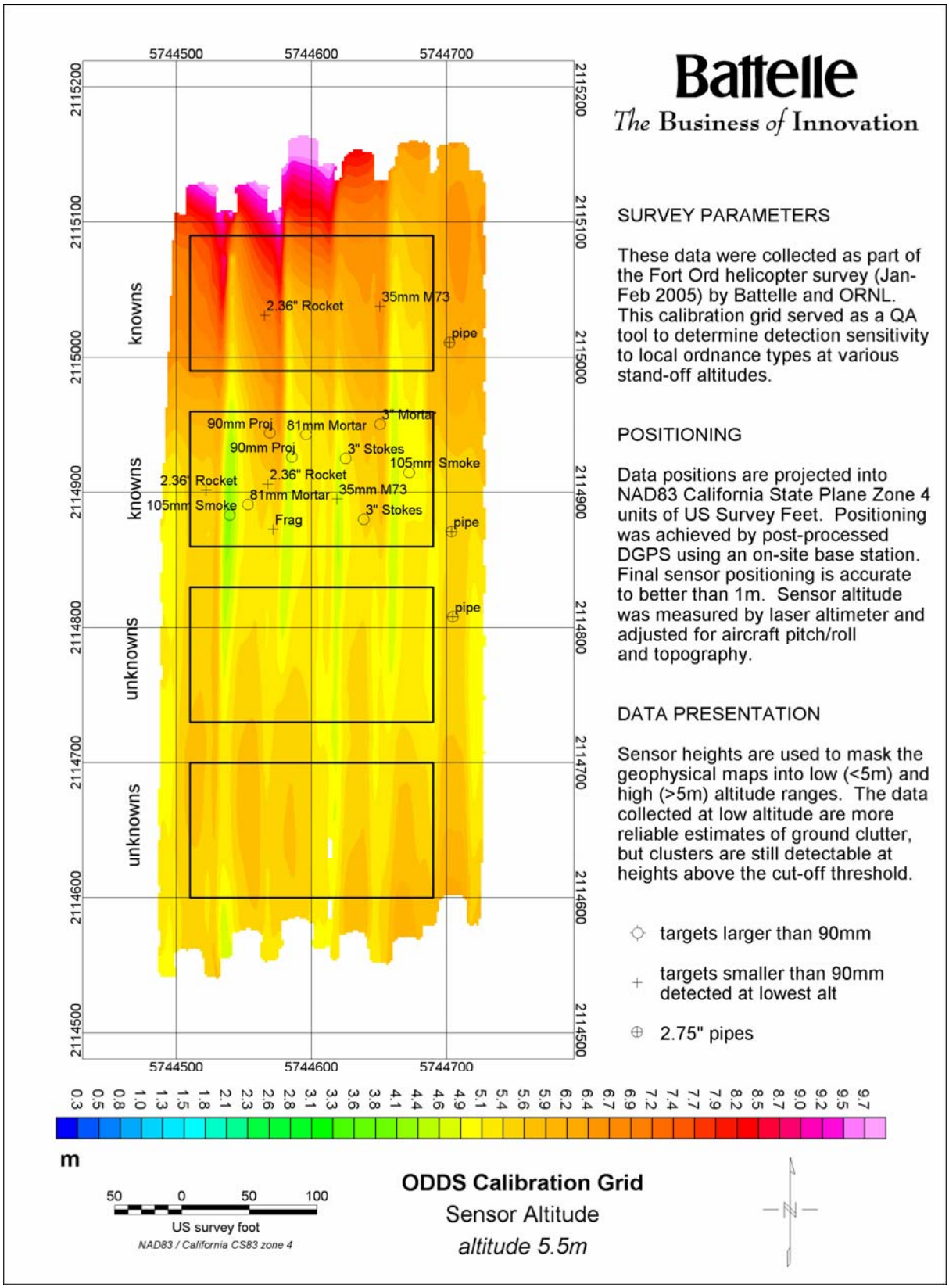

Figure 6.3: Altitude for nominal 5.5m survey at the ordnance calibration site.

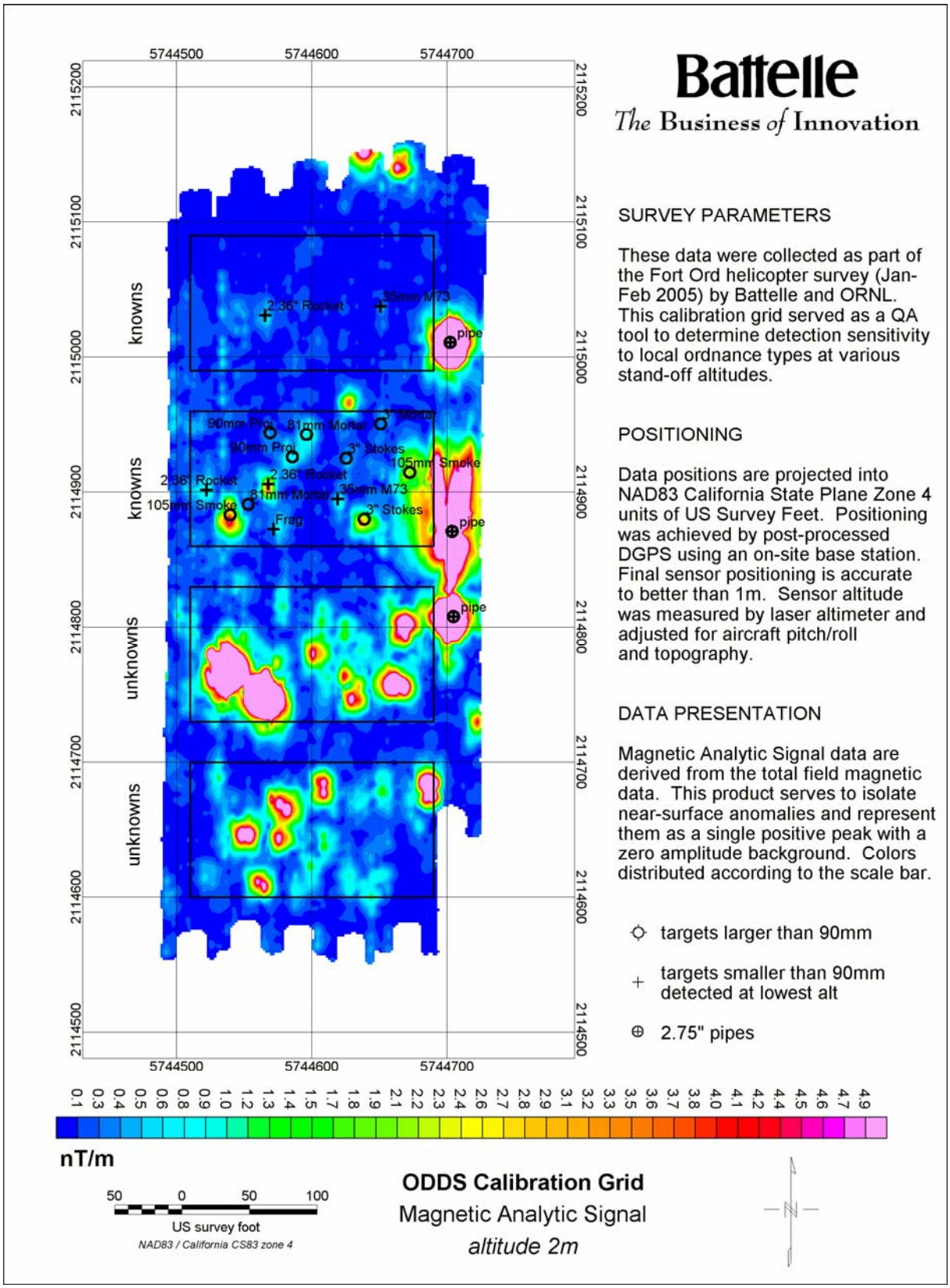

Figure 6.4: Analytic signal for nominal 2m survey at the ordnance calibration site.

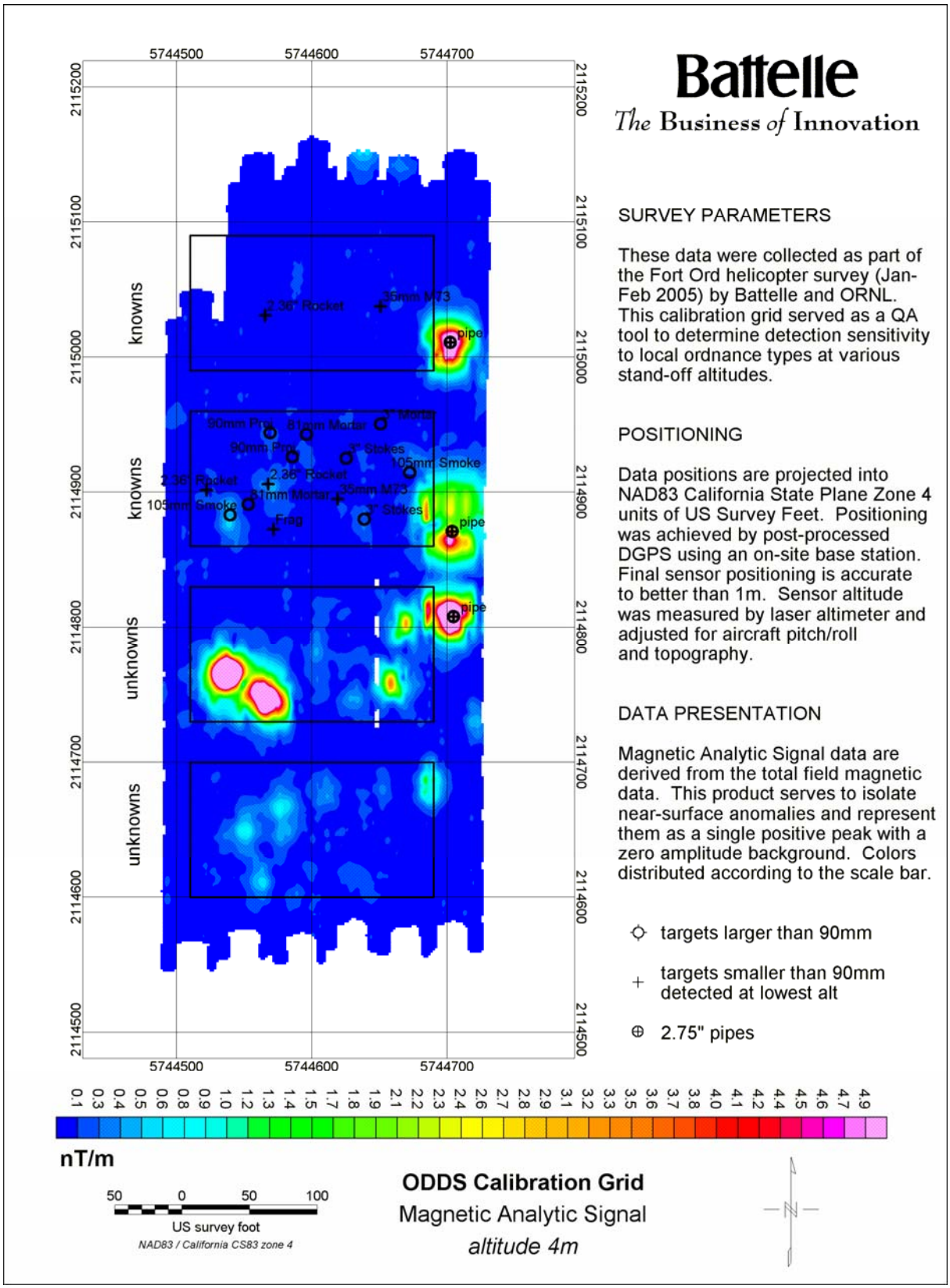

Figure 6.5: Analytic signal for nominal 4m survey at the ordnance calibration site.

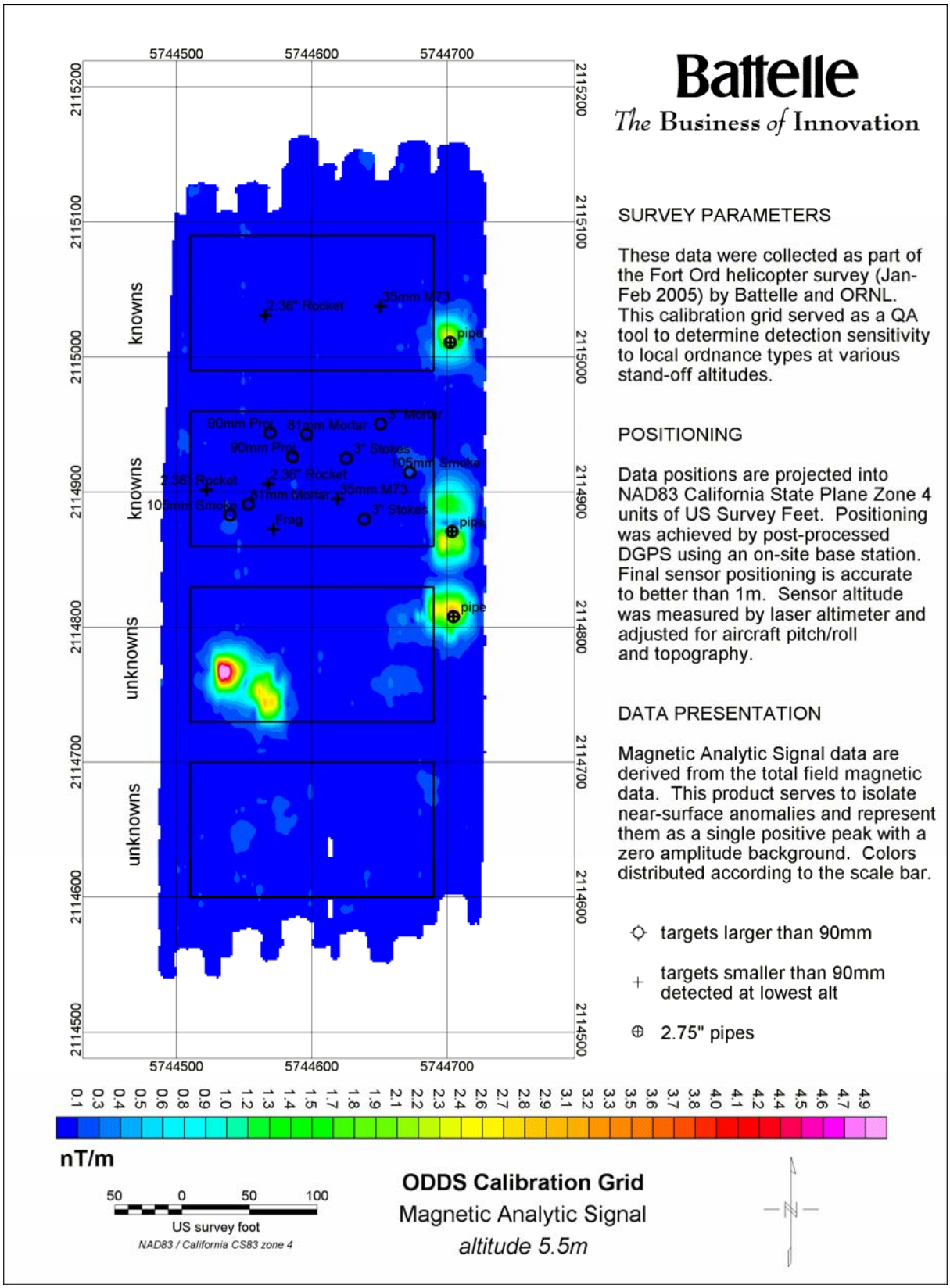

Figure 6.6: Analytic signal for nominal 5.5m survey at the ordnance calibration site.

The analytic signal map at the 2m flight height indicates that targets larger than 90mm diameter can be detected with a high degree of certainty where very low altitudes can be achieved. Several targets smaller than this were also detected, but with low signal-to-noise. Numerous additional targets, and possibly clusters of targets, were detected in the two "Unknown Blocks." This altitude was only rarely achieved during the actual survey (1%).

At the 4m altitude most of the discrete targets have dropped below the detection threshold. Only the pipes and the largest of the single targets are clearly visible. The presumed clusters in the "Unknown Blocks" are still clearly above the detection threshold. Data at this altitude and lower represent 61% of the total survey block.

The 5.5m altitude data are above the cut-off threshold used for the main survey block, but the pipes and the largest of the clusters are still visible. Discrete objects, however, cannot be detected unless they are as large as the pipes. Data at this altitude and below represent 88% of the total survey block. This evidence supports the decision to use a 5m altitude cut-off threshold for detection of clusters of ordnance and debris. The MRS-16 site, however, was largely flown at altitudes greater than this. It is unlikely that clusters of this size would be detectable at the 6.4m median altitude flown over that block.

Further support for the cut-off thresholds was derived from actual survey data over Ranges 43&48. Figure 6.7 shows the sensor altitudes with anomaly peaks shown as black dots. (Note that the color scale in this map has been altered from the main map thumbnailed in Fig 7.2 to enhance the altitude range of interest.) Target debris was assumed to be relatively uniformly distributed across the area. The irregular black polygon indicates an area where the anomalies show very little correlation with altitude even though much of the survey was flown below 4m. This would imply that the debris is not as uniformly distributed as originally thought. The general distribution of anomalies, however, clearly indicates that higher altitudes detected far fewer anomalies.

The black ovals plotted on the map indicate areas where discrete anomalies were detected at altitudes higher than 6m. This is an unusual situation and is probably the result of very large targets. The remaining ovals highlight areas between 4-5m altitude. The red ovals show areas where anomalies were detected, while the blue ovals are areas where no anomalies were detected but were expected. These gaps in the detection at 5m altitude are too small and too few to alter the overall interpretation of the data, but presentations of the data with a 4m cut-off are also provided to display the data with a higher level of sensitivity and overall confidence.

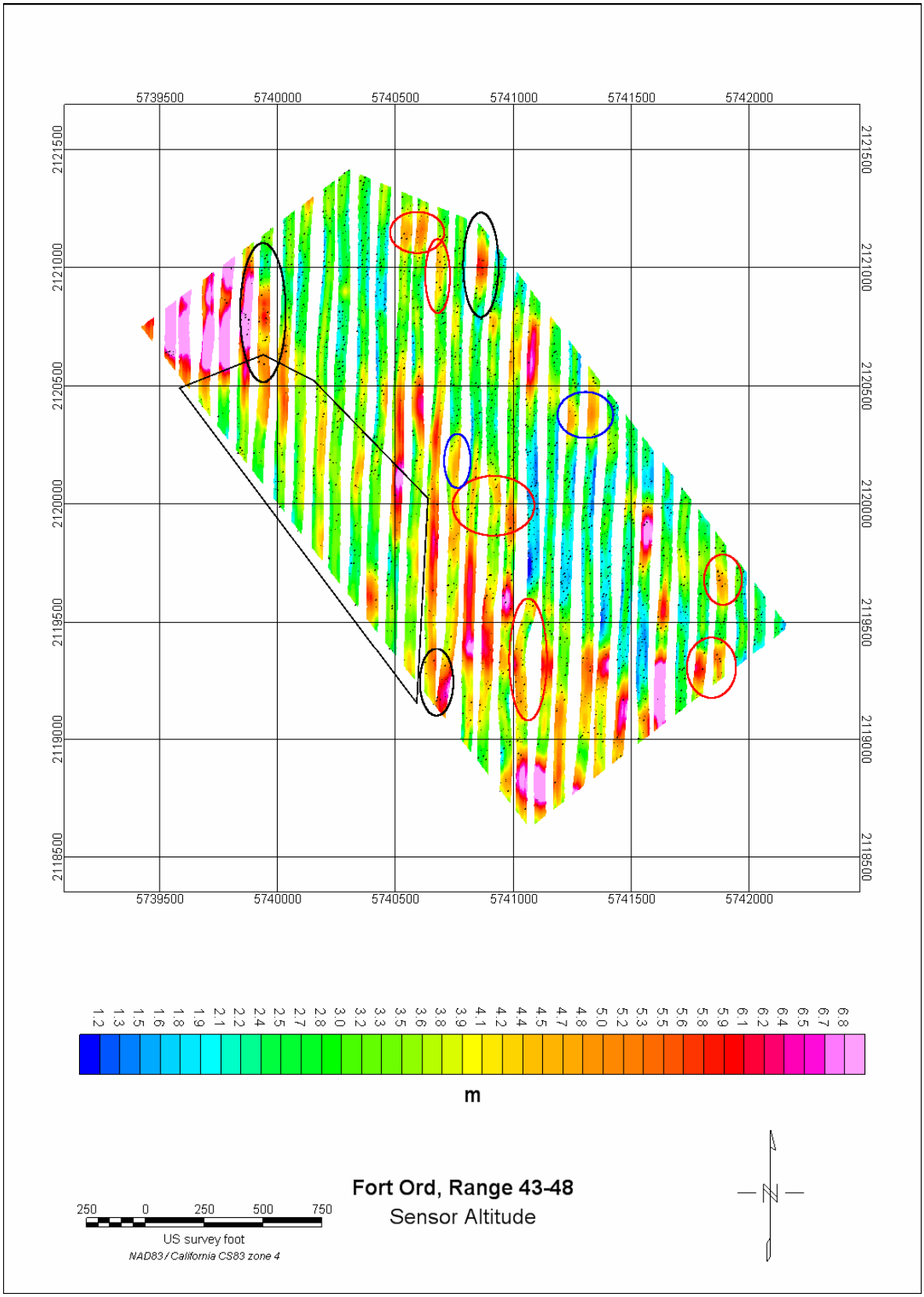

Figure 6.7: Sensor altitude plot over Ranges 43&48 with analytic signal anomaly peaks.

6.2. EM Data: Resistivity Calibration Site and Ordnance Calibration Site

The electromagnetic system used a calibration test site outside the impact zone as a resistivity calibration grid. A sub-area of the resistivity calibration grid was surveyed with ground magnetometry and with an EM-31 ground conductivity meter. The ground surveys indicated the area was relatively clear of metallic debris, and the EM-31 showed only modest variations in resistivity between 70 ohm-m and 130 ohm-m. As shown in Figure 6.8, the leveled, gridded helicopter EM response was also smooth and of low variation over the area, as confirmed by the ground assessment. However, we were unable to use the resistivity calibration grid data to estimate ground resistivity. The at-altitude EM response of the system is as large as or larger than the response at 2-m altitude over ground that, from inspection, is presumably free of metallic debris. The ground at this location is essentially unresponsive to the TEM system. This also proved to be the case inside the impact zone.

The focus of the EM portion of the Fort Ord survey was twofold: 1) to detect UXO and 2) to attempt to use of the EM system to obtain estimates of soil resistivity that might be associated with contaminants. The latter goal was untested, and presented a challenge, as the system was designed for UXO detection. We flew the ordnance calibration site on only one occasion because of the limited time allotted by the client for deploying this system over two specified areas. Shown in Figure 6.9 is the bin 2 EM response over the site. The response of the system was low throughout the site, and the anomalies shown in the figure do not correlate well with magnetic anomalies over the same area. Although small anomalies from the marker pipes used to QC the magnetic survey appear in the data, most of the anomalies appear to be related to an unusual variable frequency oscillation, the source of which we have not been able to ascertain. This noise is further discussed in section 8.2.

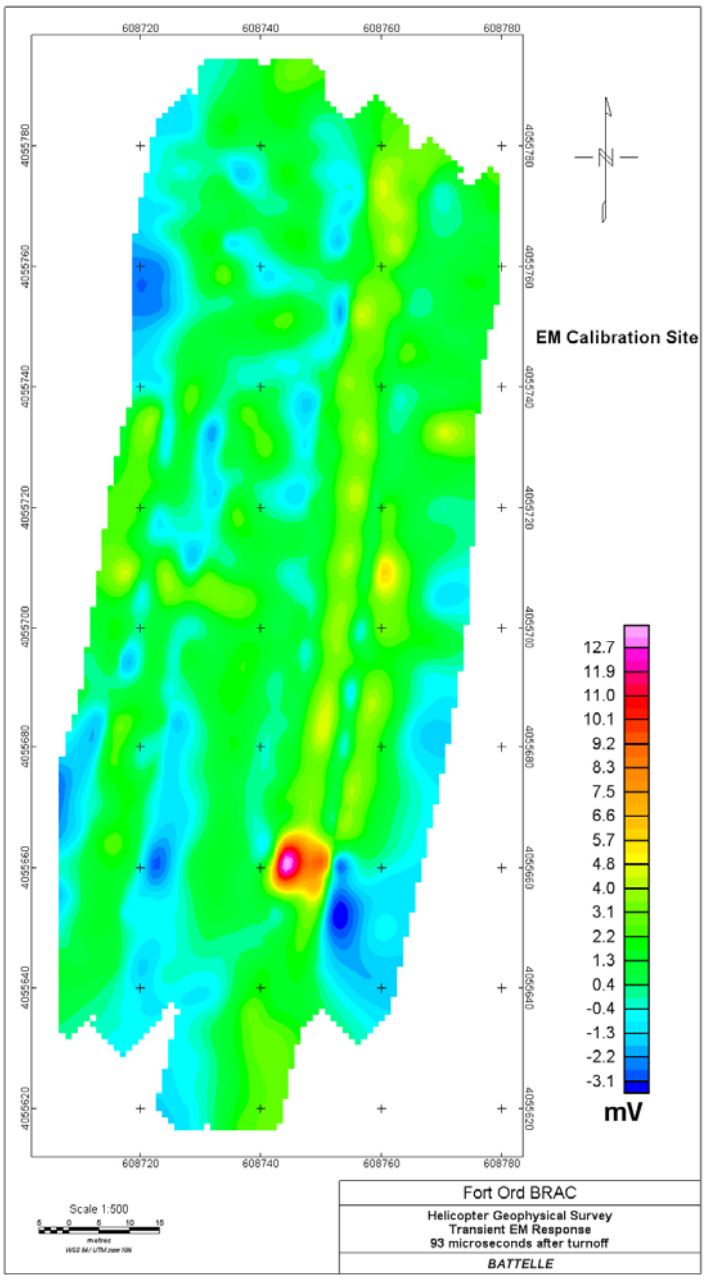

Figure 6.8: EM response (mV) for time bin 1 at the resistivity calibration site.

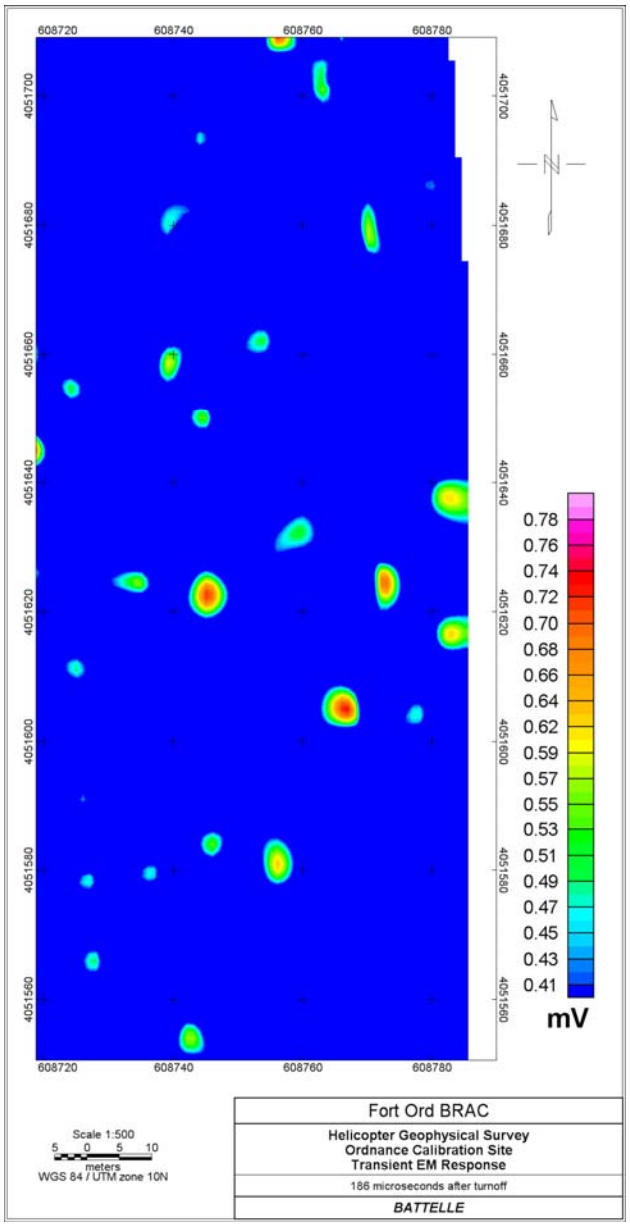

Figure 6.8: EM response (mV) for time bin 2 at the ordnance calibration site.

7. Magnetic Products and Interpretation

7.1. Introduction

The maps referenced in this section are provided in several formats. They include full size plates provided as an attachment to this report, thumbnail figures in the text of the report, and a variety of digital formats as detailed in Section 7.8. The magnetic interpretation is divided into the main survey area, and the MRS-16 site flown at the request of the BRAC office. Due to the relatively high flight height over the MRS-16 site, most of the interpretation focuses on the main survey area.

7.2. Total magnetic field

The dominant feature of the total field map (Figure 7.1[1]) is the regional N-S trend. This can generally be ignored as irrelevant to the survey objectives, but it makes interpretation difficult. In most cases, the regional field dominates so that discrete anomalies of interest are compressed into a narrow band of the color spectrum, and become difficult to discern. In order to produce a residual magnetic map to show localized geology and ordnance, large scale features must be removed. Residual calculations using a plane and the International Geomagnetic Reference Field (IGRF) only removed a portion of the regional effect and were discarded. The remaining deep-seated geology still dominated. Residual calculations using standard B-spline techniques (such as those used on the field QC maps) produced a visually appealing map, but distorted many of the near-surface anomalies. This was especially true of those on the flanks of deeper geologic features. In comparison, some mid-depth features exceeded the residual cut-off threshold and produced false anomalies. These could be discounted by comparing the residual and total field, but would be very time consuming on a survey-wide basis. The variation in survey altitude (Figure 7.2) also made it difficult to set a single residual cut-off threshold, because changes in altitude shift the spatial spectrum of the anomalies. It was decided, therefore, to concentrate interpretation on the vertical gradient and analytic signal maps and discard the residual maps created for QC in the field.

[1] The figures printed in this section are thumbnails only. The resolution here is insufficient for detailed interpretation. Please refer to the full suite of larger scale maps included in the attachments.

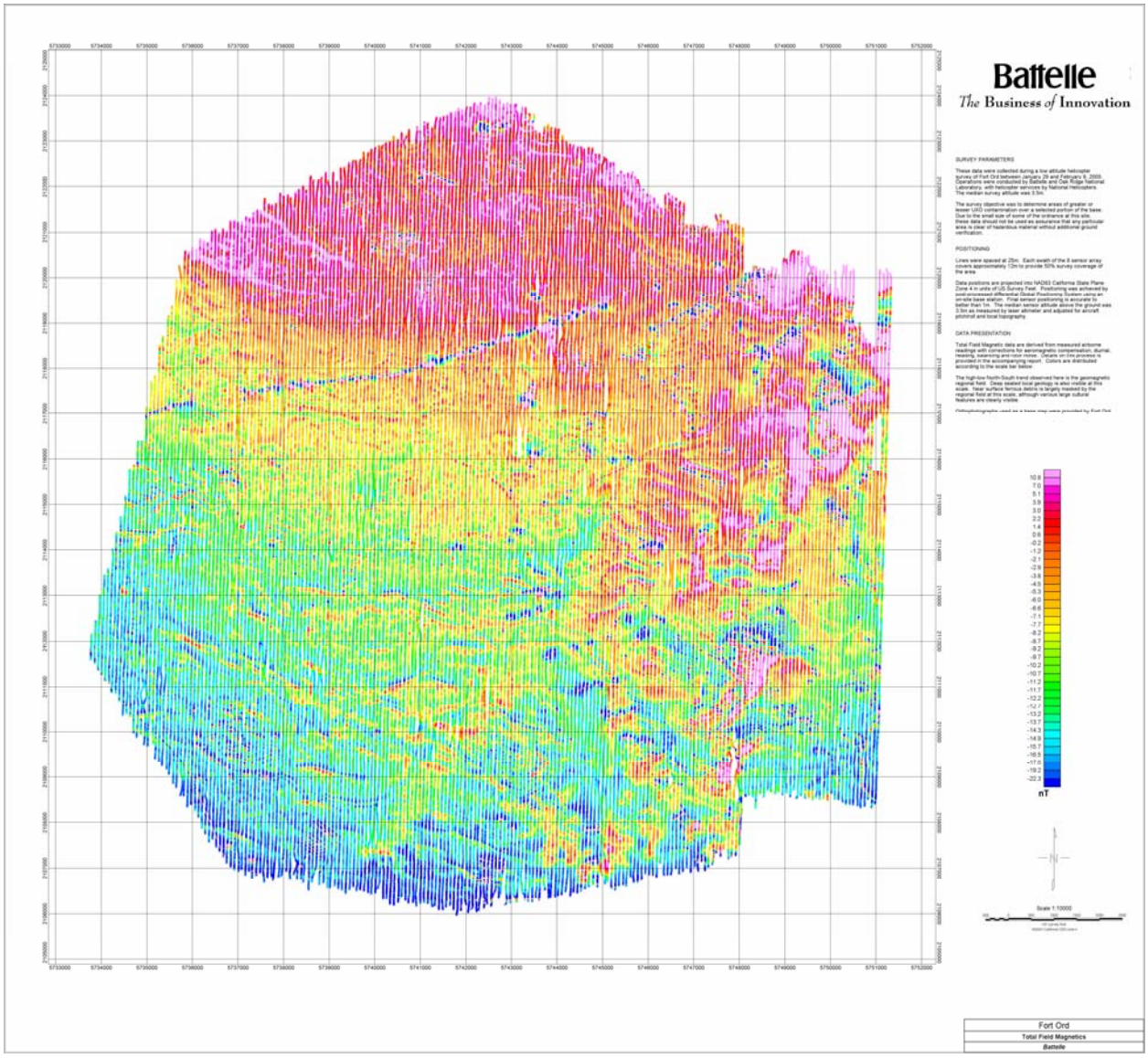

Figure 7.1: Thumbnail of total magnetic field map of the survey area at Fort Ord.

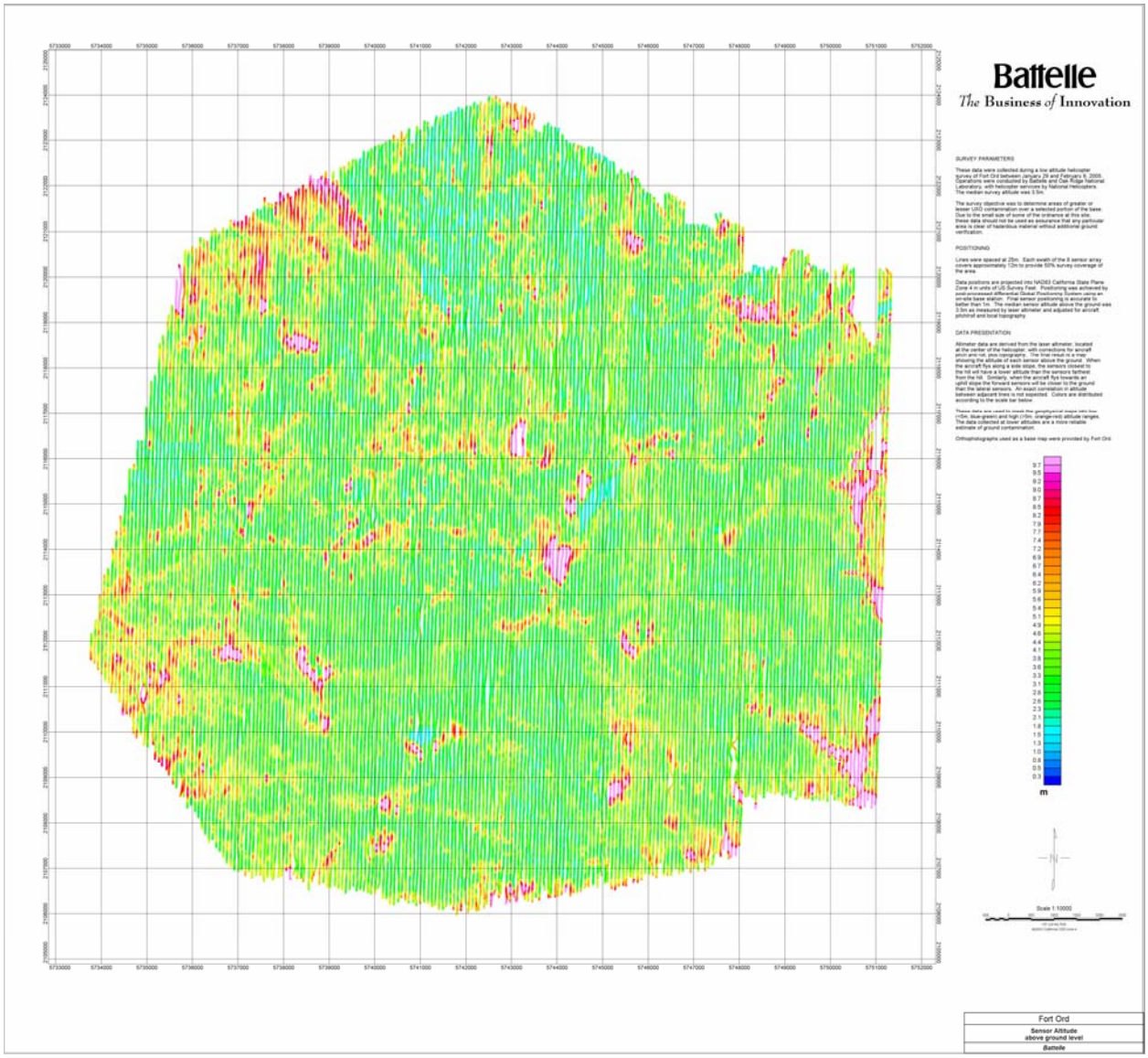

Figure 7.2: Thumbnail of sensor altitude above ground level map of the survey at Fort Ord.

7.3. Vertical gradient

The vertical gradient map (Figure 7.3 and 7.4) was calculated from the gridded total field data using a FFT vertical derivative function. This is an intermediate product between the total field and the analytic signal which is visually similar to the residual total field. Near-surface anomalies appear as dipolar responses with a small spatial extent. The amplitude of the response is dependent upon the sensor height, magnetic susceptibility, size, and mass distribution of the source. The sensor height is particularly important because it is the only one that is independent of the target. These data must be analyzed with due consideration given to the actual sensor altitude achieved at each anomaly. To restrict the presented data to an acceptable range of sensor heights, results were masked for those portions of the survey area where the flight height was greater than 5m (Figure 7.3). The masked areas comprise approximately 17% of the total map area, and represent places where vegetation or topography prevented successful acquisition of data suitable for detection of individual UXO items or clusters at this site. Supplemental maps with a 4m altitude cut-off (Figure 7.4) allow the user to see the effect of altitude with respect to reduced area coverage and increased target sensitivity. In general the 5m data were used for interpretation, with a greater level of confidence implied for the 4m data.

The dominant feature of the vertical gradient map is the linear pipeline running ENE from the west side of the survey block. Areas of high contamination are highlighted as red/blue pockets against the yellow "zero-mean" response. Areas of moderate debris are less obvious orange/green responses. Some low amplitude linear features undulate across the area in a general E-W direction. These are interpreted as geologic or topographic sources.

It should be noted that there is a strong correlation between geology, topography, cultural and historic land use, and survey altitude. For example, geology often controls topography; cultural features such as roads, trails, power lines and impact ranges are often dictated by topography; and survey height is strongly controlled by the necessity to avoid both topography and cultural obstacles. This makes detailed interpretation regarding the source of each geophysical anomaly difficult. This level of analysis is not, however, an objective of this project. If such an analysis is conducted, the altimeter data must be considered as a primary factor.

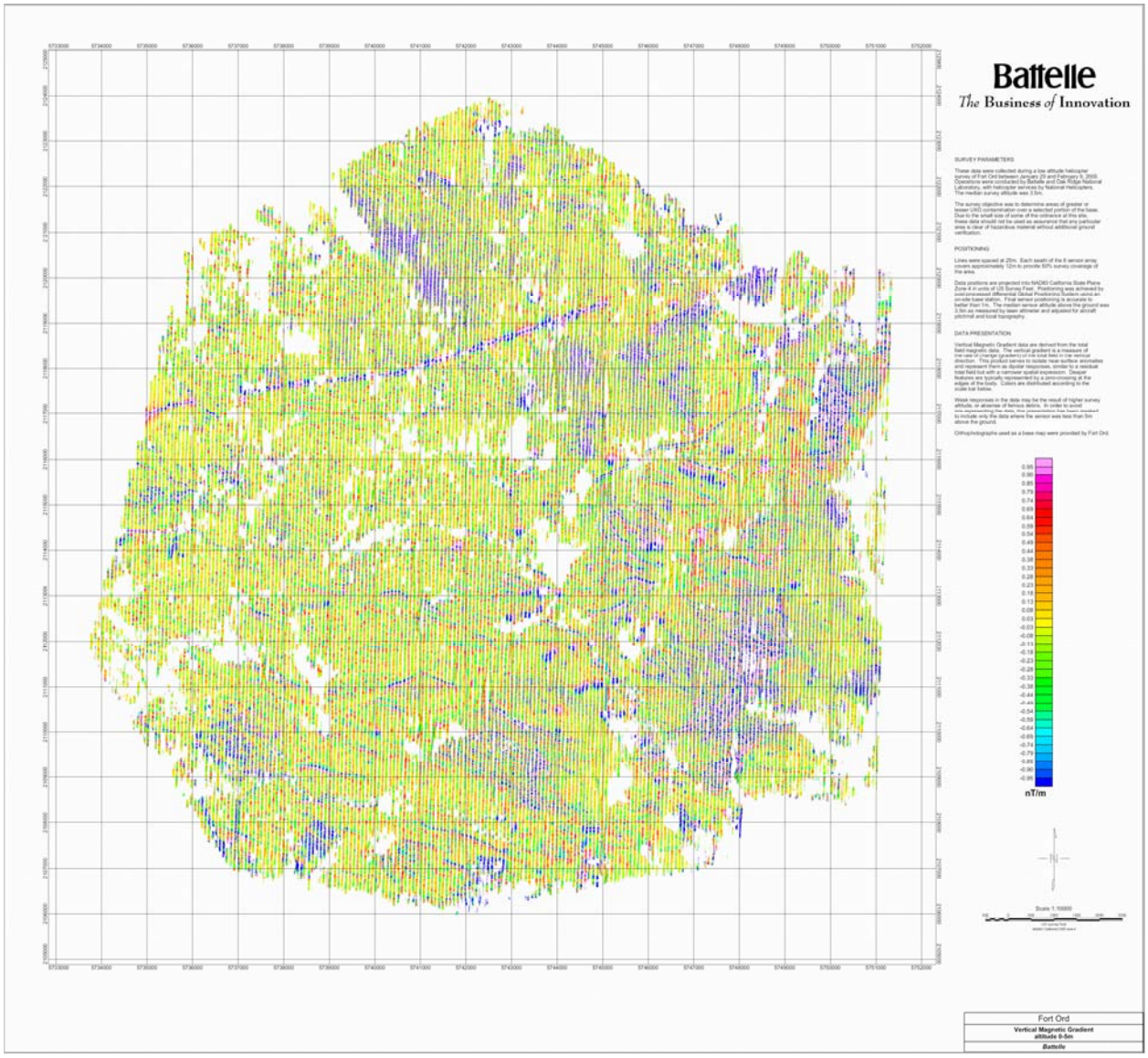

Figure 7.3: Thumbnail of vertical magnetic gradient map of the survey area at Fort Ord for altitudes <5m.

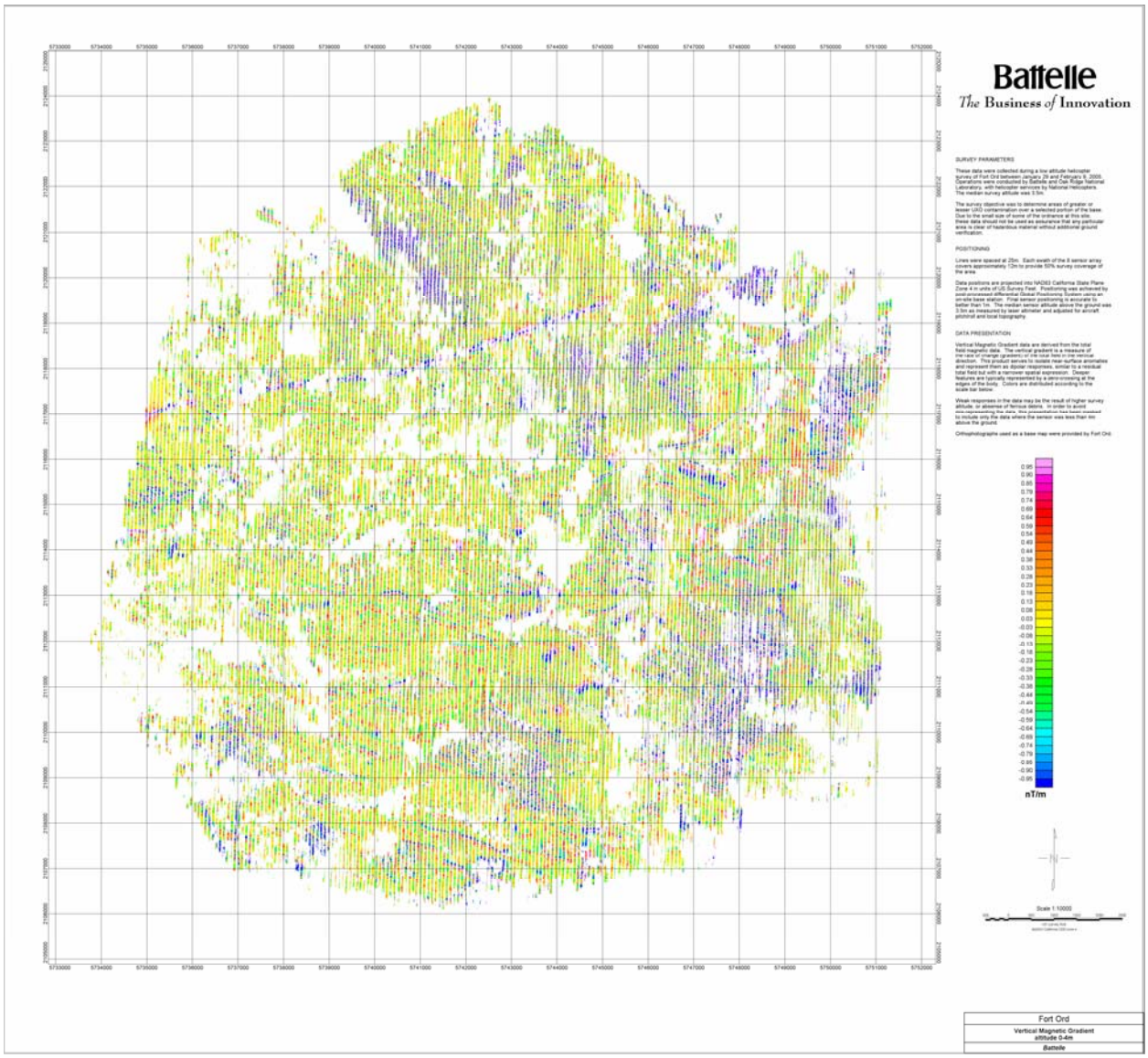

Figure 7.4: Thumbnail of vertical magnetic gradient map of the survey area at Fort Ord for altitudes <4m.

7.4. Analytic signal

An analytic signal map is presented in Figure 7.5 and Figure 7.5. As described in Section 4.11, the analytic signal can be understood as the total gradient. It is similar to the vertical gradient, but it factors in the horizontal gradients as well. The result is a "zero-minimum" product with all peaks being positive, and the amplitude proportional to the size and magnetic susceptibility. In most magnetometer UXO surveys, this map serves as the basis for UXO detection. For this project, anomaly peaks and most of the interpretation were based on this product.

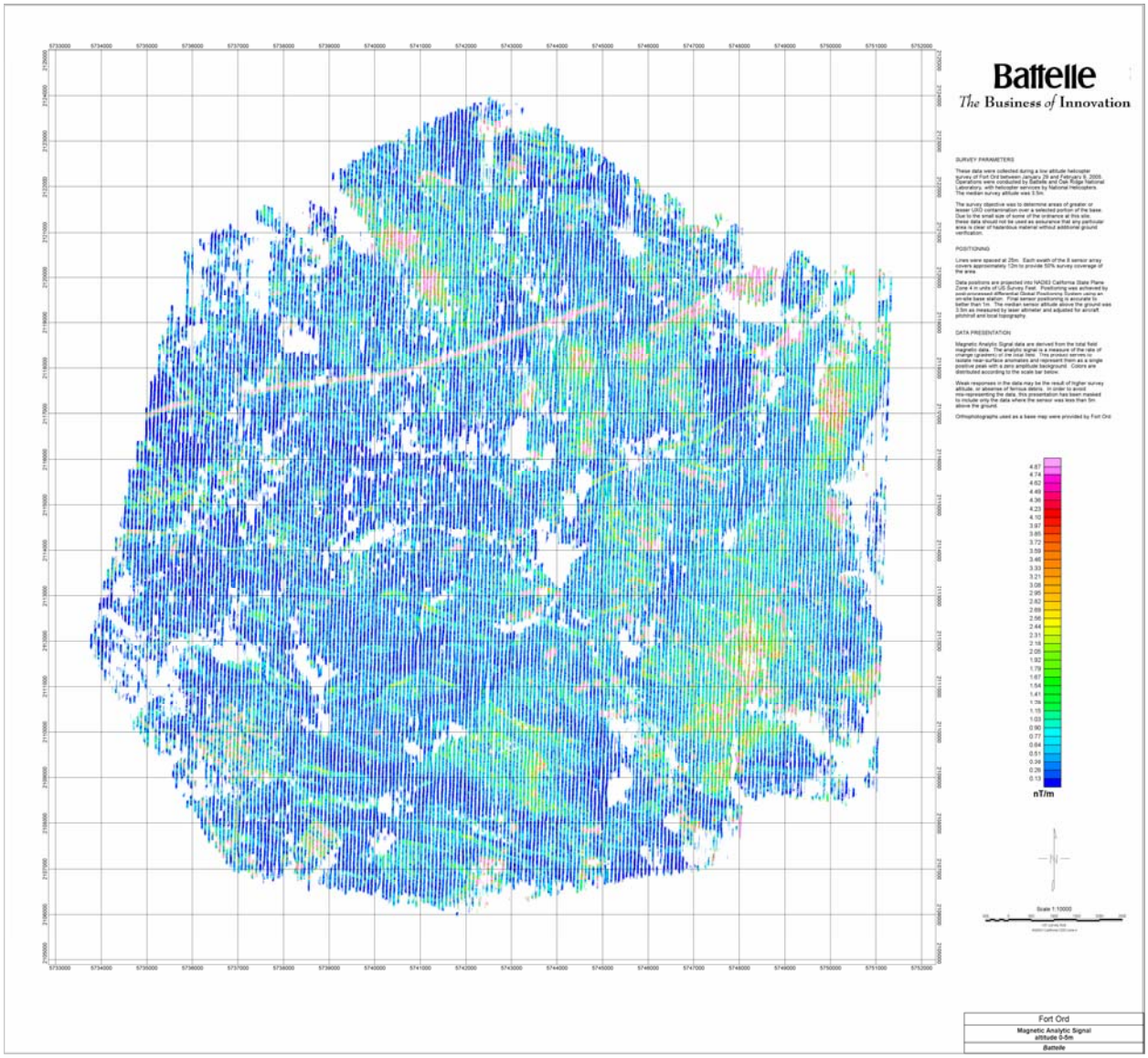

Figure 7.5: Thumbnail of analytic signal map of the survey area at Fort Ord for altitudes <5m.

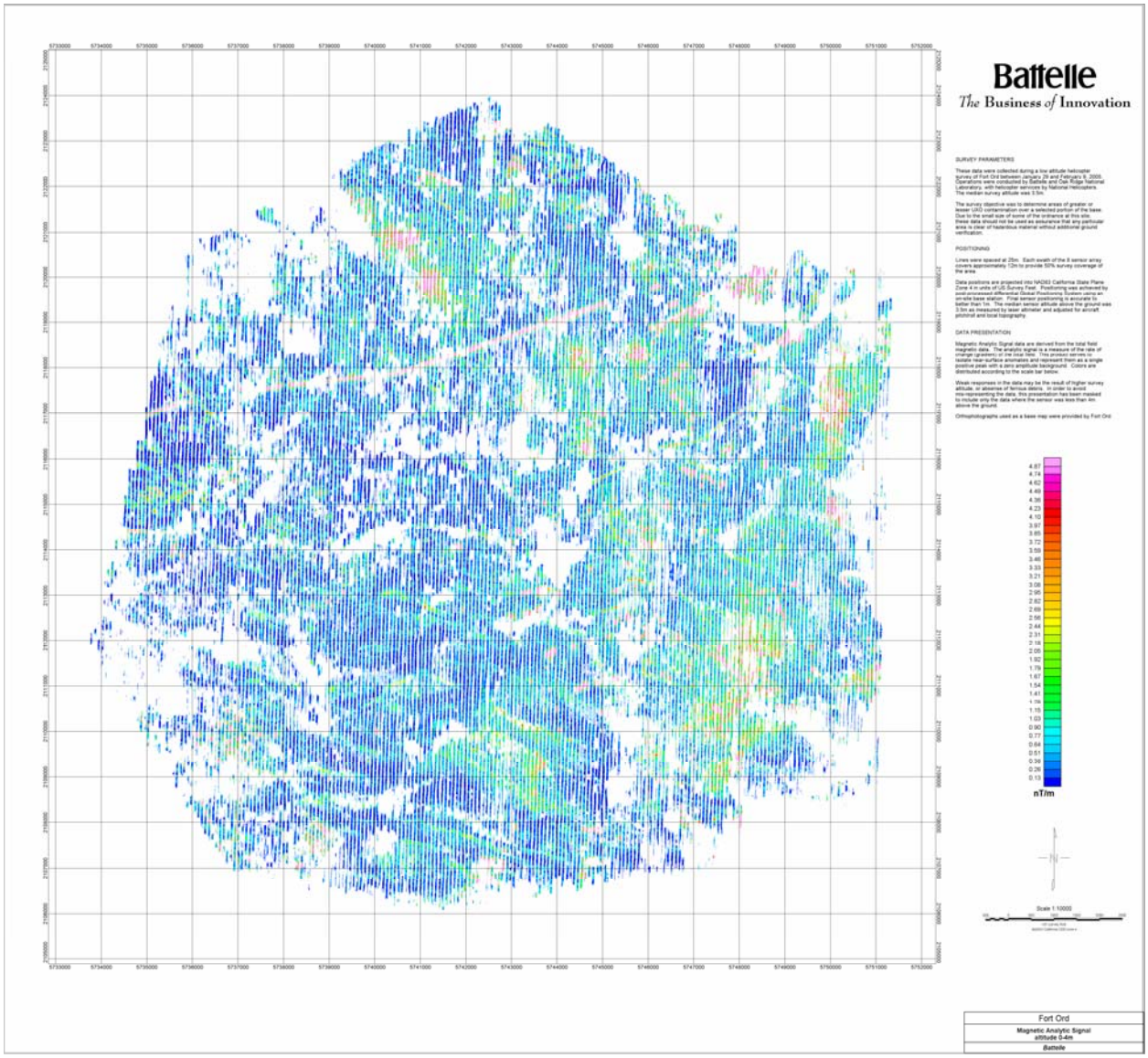

Figure 7.6: Thumbnail of analytic signal map of the survey area at Fort Ord for altitudes <4m.

7.5. Interpretation Map

From the analytic signal map, various linear features that were associated with roads, tracks, pipelines or other cultural features were plotted by hand. These features appear on the interpretation map (Figure 7.8) as black line segments. The most obvious of these is the interpreted pipeline across the northern portion of the survey block. This response is discontinuous, presumably because sections have been removed from the ground. A smaller discontinuous line runs through the center of the block. A third line along the SW boundary of the block is interpreted as associated with a boundary fence.

Other linear features were mapped with red and blue lines. The red lines correspond to analytic signal anomalies which trace topographic ridge lines. These may be geologic in origin. The blue lines correspond to analytic signal anomalies which trace topographic troughs. These may be associated with collections of debris that have settled in local depressions.

In addition to linear trends, anomaly peaks in the analytic signal were analyzed and collected into various groups. A histogram of the analytic signal map (Figure 7.7) shows that the background noise level is 0.2nT/m. From this basis, amplitude thresholds were established at 10:1 (2nT/m) and 2.5:1 (0.5nT/m) signal-noise ratios for strong and weak anomalies respectively. Anomalies were thus divided into low (0.2-0.5nT/m) medium (0.5-2.0nT/m) and high (>2nT/m) amplitude responses. The low amplitude anomalies are not included in this analysis. The remaining anomalies are divided 80/20% between medium and high amplitude responses. These were manually grouped into contiguous blocks and plotted on the interpretation map. Very high amplitude anomalies (>20nT/m or 100:1 signal-noise) represent 3% of the total anomaly count.

Large contiguous blocks (two or more lines) of high amplitude response (>2nT/m) were outlined with hand-drawn polygons in grey. The boundaries of these polygons should not be taken as physical target boundaries. They are merely an attempt to outline the highest amplitude responses. In many cases, dozens or hundreds of individual items may be combining to create a single anomaly that effectively saturates the system's ability to resolve them. Also, many responses are caused by sources that have forced the survey altitude above the 5m altitude threshold. In this situation, the boundaries of the response are impossible to define because the relevant data have been masked out.

Other polygons were drawn in red around blocks of medium amplitude response (>0.5nT/m) which may be associated with lesser densities of debris. That is not to say that ordnance does not exist outside the polygons shown, but the responses outside the blocks appear to be more consistent with geologic sources than the ordnance types expected at this site and at the actual survey altitude. Several of these moderate amplitude responses exist within the survey area, but these are interpreted to be more likely geologic in nature. This would be the result of magnetically susceptible rocks eroding in from other locations; although random rock samples were tested with a susceptibility meter and were not found to be particularly magnetic. The true source of these moderate amplitude but lower priority anomalies cannot be ascertained without ground follow-up.

The largest contiguous block of high amplitude data in this map is in the SE corner of the survey area (A). It is part of a larger medium amplitude block that extends to the NNE and encompasses the second largest single high amplitude block (B). Blocks C-G represent a line of high amplitude blocks that are smaller in extent, but equally strong in amplitude. Blocks D-G are located on topographic highs, but block C almost completely fills a local valley. Blocks H-J represent equally strong responses and are known ranges under remediation. Numerous other high amplitude blocks have been identified and require additional ground follow-up, but we have not assigned letters to these areas. In general, these other blocks have amplitudes comparable to the lettered blocks, but are smaller in their extent.

Most of the high amplitude blocks are contained within a larger medium amplitude block. This would indicate that there is a considerable amount of scattered debris around a central cluster. Not all high amplitude blocks have an associated halo of debris, however. In these cases, the response may be caused by a single large object rather than a cluster of smaller ones. The lack of a response from a debris halo is not an indication of a lack of small ordnance however. Much of the ordnance expected at this site is below the detection threshold of an airborne magnetometer system, and the existence of a large discrete object is an indication of human activity that should be followed-up.

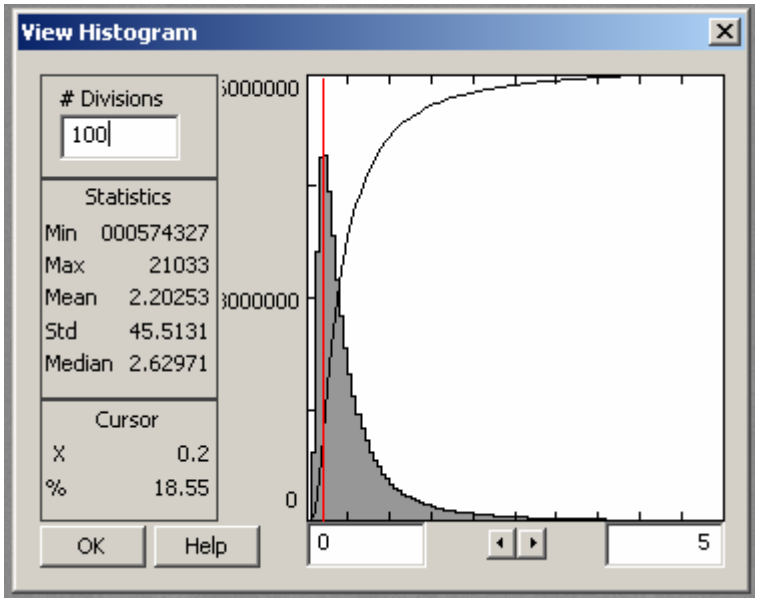

Figure 7.7: Histogram of analytic signal map showing background noise peak at 0.2nT/m.

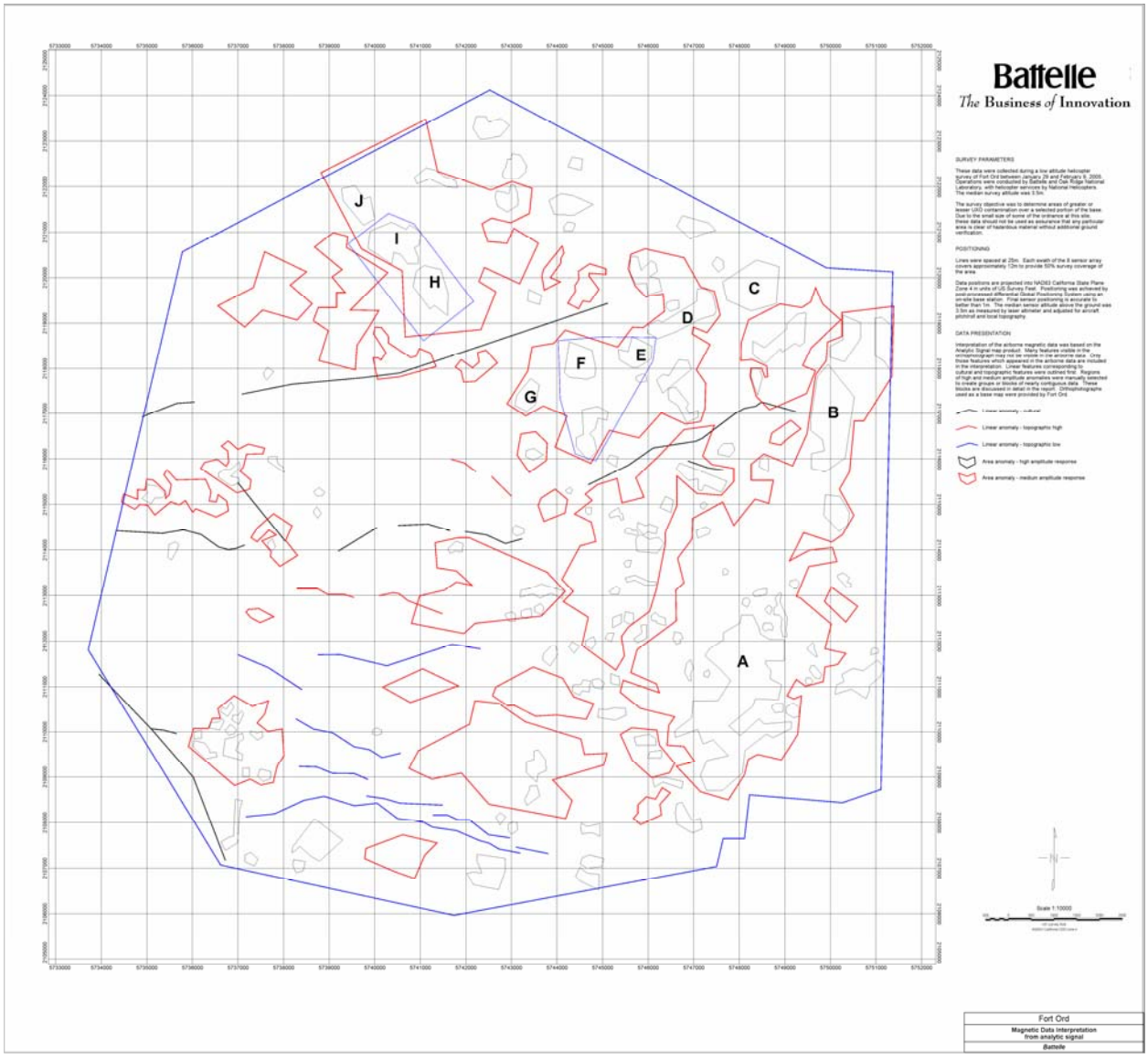

Figure 7.8: Thumbnail of interpretation map for the survey area at Fort Ord.

7.6. Anomaly density

A total of 140,166 discrete anomaly peaks were detected in the analytic signal grid with a minimum amplitude threshold of 0.5nT/m, which is 2.5 times the background noise level of 0.2nT/m. The average amplitude of these peaks was 6.5nT/m and the maximum was 21,000nT/m. Of these, 12,702 were eliminated because the associated sensor altitude was greater than 5m, leaving a total of 127,464 airborne anomaly peaks. As described earlier, 80% of the anomalies were between 0.5-2.0nT/m, and 3% of the anomalies were above 20nT/m.

Airborne anomaly density, in units of counts per hectare, were calculated from these peaks and the low altitude analytic signal coverage. These were compared to the ground magnetic anomaly density figures provided by Parsons Engineering through the Corps of Engineers. The differences in sensitivity between the two survey modes makes quantitative comparisons difficult. The ratio of the ground to airborne densities was calculated by simply dividing the airborne- and ground-based density maps. The ratios ranged from 2:1 to 9:1 with no single dominant ratio. A 5:1 ratio represents an average scaling factor between ground and airborne densities, but the numeric accuracy of such scaling is accurate only within a factor of +/-2 at best. It should be noted that low, or even zero density responses in the airborne data are insufficient justification to declare an area clear of ordnance.

The resulting map (Figure 7.9) shows a strong correlation with the polygons of the moderate analytic signal response (red polygons). Most of the linear cultural features are suppressed but not eliminated because they form longer anomalies rather than discrete peaks. The linear features associated with local topographic features are not particularly suppressed. This is because they are strings of discrete anomalies rather than a long continuous anomaly. The high amplitude analytic signal responses (grey polygons) do not show as high a correlation with the density as expected. In this product, a single large amplitude response counts with the same weight as a single low amplitude response. The analytic signal may reflect the bulk or volume or mass of metallic debris whereas the density measurement attempts to represent a count of debris pieces.

The dominant feature of this map is the very high density found in the vicinity of Range 43 and 48 (Blocks H-J). Blocks C-G have comparable anomaly densities. By comparison, Blocks A and B, which dominated the analytic signal amplitude response, show noticeably lower densities. The broad medium amplitude response block surrounding Blocks A and B shows ordnance densities comparable to those in the ODDS calibration grid.

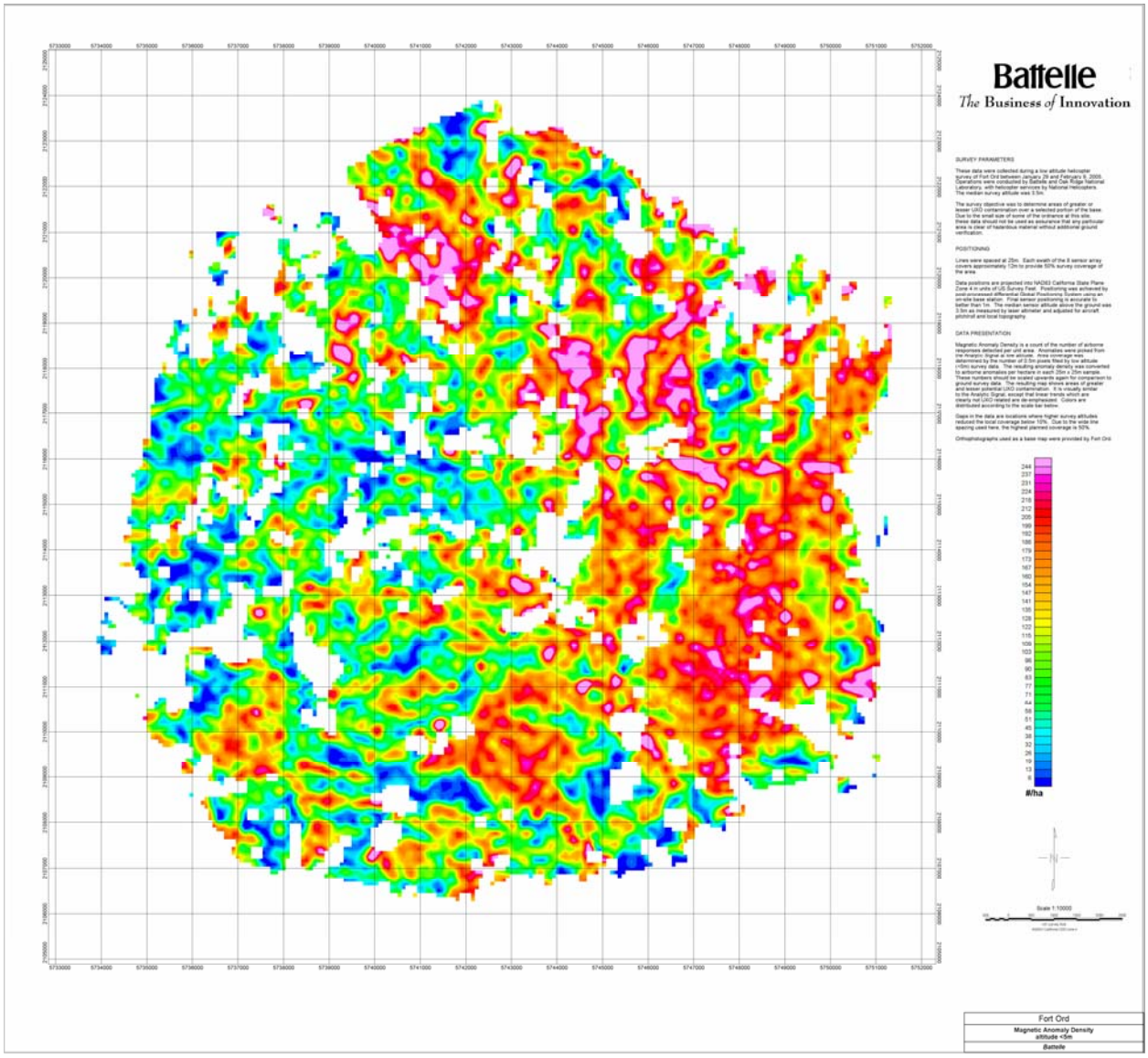

Figure 7.9: Thumbnail of anomaly density map of the survey area at Fort Ord.

7.7. MRS-16 Site

At the request of the Fort Ord BRAC office an additional block, known as the MRS-16 site was flown to the north of the main survey area. This area was heavily treed and was under consideration for clearance burning. The area was flown with full coverage using 12m line spacing. The vegetative cover prevented low level surveying in all but one small section of the area. Although the range of altitudes was comparable to the main survey block, the median height was approximately double at 6.4m. Figure 7.10 shows the histogram and general statistics for the MRS-16 site. The vertical red line shows the cut-off altitude used on the main block.

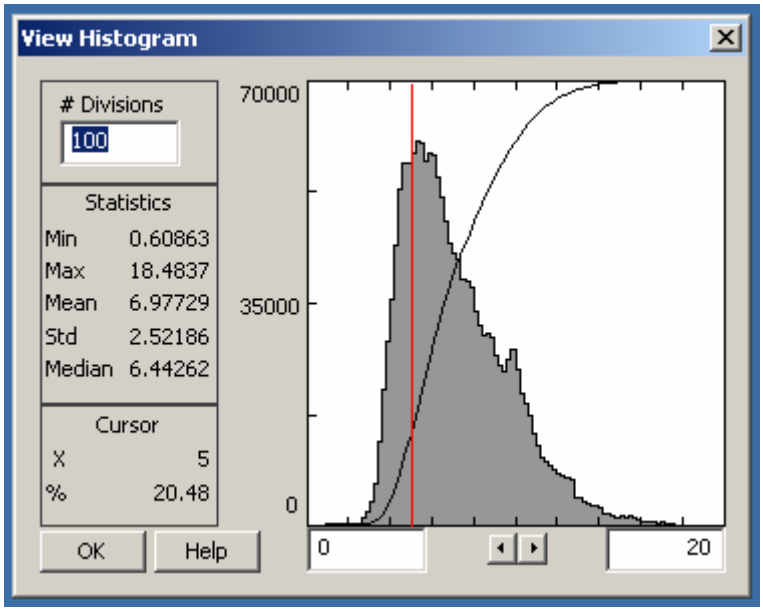

Figure 7.10: Histogram of altitude data at the MRS-16 site. The median altitude is 6.4m. The 5m cut-off threshold used in the main survey area would eliminate 79.5% of the data from consideration.

In general, the survey height was too great to discriminate individual objects. Clusters of objects may also be masked at this altitude. Infrastructure such as fences and roads are the most likely source of the observable anomalies, however there about a dozen small, discrete anomalies that should be assessed. These are marked on analytic signal map (Figure 7.11) and interpretation map (Figure 7.12). The approach to interpretation was similar to that used for the main survey area. Linear and cultural features were traced by hand, as were areas of high and moderate anomaly intensity. In addition, several discrete anomalies which occurred outside the moderate intensity polygons are recommended for assessment by the BRAC office.

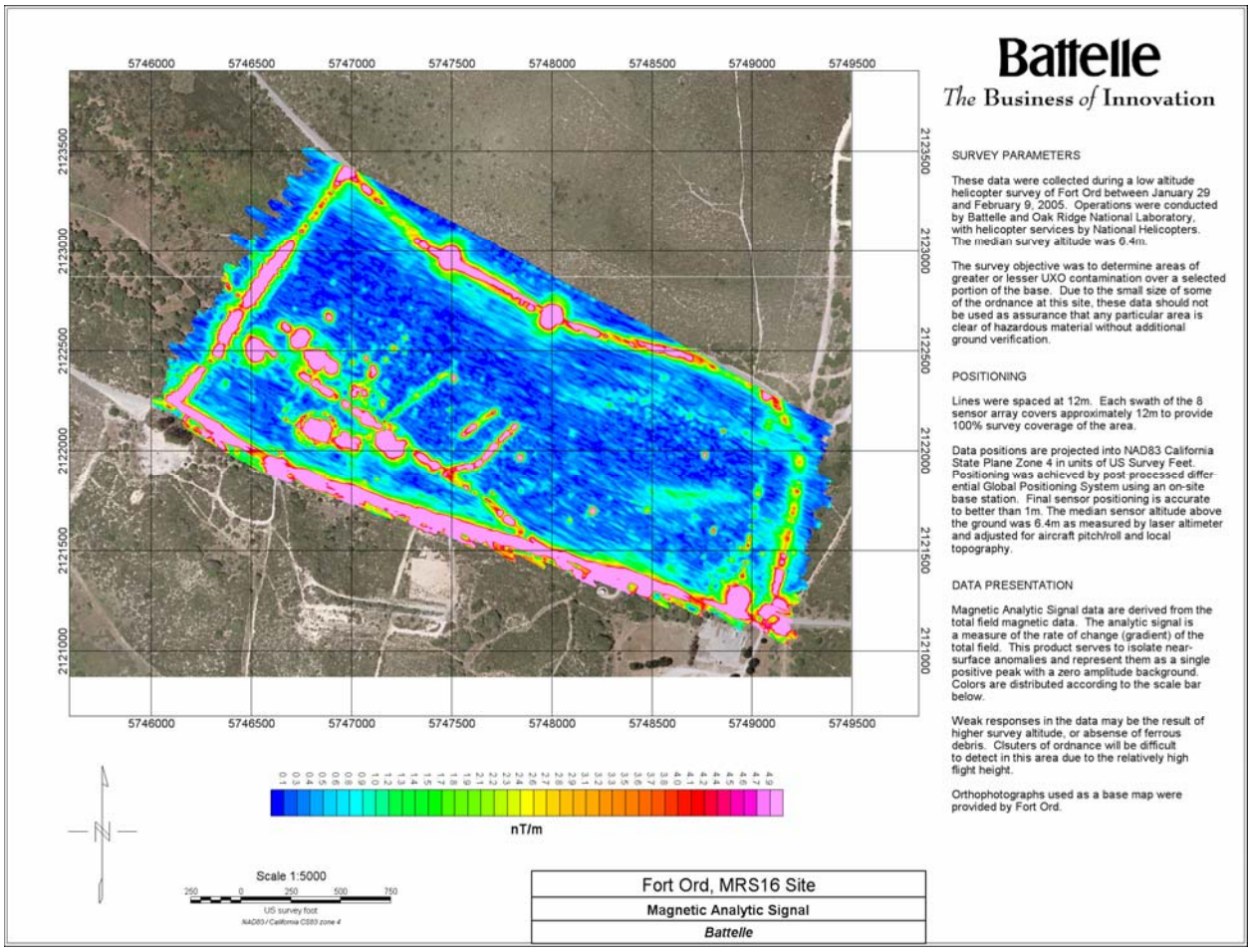

Figure 7.11: Thumbnail of analytic signal map of the MRS-16 area at Fort Ord.

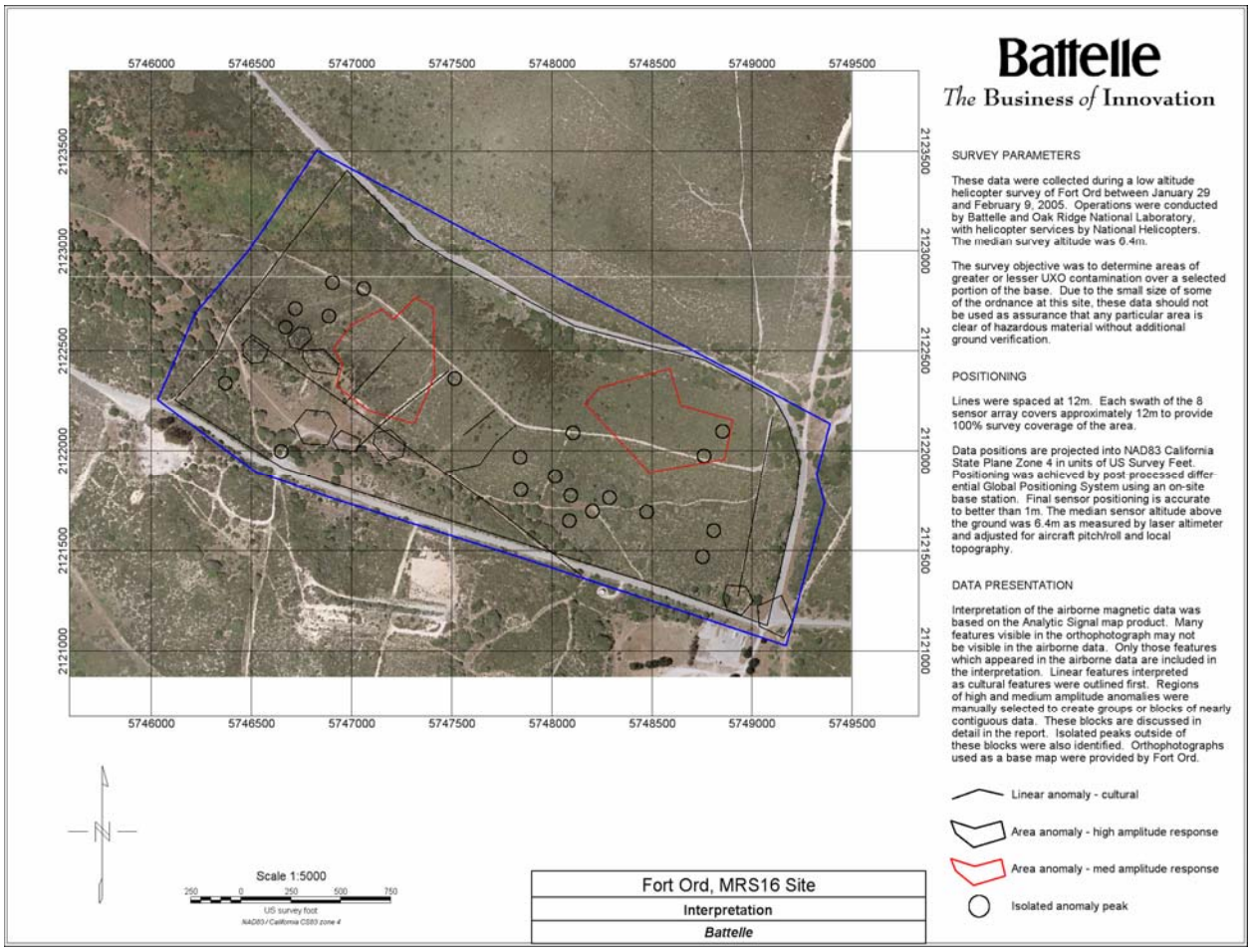

Figure 7.12: Thumbnail of interpretation map of the MRS-16 area at Fort Ord.

7.8. Data and Image Archive

Original Geosoft format files are provided as the principal digital format. This includes database files with georeferenced point data (GDB), and interpolated grid files (GRD). A free data viewer is included with the digital data or is available online at www.geosoft.com (Oasis Montaj Viewer 6.1). Supplemental copies of map data are provided as image files in compressed TIF format in addition to the smaller reproductions included in this report. These maps are provided with a digital resolution of 150 and 300 dpi. GeoTiff format files of the geophysical data alone are provided for quick inclusion into other GIS platforms, but the resolution is not as high as the original Geosoft GRD files.

The Geosoft databases (GDB) are the primary data source. They represent the highest data resolution, but have no visual component. Files are named “ord_final_A”, where A designates the survey area covered. Areas include the calibration grid (calgrid), area MRS16, and the main survey block broken roughly into four quadrants (q1, q2, q3, q4). Lines in the database represent the trace of a single sensor as it travels down the line. Lines are numbered “Q####.S”, where Q

is the quadrant number, #### is the survey line number and S is the sensor number (0-7 from left to right across the array). Data columns or channels in the database are bulleted below.

- X_UTM Easting coordinate in NAD83 UTM Zone 10N meters.
- Y_UTM Northing coordinate in NAD83 UTM Zone 10N meters.
- Z_agl Sensor altitude above ground level in meters.
- Mag_tf Total field magnetic values in nanoTesla.
- Mag_resid Residual total field magnetic values in nanoTesla.

The Geosoft grids (GRD) are the database values interpolated onto a regular grid for contouring and visualization. Additional products, such as vertical gradient and analytic signal are calculated exclusively in gridded format. Gridded data use the naming convention "A_PROD_SPC", where A is the survey area (calgrid, MRS16, ord). The calibration grid data are divided into three heights of 5ft, 10ft, and 15ft above ground level. PROD is the data product as described in the bullets below. The SPC extension is included to remind users that the coordinates for the gridded data use the California State Plane Coordinates, NAD83 Zone4, US survey feet.

- TF Total field magnetic values in nanoTesla
- VGhi Vertical gradient values above 5m sensor height in nanoTesla/meter.
- VGlo4 Vertical gradient values below 4m sensor height in nanoTesla/meter.
- VGlo5 Vertical gradient values below 5m sensor height in nanoTesla/meter.
- AS Analytic signal values for all heights in nanoTesla/meter.
- AShi Analytic signal values above 5m sensor height in nanoTesla/meter.
- ASlo4 Analytic signal values below 4m sensor height in nanoTesla/meter.
- ASlo5 Analytic signal values below 5m sensor height in nanoTesla/meter.
- ALT2 Sensor altitudes above ground level in meters.
- DENS Magnetic anomaly density in peaks/hectare.

Geosoft maps (MAP) present the gridded data at 1:10,000 scale (1:5,000 scale for MRS16) with orthophoto background, coordinate grids, title blocks and legends. These are the files that are used for the final data presentation. The naming convention is identical to that of the GRD files, except that the SPC designation has been dropped and interpretation maps (interp) have been added to the product list. TIF files of these maps have been prepared at 150 and 300dpi. The naming convention is the same as the MAP files with the addition of the image resolution information (_MAP150 or _MAP300).

GeoTIF files have been prepared GRD files at 150 dpi resolution. These are similar to the TIF files described above, except that they include the data only (no orthophoto background, title blocks, etc) and include supplementary files (IPJ) for georeferencing the images. The naming convention is the same as the GRD files with the addition of the image resolution information (_DATA150). The prefix DATA has been used to differentiate these files from the TIF of the MAP files which include background information.

8. Electromagnetic products and interpretation

8.1. Time-domain electromagnetic response

Electromagnetic data were collected in only two sizeable areas: EM Block A (35 ha/86 acres) and EM Block B (37 ha/92 acres). EM data were also collected at the geophysical prove-out grid and at a site designated as the resistivity calibration area. Maps were made of EM response in millivolts for data averaged over specific time windows. Table 8.1 shows details of the six time bins with units in microseconds after the end of the transmitter pulse. Figure 8.1 shows the typical decay of the EM response over a good conductor. Over most metallic conductors found in EM Blocks A and B, the EM response decays to background levels usually by the fourth time bin, i.e. by about 1.4 milliseconds after transmitter turnoff. However, a few conductors in both areas showed above-background responses through all six time bins.

Table 8-1: Time bins for ORAGS-TEM system

Time Bin	Decay Samples Averaged	Start time (microseconds)	End time (microseconds)	Mean Bin time (microseconds)
1	1	92.5	92.5	92.5
2	2,3	185	277.5	231
3	4,5,6,7	370	647.5	509
4	8,9,10,11,12,13,14,15	740	1387.5	1064
5	16,17,18,19,20,21,22,23	1480	2127.5	1804
6	24,25	2220	2312.5	2266

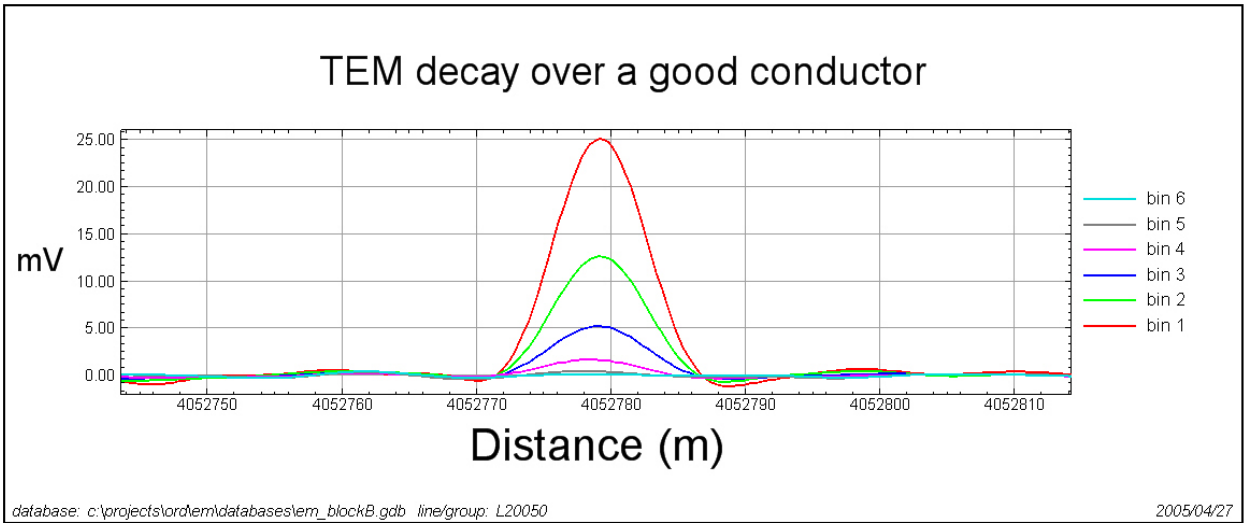

Figure 8.1: Typical EM response over a metallic conductor. Time bins correspond to those listed in Table 8.1.

Our experience with the ORAGS-TEM system in tests at the Badlands Bombing Range (BBR) led us to believe that we might see EM response change with (assumed) changes in soil conductivity (ORNL, 2003). At BBR, the earliest time gates showed long period variations superimposed on the short period anomalies from UXO. The source of this long period variation was never firmly established. At Fort Ord neither of the EM survey blocks shows unambiguous responses from soil cover. All anomalies appear to be produced by large metallic debris, or collections thereof. Most of the time the high altitude EM background was virtually indistinguishable from the EM response near the ground surface in areas clear of large conductors. Figure 8.2 shows data from time bin 2 (185 microseconds after transmitter turnoff) collected along a survey line at an altitude of about 2 m AGL and also along a high altitude background excursion at over 80 m AGL. The mean millivolt response at 2m is virtually indistinguishable from the high altitude millivolt response. Based on this and other results, we concluded that it would not be possible to use the Fort Ord TEM data for ground conductivity mapping.

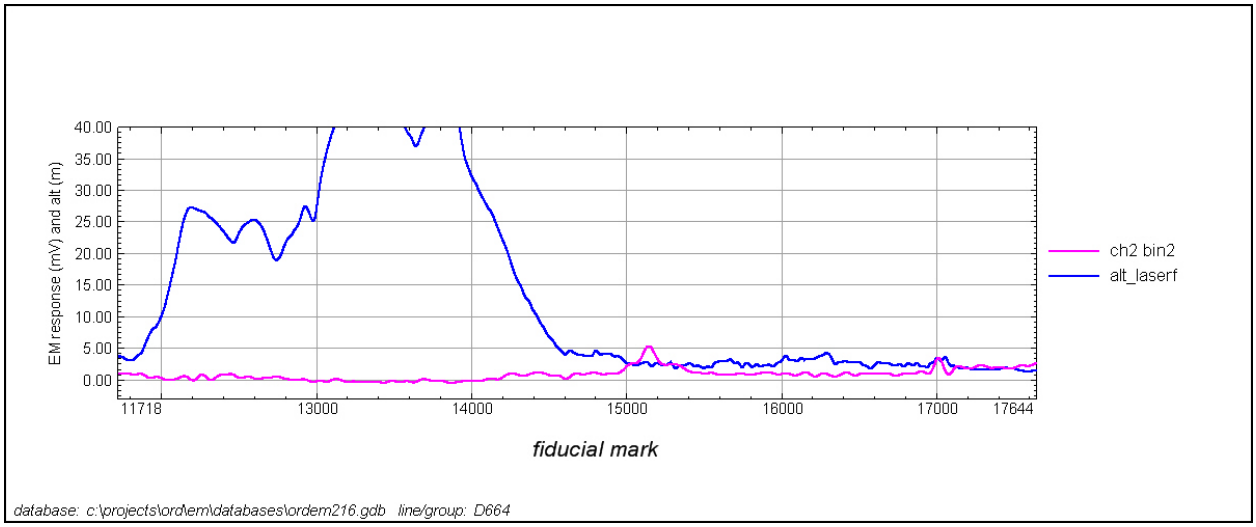

Figure 8.2: The insensitivity of Fort Ord soils to ORAGS-TEM: the EM response near the ground (fids 15000-17000) is virtually the same as the at-altitude response (fids 13000-14000).

8.2. Interpretation of Electromagnetic Data

ORAGS-TEM data were collected in only two large areas at Fort Ord. The locations of EM Blocks A and B are shown by the red polygons in Figure 3.1. EM Block A is roughly rectangular, and comprises 35 ha. EM Block B is somewhat triangular in shape and comprises 37 ha.

For small targets and small transmitter and receiver coils, the EM response falls off with coil-to-target separation R at about $1/R^6$. The ORAGS-TEM system has a transmitter that is large with respect to the UXO target, and we have found that fields from most UXO sources decay as $1/R^5$ to $1/R^4$, a rate that is nonetheless more extreme than the $1/R^3$ falloff in the case of magnetic

fields. The ORAGS-TEM system therefore shows even more height dependence than do the magnetic systems. This is particularly apparent in EM Block A, where taller vegetation forced higher survey altitudes (3-5 m AGL) in the southwest half of the area. On this side of the survey block there are virtually no anomalies, as can be seen in Figure 8.3, which shows the EM response of time bin 2. On the northeast half, where survey heights were generally at or below 2 m AGL, EM anomalies are prevalent. Most sources appear to be from clusters of UXO rather than individual items.

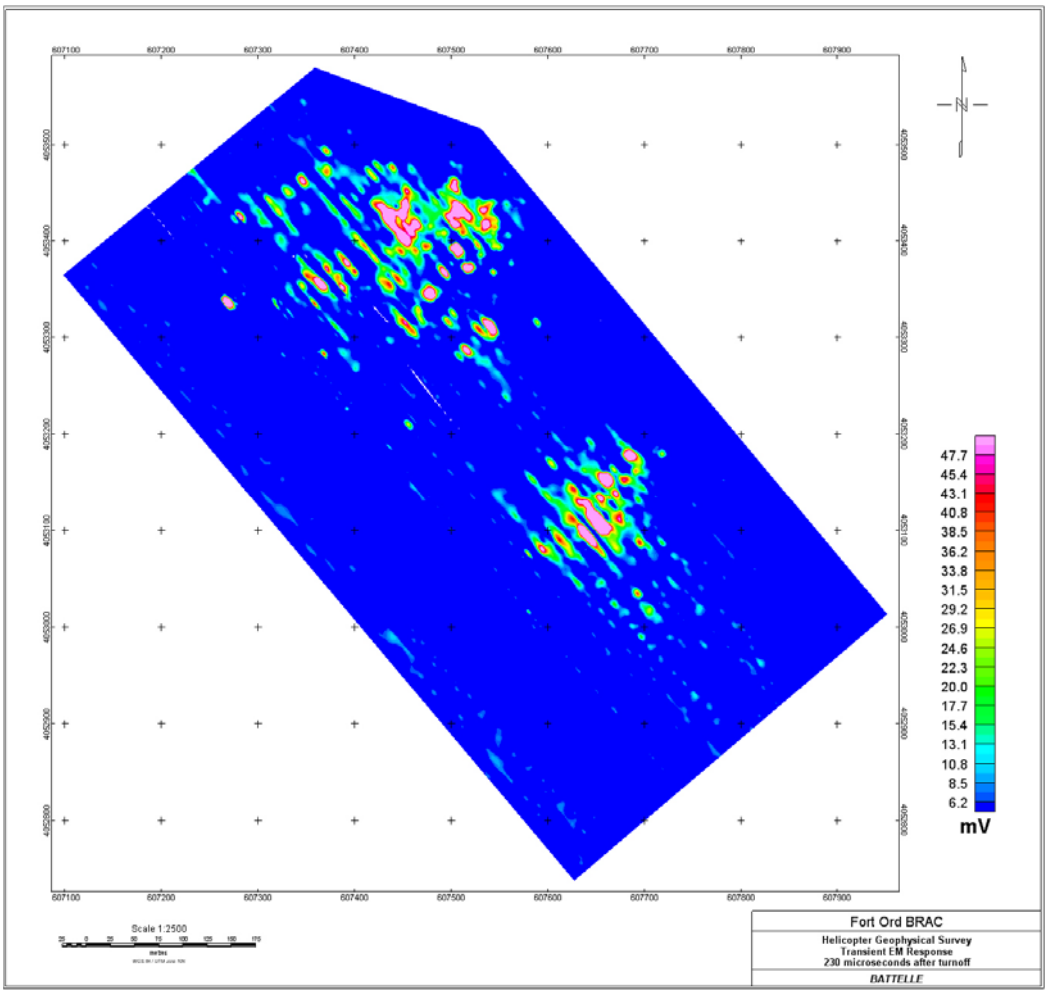

Figure 8.3: EM response of EM Block A, 230 microseconds after transmitter turnoff (time bin 2).

Comparing the EM map with the analytic signal map derived form magnetic field data over EM Block A, we see that the analytic signal appears more sensitive to smaller items than does the EM system. The analytic signal shown in Figure 8.4 shows small anomalies even over the southwest half of the area where survey heights were in the vicinity of 5 m. The EM map also appears more striped than the analytic signal map. The magnetic sensors were 1.7 m apart, and the change in signal between adjacent sensors from height differences is small. In contrast, the centers of the port and starboard EM receivers were 10 m apart, and small changes in helicopter roll can produce substantial EM response differences. For example, a 2 degree roll can produce

a 24 cm height difference in the receivers. This can in turn produce up to a 100% difference in the EM responses of the port and starboard sensors. These line-to-line response differences cause the EM anomalies to appear discontinuous, and give the two-receiver data a corrugated or striped appearance.

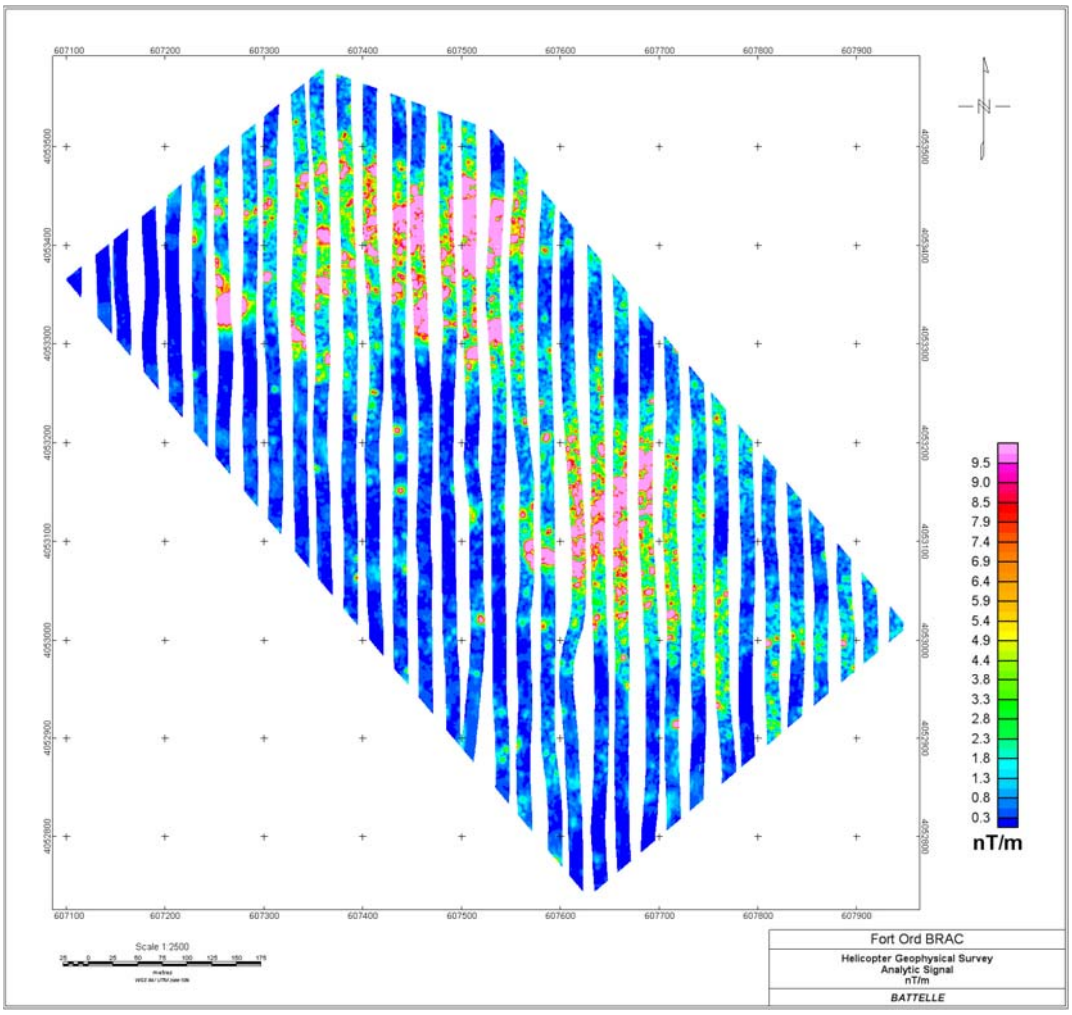

Figure 8.4: Analytic signal of total magnetic field measured over EM Block A.

The situation in EM Block B is similar to that of EM Block A. Again, the EM data mainly show what appear to be concentrations of UXO or scrap, and do not show small individual items. A comparison of the EM bin 2 response in Figure 8.5 with the analytic signal in Figure 8.6 shows that virtually every clearly visible EM anomaly corresponds to a large analytic signal anomaly. Ordnance *concentrations* can be well-located using the Fort Ord EM data. It is the small individual ordnance items that are difficult for EM to define in the Fort Ord data sets. Survey altitudes in EM Block B ranged from 1 m to over 7 m, and averaged 2.6 m AGL.

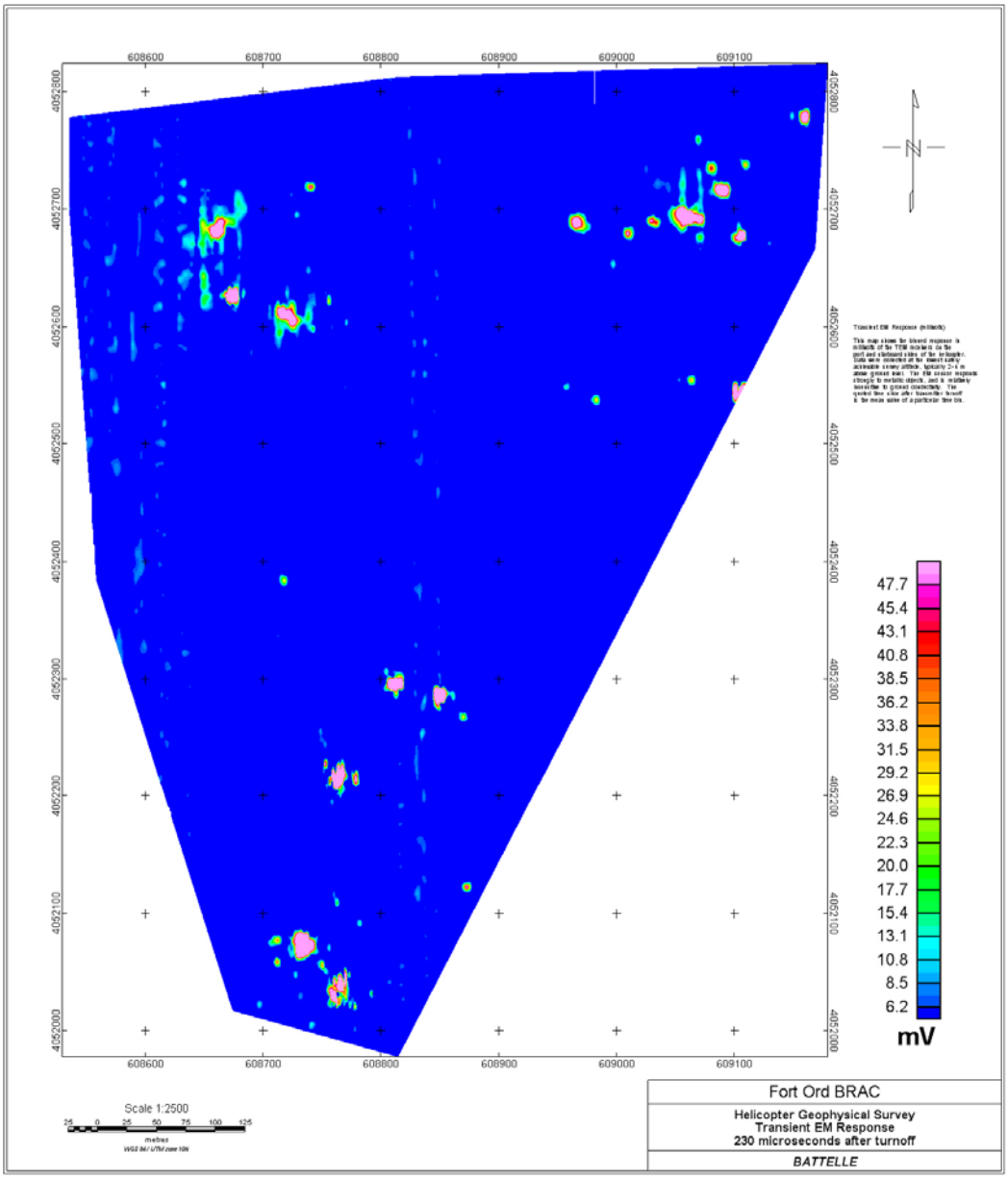

Figure 8.5: EM response of EM Block B, 230 microseconds after transmitter turnoff (time bin 2).

In tests at the Badlands Bombing Range, individual M-38 practice bombs were clearly visible in low altitude data (Beard et al, 2004), and items as small as 81-mm mortars could be detected, although less consistently. However, at Fort Ord, taller vegetation and rougher topography forced the pilot to consistently fly above 2.5 m AGL, and at these heights items smaller than individual bombs cannot be seen.

Another problem with the Fort Ord EM data was a variable period oscillation that appeared in the data. We have not yet ascertained the source of the oscillation. The most likely sources are either on overdriven transmitter, or boom vibration. In some cases the oscillation is substantial – over 10 mV – and could hide small anomalies produced by individual ordnance items.

All EM maps for EM Blocks A and B, including EM sensor altitude and a comparison with analytic signal, are shown in Appendix 2.

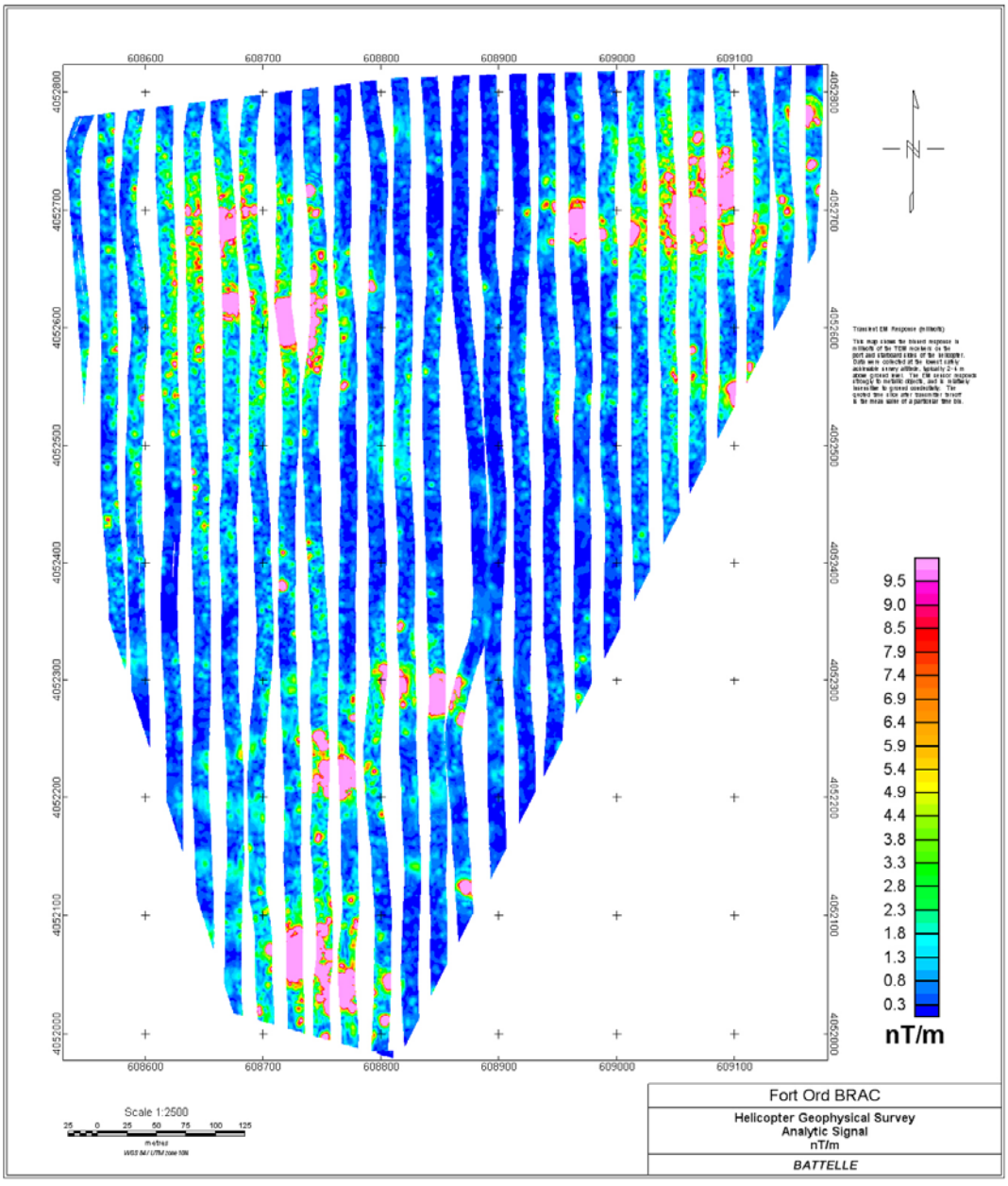

Figure 8.6: Analytic signal of total magnetic field measured over EM Block B.

8.3. EM Data and Image Archive

Geosoft format files are provided as the principal digital format. This includes database files with georeferenced point data (GDB), and interpolated grid files (GRD). Copies of map data are provided as image files in JPG format in addition to the smaller reproductions included in this report. These maps are provided with a digital resolution of 100 dpi. Eight JPG files have been made for both of the EM survey areas: six EM response bins, altitude, and analytic signal. The EM response files are named to describe time bin and the survey block, e.g. em1A.jpg.

The Geosoft databases (filename.gdb) containing the electromagnetic data are named after the 100 acre areas where EM data were collected. They are "EM_blkA.gdb" and "EM_blkB.gdb". Lines in the database represent the trace of a single sensor as it travels down the line. Data columns or channels in the database are bulleted below.

- Xm Easting coordinate in NAD83 UTM Zone 10N meters.
- Ym Northing coordinate in NAD83 UTM Zone 10N meters.
- date year/month/day.
- hae Sensor height above ellipsoid.
- alt Sensor altitude above ground level in meters.
- gps_synch GPS synchronized time in seconds.
- line Flight line number.
- line2 Flight line number with receiver indicator (0, port; 1, starboard).
- em1ffB Levelled, filtered EM channel 1—93 μs after transmitter turnoff.
- em2ffB Levelled, filtered EM channel 2—230 μs after transmitter turnoff.
- em3ffB Levelled, filtered EM channel 3—510 μs after transmitter turnoff.
- em4ffB Levelled, filtered EM channel 4—1065 μs after transmitter turnoff.
- em5ffB Levelled, filtered EM channel 5—1085 μs after transmitter turnoff.
- em6ffB Levelled, filtered EM channel 6—2270 μs after transmitter turnoff.

Geosoft grid files (filename.grd) are the database values interpolated onto a regular grid for contouring and visualization. The grids are NAD83 Zone10N, meters. Grids were made for the two survey areas: block A and block B. The eight grids for each block consist of one altitude grid, and analytic signal magnetic grid, and grids for each of the six time bins. For example, em1ffB_A.grd represents the grid for time bin 1 in block A.

Geosoft maps (filename.map) present the gridded data at 1:2500 scale with coordinate grids, title blocks and legends. These are the files that are used for the final data presentation. The maps for the six EM time bins are named according to time bin and block. For example, the EM response of time bin 3 in block B is em3_B.map.

9. Conclusions

Data acquired during this survey are suitable for use by the Fort Ord BRAC Office and their contractors in a variety of characterization, screening-level, and removal activities associated with determination of the extent of potential UXO-related contamination at the site. The main survey consisted of a 1281 ha magnetic survey using the transect survey method on alternating lines (providing an effective coverage of 2562 ha). Rough topography and tall vegetation increased flight height and reduced the survey data coverage from 50% to 42% of the effective total. Clusters of ordnance, however, represent a legitimate target for this technology over the entire 2562 ha, allowing for interpolation between lines and across gaps caused by increased flight height.

A 72 ha electromagnetic survey was also conducted within the main area and was flown at full density (10m line spacing). In addition, a supplemental 41 ha magnetic survey was flown at as the MRS-16 area at full coverage (100% at 1.7m line spacing) at the request of the Fort Ord BRAC Office. A well-established and documented geophysical prove-out site containing inert ordnance items was used as calibration targets for this survey.

Map products that were developed for the main magnetic survey area include total magnetic field, vertical magnetic gradient, analytic signal, anomaly density, and interpretation maps. These are suitable for ground follow-up and other analyses intended to understand the relationship between concentrations of airborne anomalies and the density of UXO at the site. The airborne data are NOT suitable for declaring an area free of contamination, as some ordnance types fall below the detection threshold of the system, and only a percentage of other ordnance types will be detected. This is particularly true for the transect method that was employed in the main survey area at Fort Ord, in which only about half of the area of interest was surveyed. Further, areas of rough topography or tall vegetation forced increased flight height in those areas (as in the MRS-16 area), and renders a portion of the data unsuitable for detection of the targets of interest. These factors are consistent with the goal of the project, which was to delineate areas of magnetic anomalies, many of which may be indicative of targets where an abundance of MEC and UXO may be found.

In general, the survey height in the MRS-16 area was too great to discriminate individual objects. Clusters of objects may also be masked at this altitude. Infrastructure such as fences and roads are the most likely source of the observable anomalies, however there about a dozen small, discrete anomalies that should be assessed. Several discrete anomalies outside the moderate intensity polygons are recommended for assessment by the BRAC office.

The ORAGS-TEM system shows even more height dependence than the magnetic system. This is particularly apparent in EM Block A, where taller vegetation forced higher survey altitudes (3-5 m AGL) in the southwest half of the area. On this side of the survey block there are virtually no anomalies. On the northeast side, where survey heights were generally at or below 2 m AGL, EM anomalies are prevalent. Sources appear to be both clusters of UXO and individual items.

10. References

Beard, L.P., Doll, W.E., Holladay, J.S., Gamey, T.J., Lee, J.L.C., and Bell, D.T., 2004. Field tests of an experimental helicopter time-domain electromagnetic system for unexploded ordnance detection: Geophysics 69: 664-673.

Billings, S. D., Pasion, L. R., Oldenburg, D. W. and Foley, J., 2003. The influence of magnetic viscosity on electromagnetic sensors: EUDEM-SCOT2 2003, International Conference on Requirements and Technologies for the Detection, Removal and Neutralization of Landmines and UXO, Brussels, September 15-18, 2003.

ORNL, 2003. Demonstration of airborne electromagnetic systems for detection and characterization of unexploded ordnance at the Badlands Bombing Range, South Dakota: ESTCP Project 200101 Final Report, 60 pp.

MACTEC Engineering and Consulting, Inc., 2005. Fort Ord Cleanup website: http://www.fortordcleanup.com/foprimer/.

Telford, W.M., L.P. Geldart, and R.E. Sheriff, 1990. Chapter 5—Electrical properties of rocks and minerals in Applied Geophysics, 2nd Ed., Cambridge University Press, New York, 770 pp.

Appendix A
Daily QC Results

A single swath was flown over a line of pipes laid out on the surface of the ground at the start of each day. The results were analyzed for positional accuracy and sensor functionality. The following plots show the analytic signal in nT/m for the North-bound and South-bound lines separately. Altitudes varied slightly from line to line, but averaged 2m. Dates are shown on the map in a m-dd format. The target pipes were moved after positioning problems were detected and resolved on January 29/05 (1-29). This accounts for the difference in response on that day.

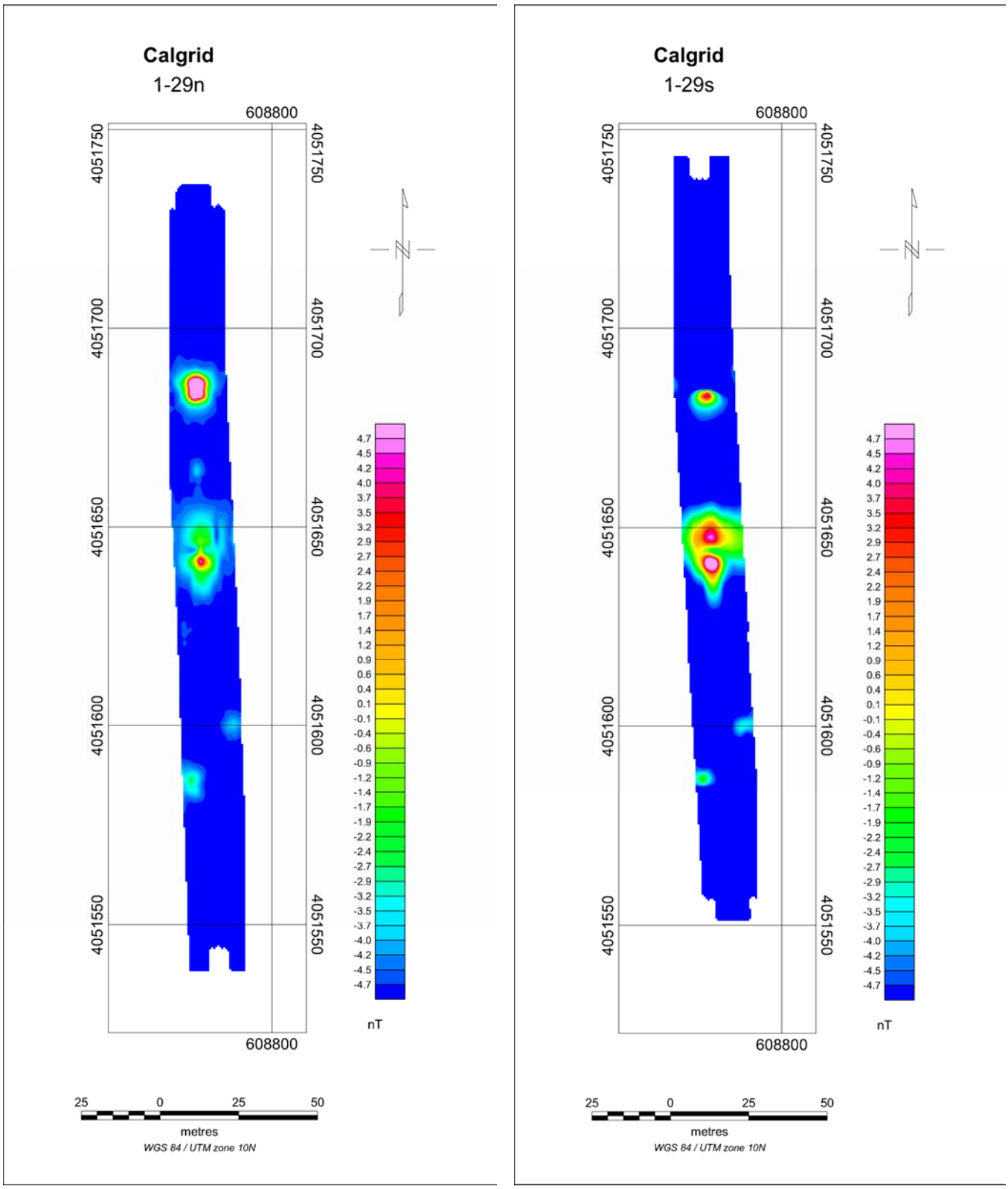

Figure A1: Magnetic QC lines from Jan 29/05.

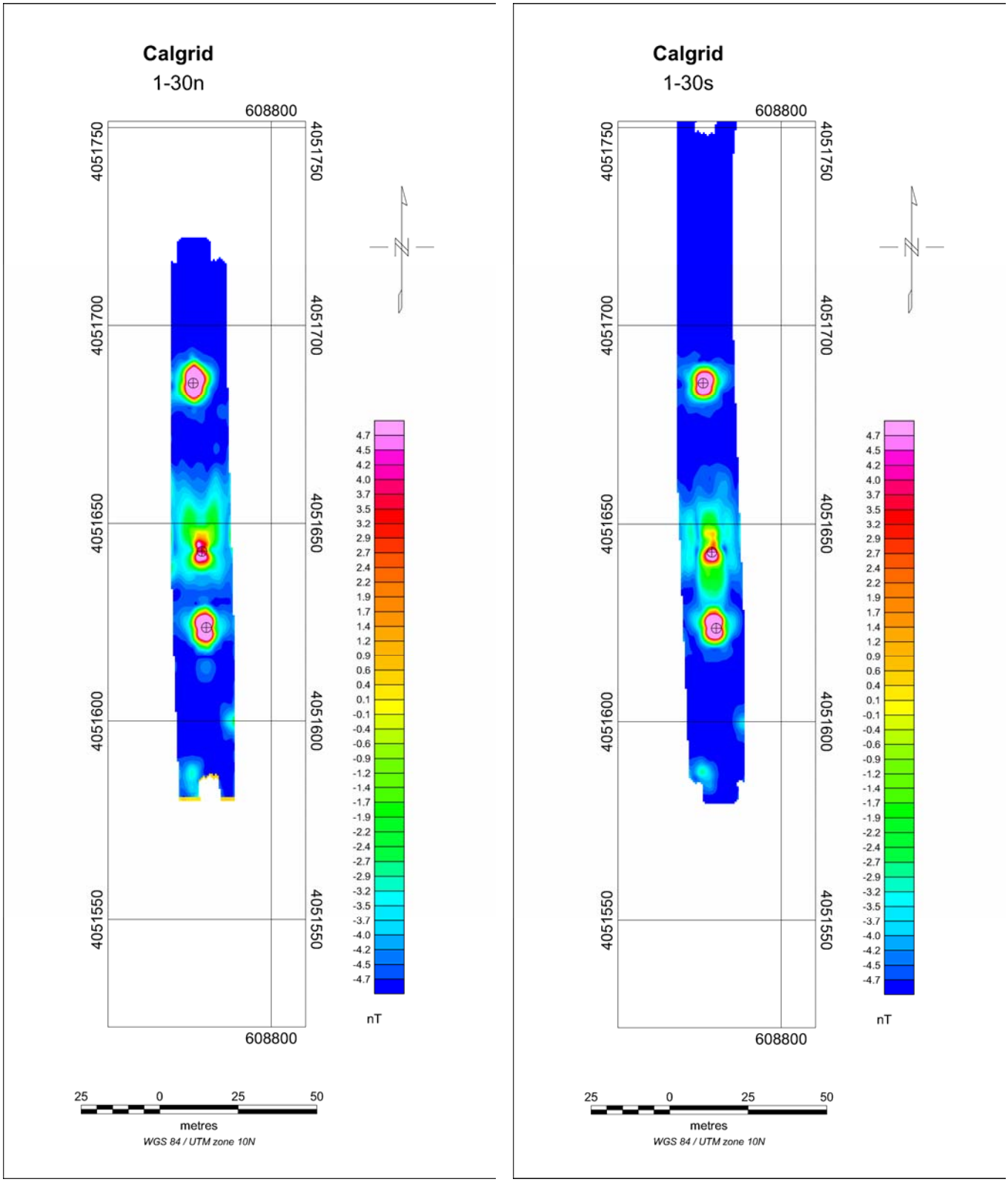

Figure A2: Magnetic QC lines from Jan 30/05.

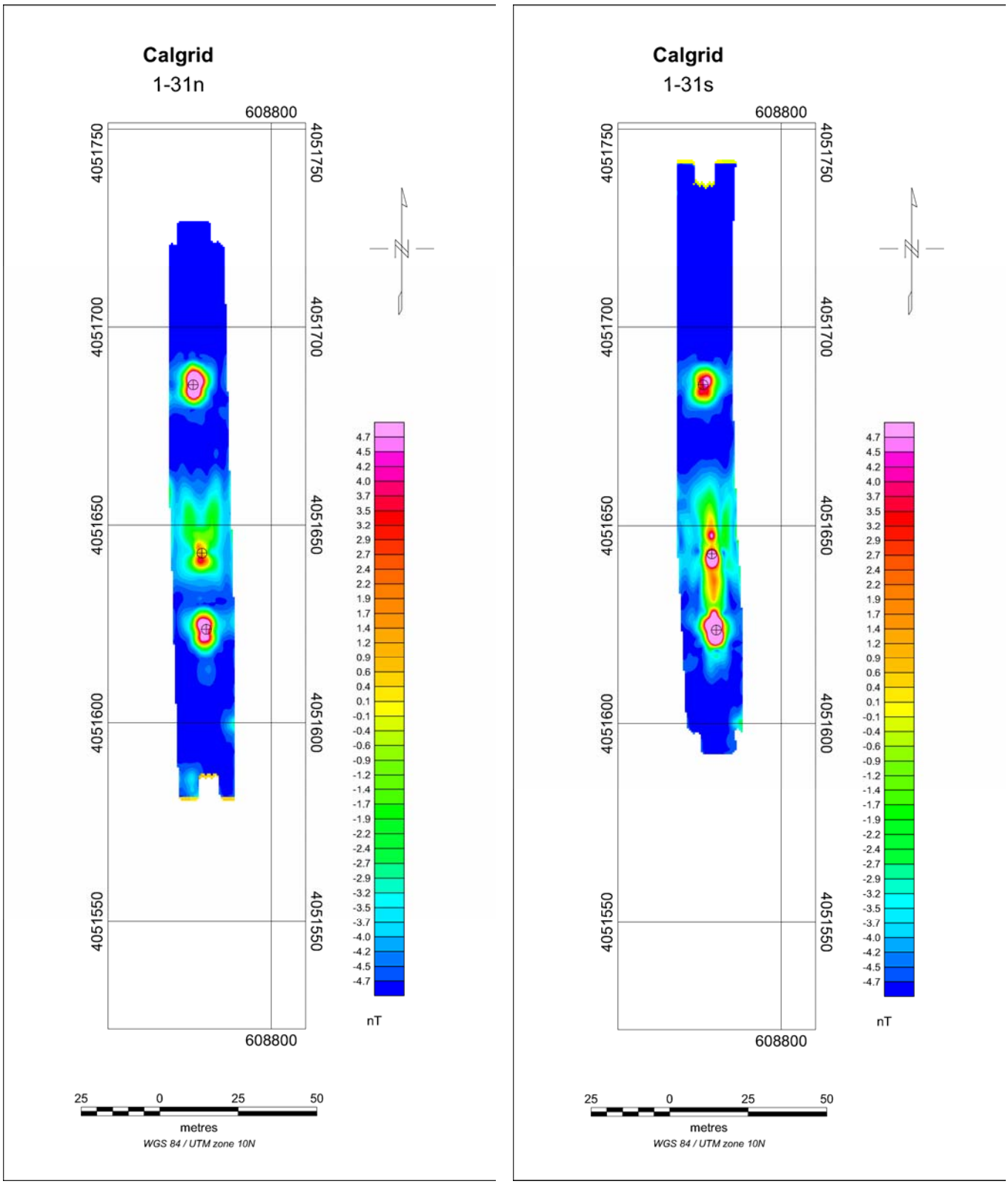

Figure A3: Magnetic QC lines from Jan 31/05.

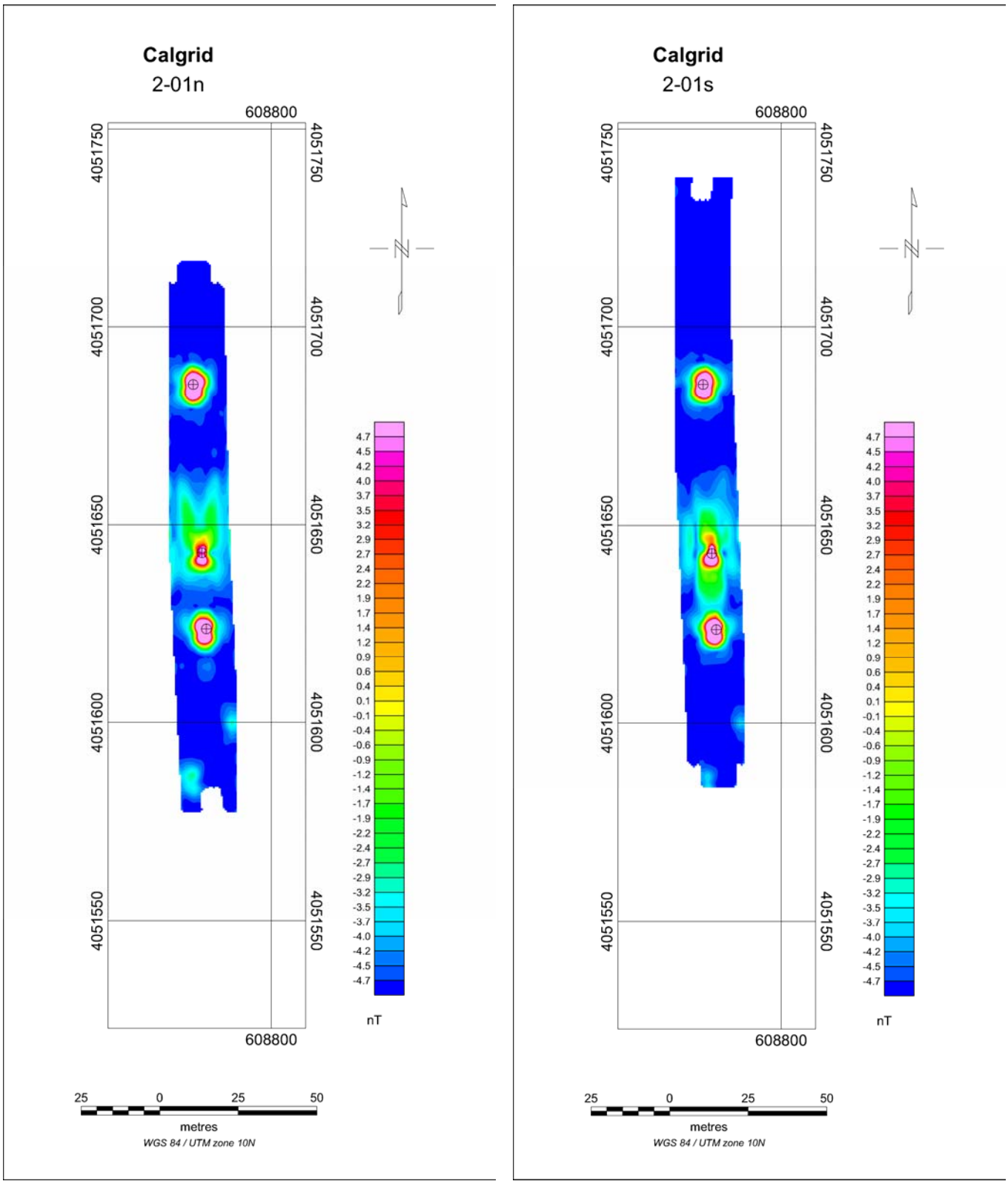

Figure A4: Magnetic QC lines from Feb 01/05.

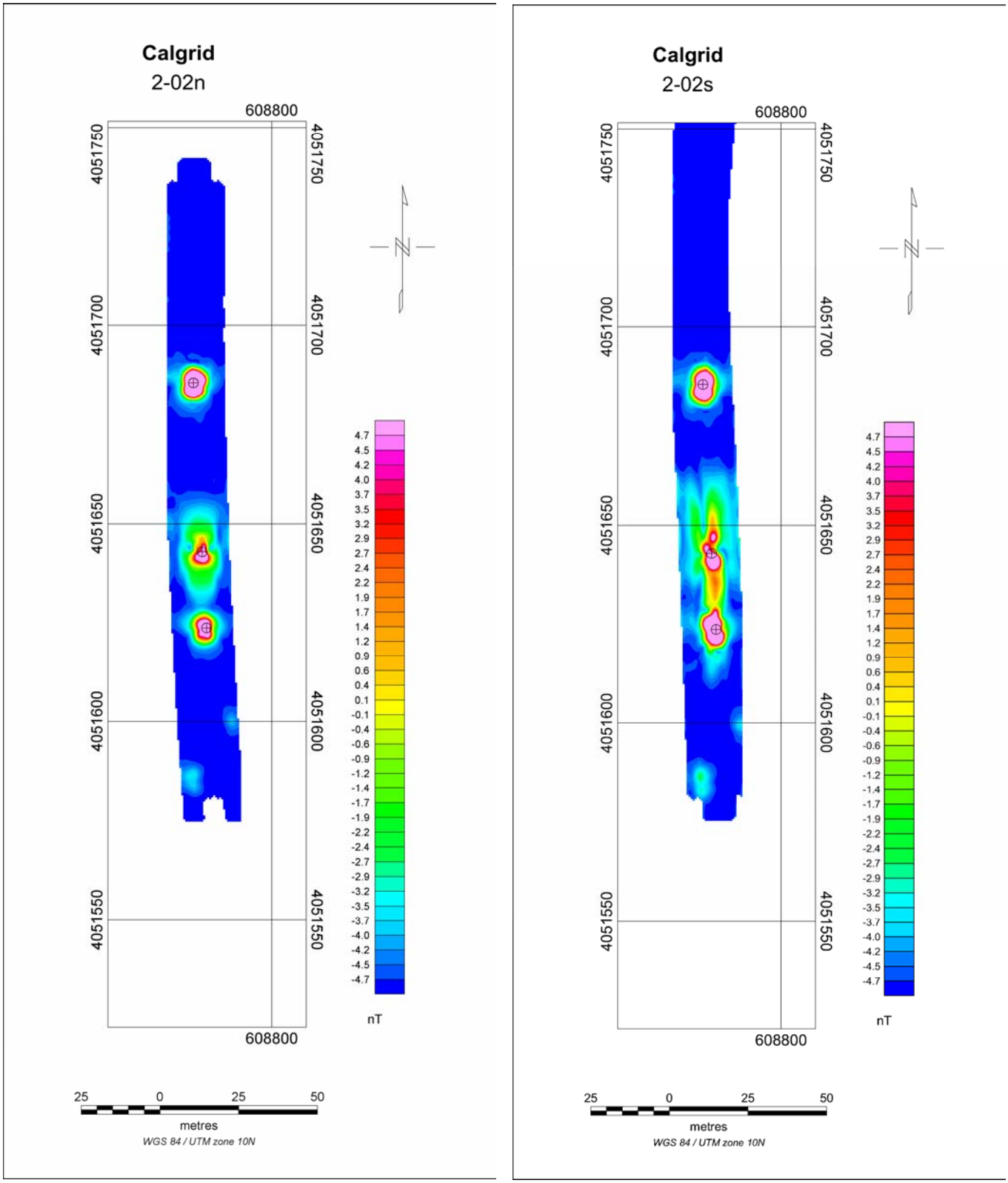

Figure A5: Magnetic QC lines from Feb 02/05.

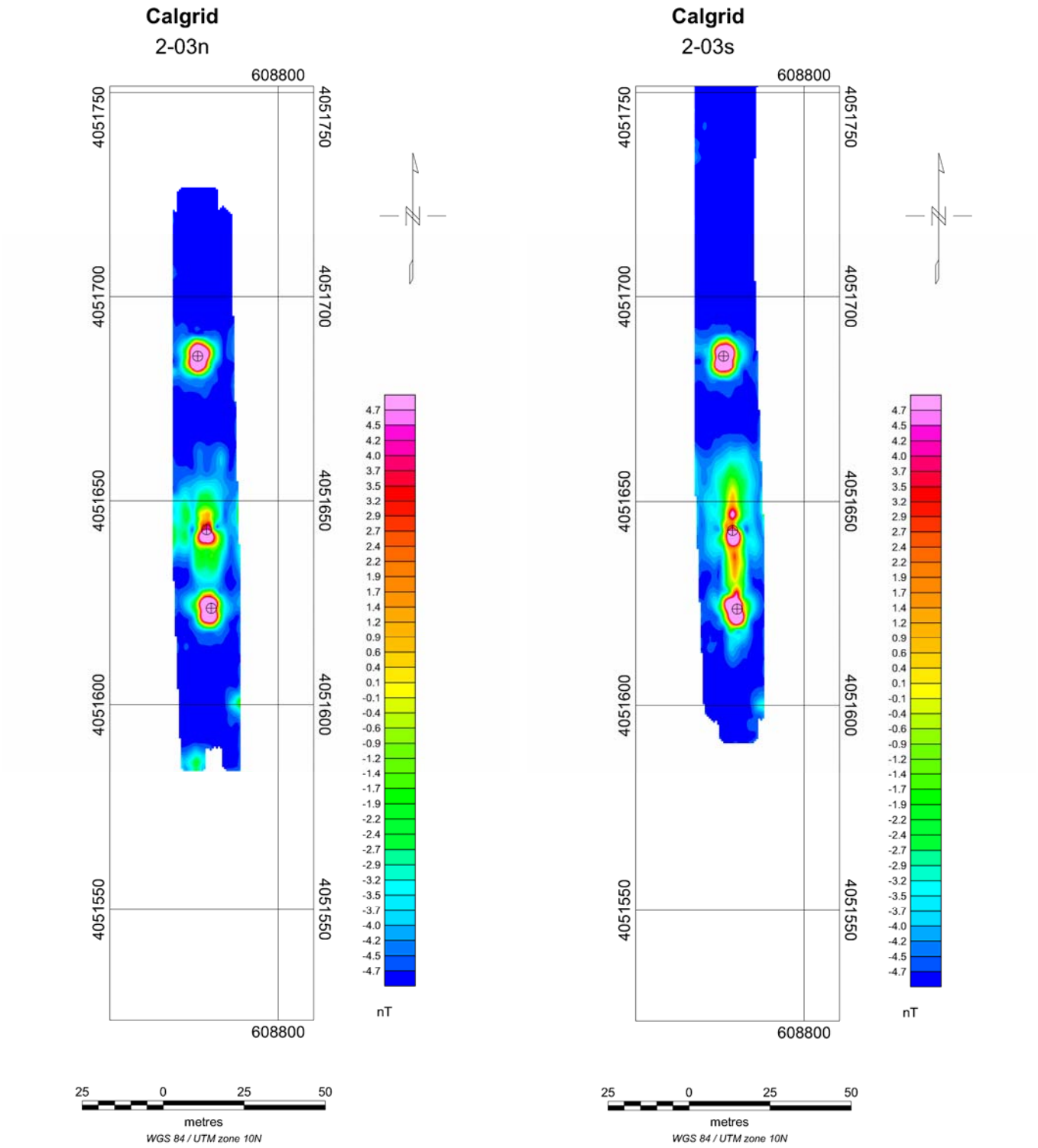

Figure A6: Magnetic QC lines from Feb 03/05.

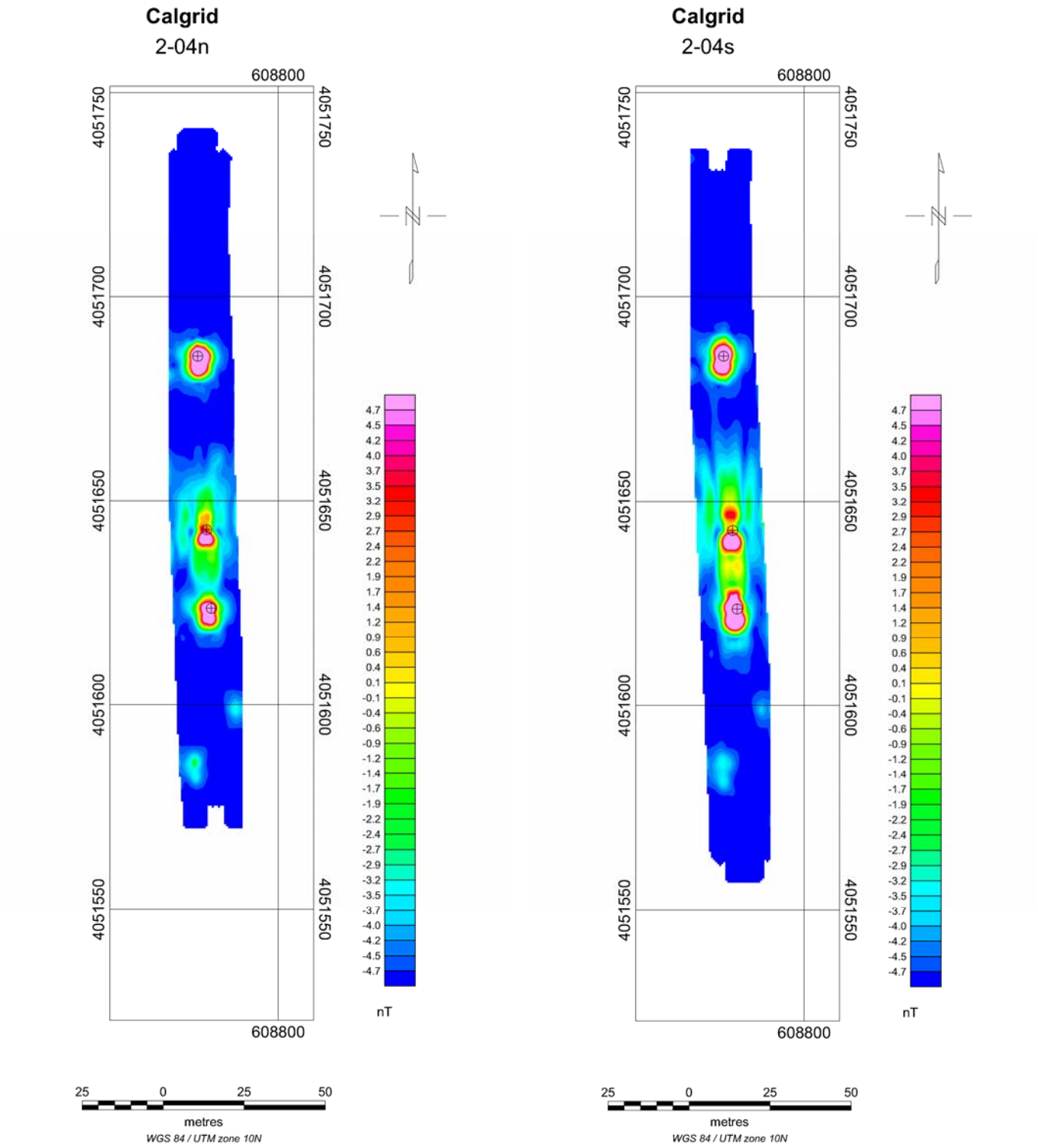

Figure A7: Magnetic QC lines from Feb 04/05.

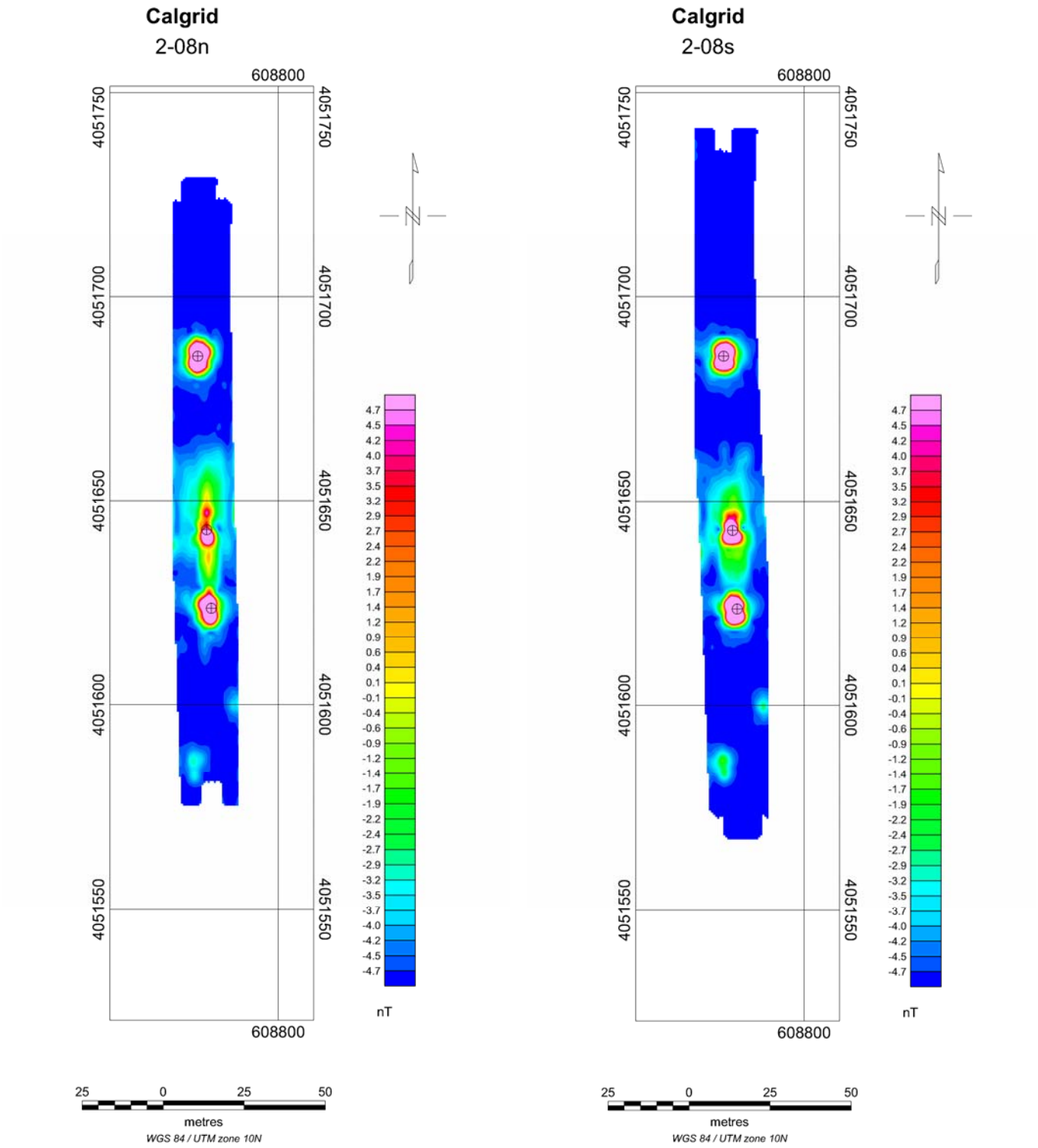

Figure A8: Magnetic QC lines from Feb 08/05.

Appendix B
Electromagnetic data

The maps shown in this appendix depict six electromagnetic time-decay snapshots (bins 1-6), EM sensor altitude AGL, and analytic signal data from the EM blocks A and B.

EM Block A

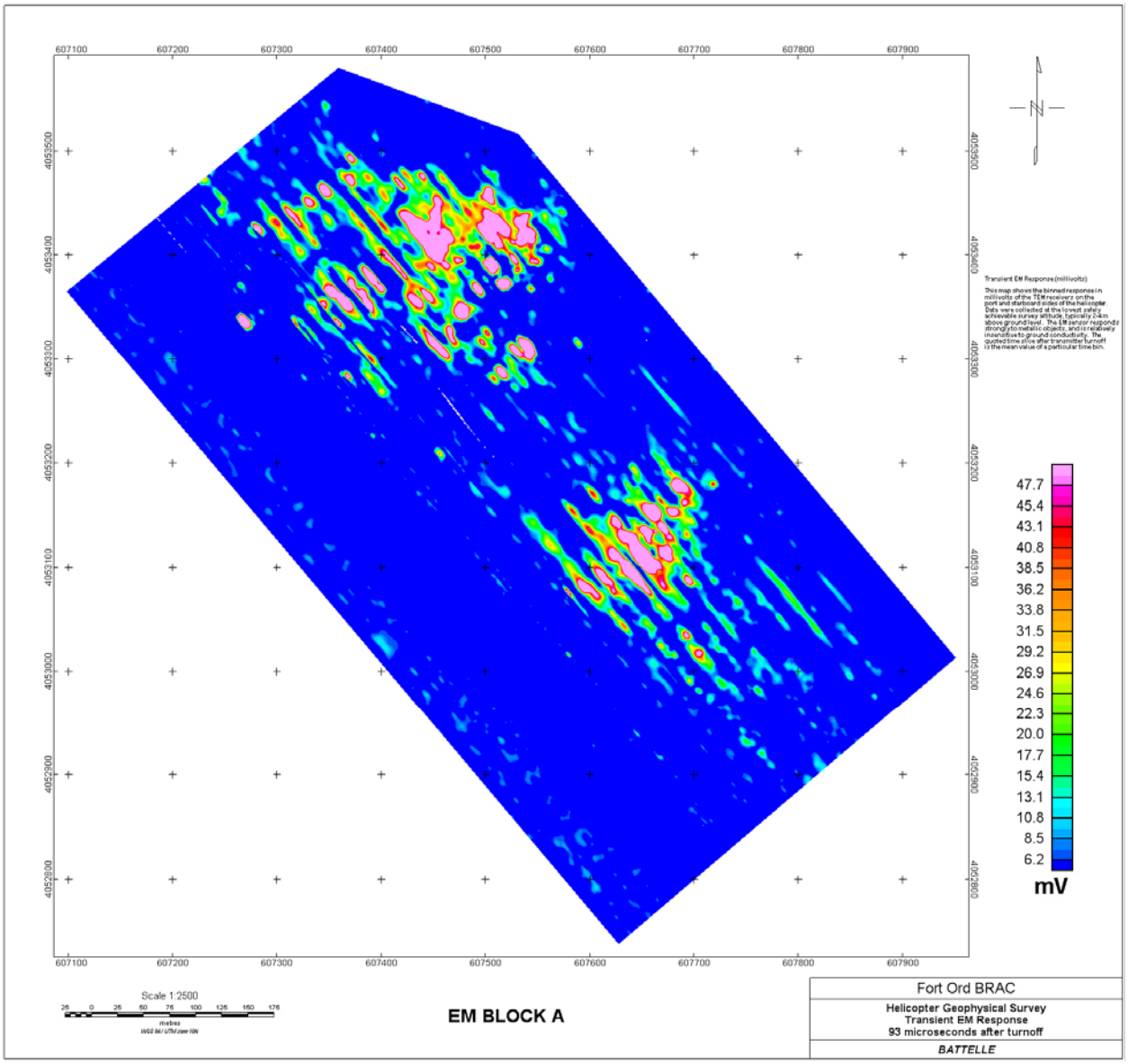

Figure B1. EM response (mV), time bin 1—93 microseconds after turnoff.

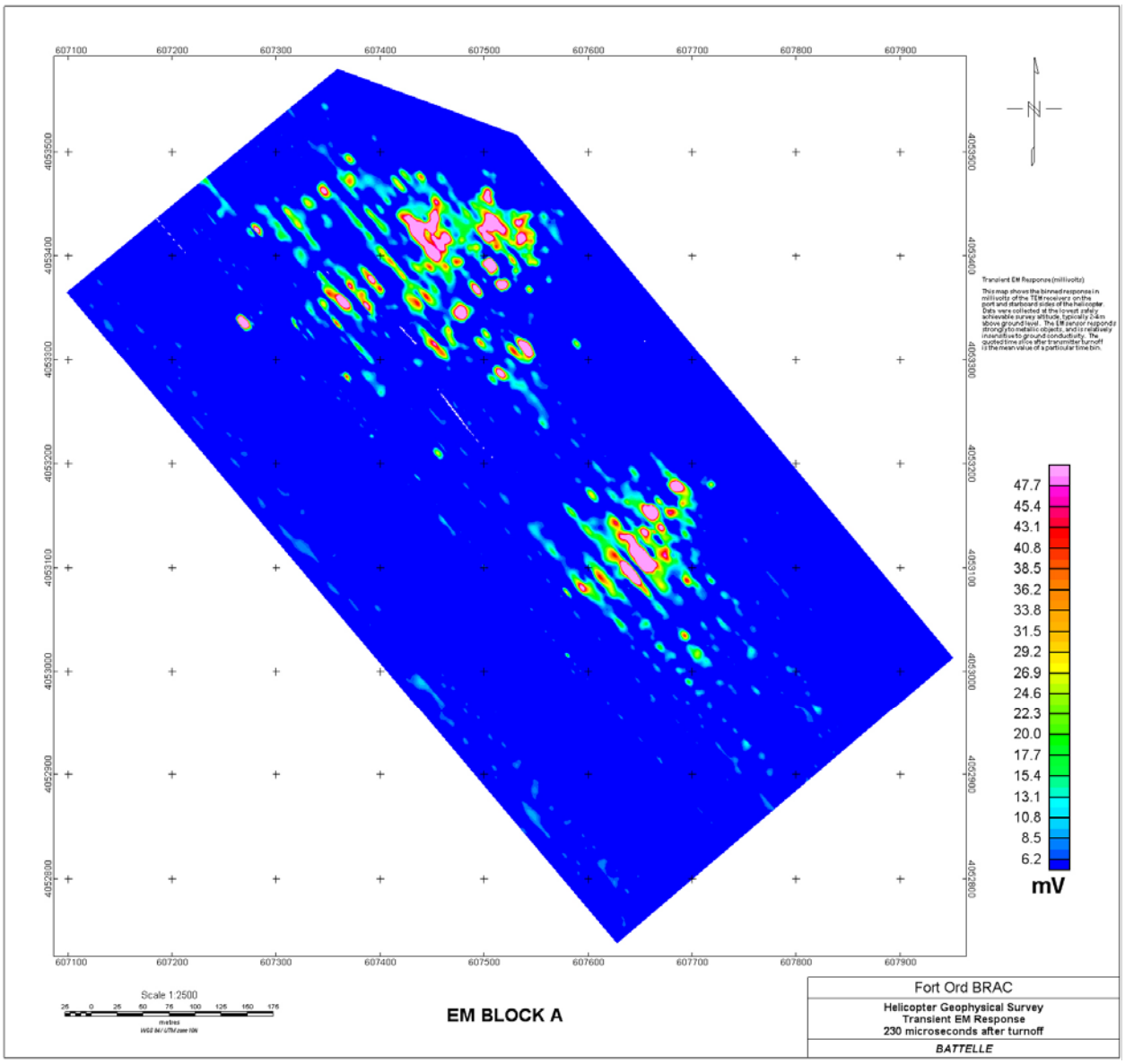

Figure B2. EM response (mV), time bin 2—230 microseconds after turnoff.

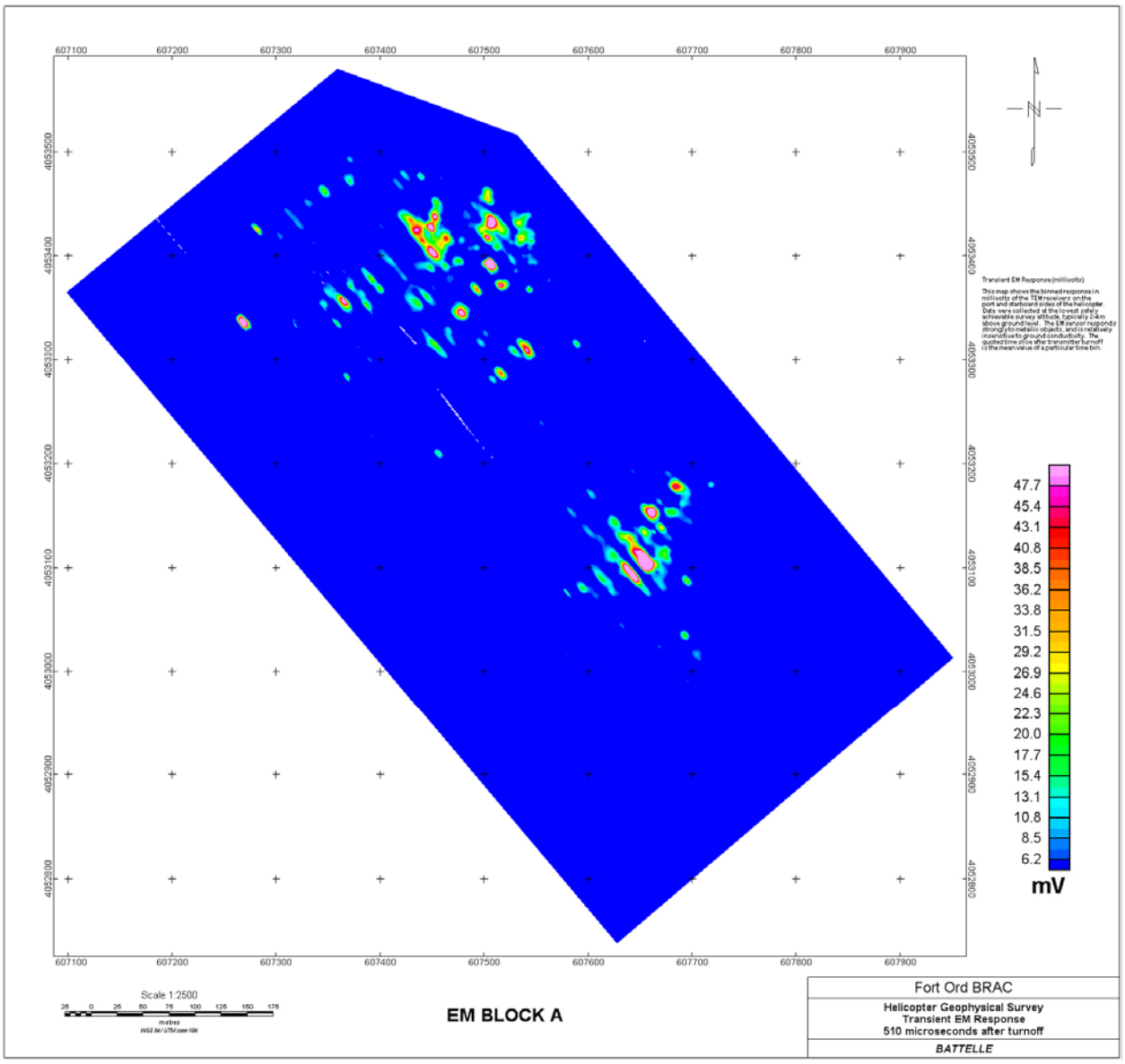

Figure B3. EM response (mV), time bin 3—510 microseconds after turnoff.

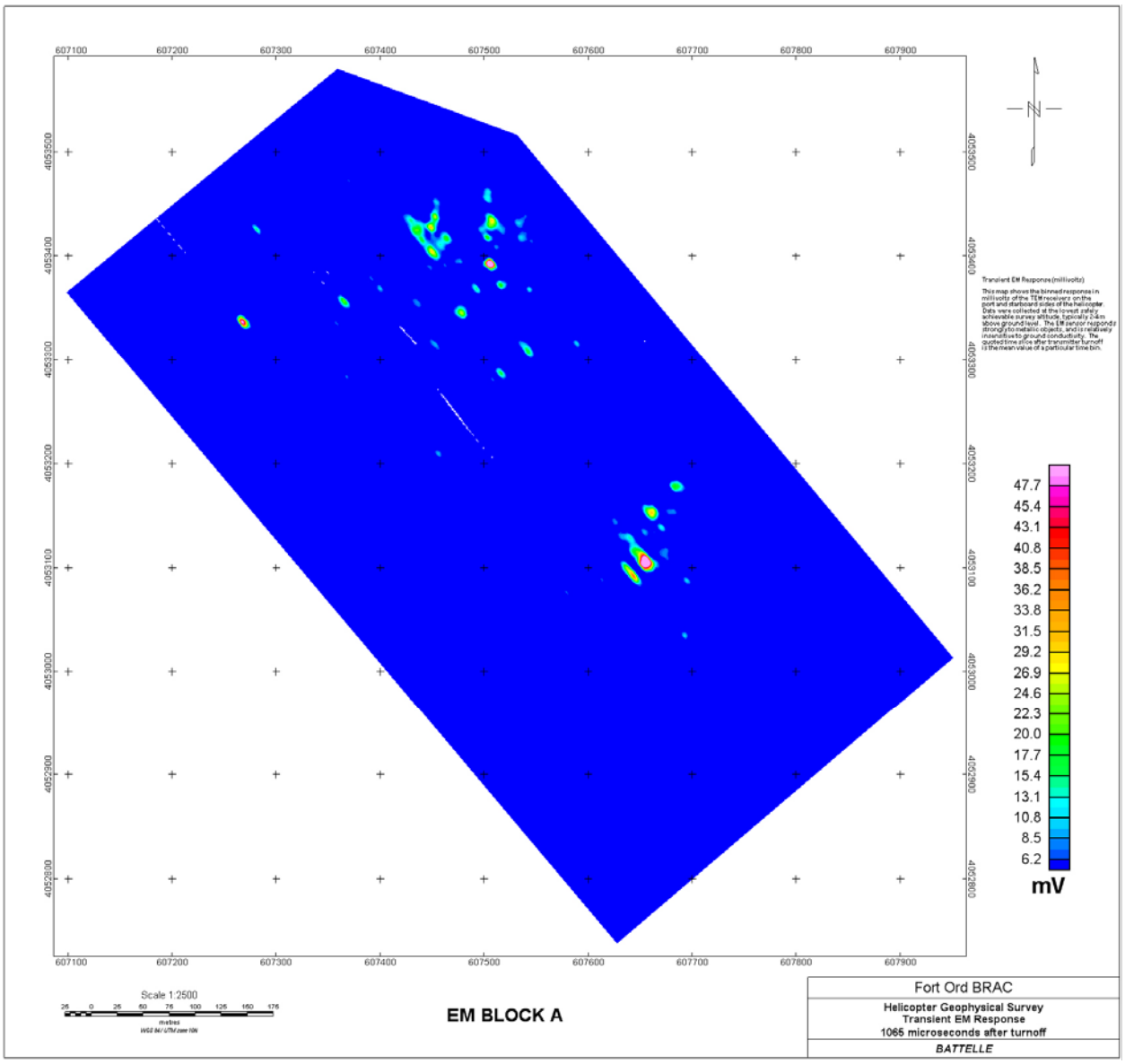

Figure B4. EM response (mV), time bin 4—1065 microseconds after turnoff.

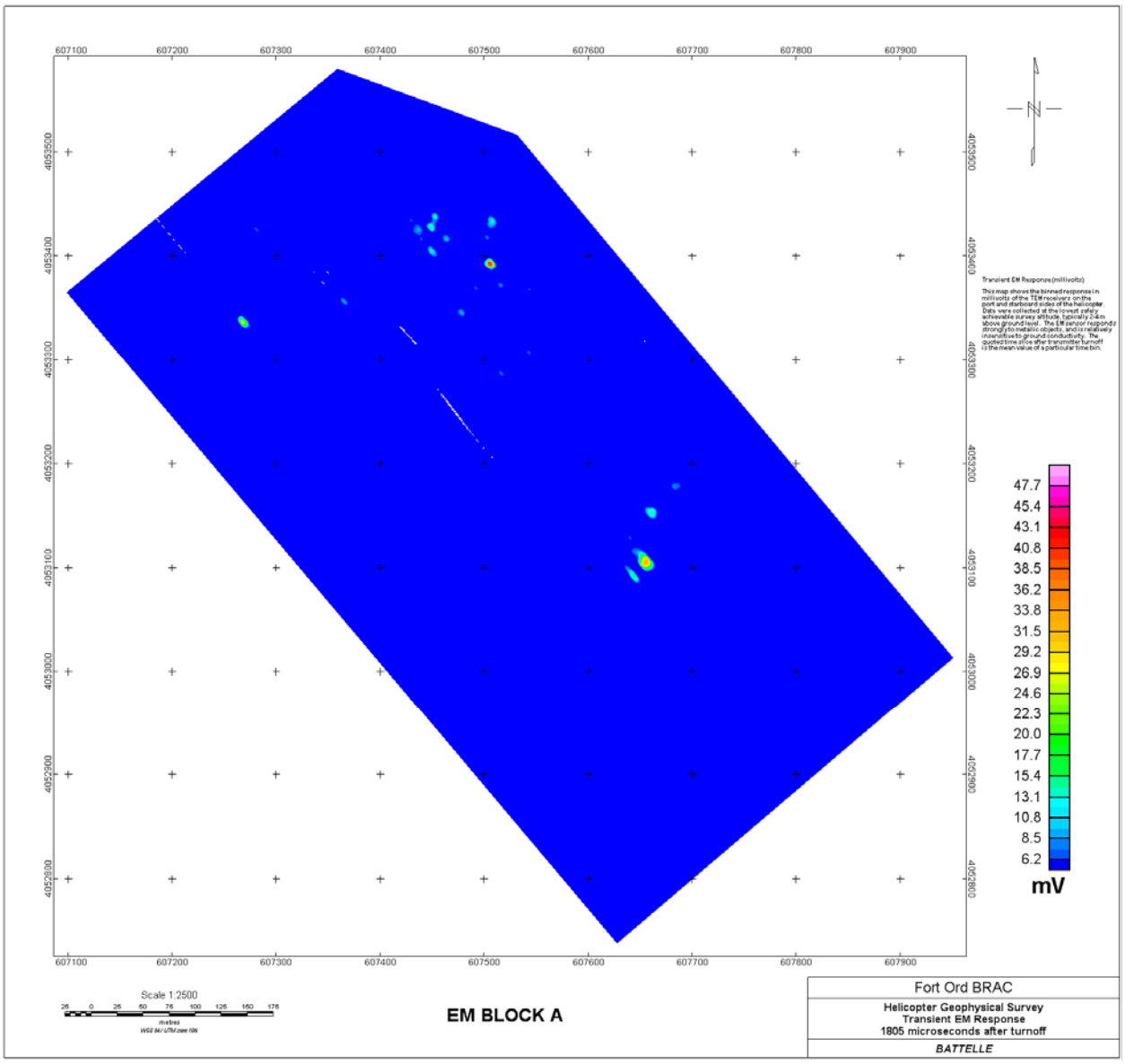

Figure B5. EM response (mV), time bin 5—1805 microseconds after turnoff.

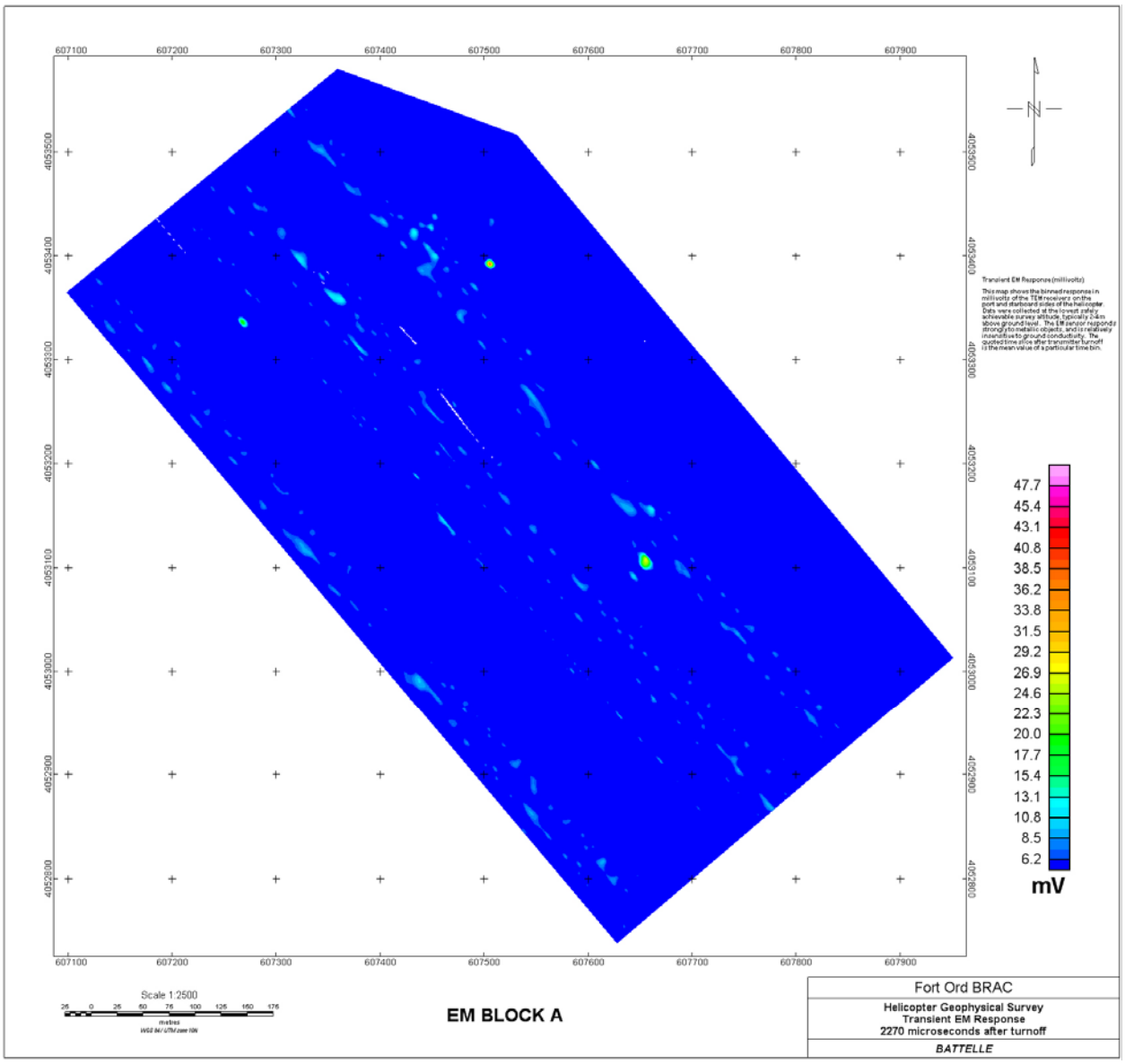

Figure B6. EM response (mV), time bin 6—2270 microseconds after turnoff.

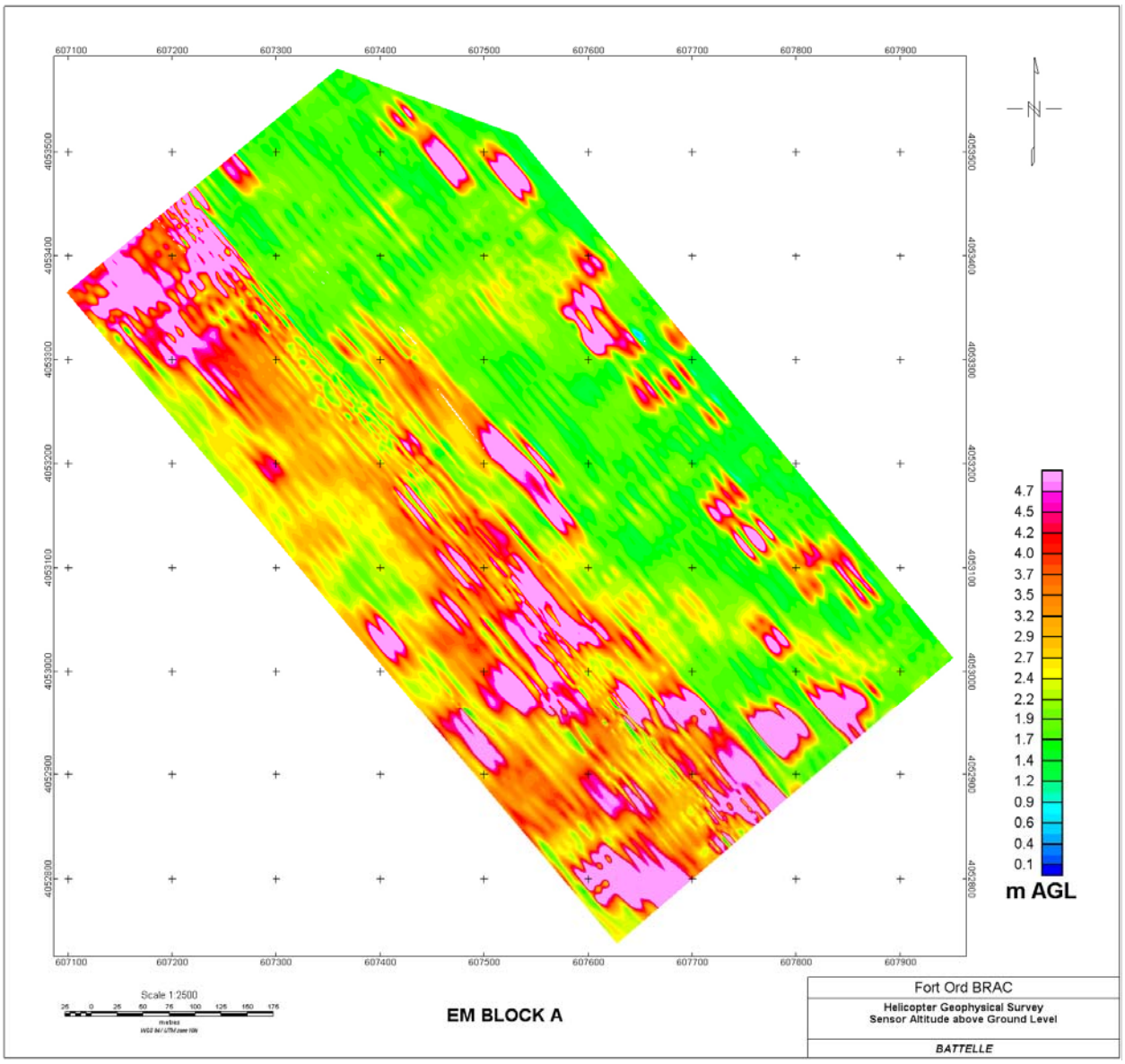

Figure B7. EM sensor altitude.

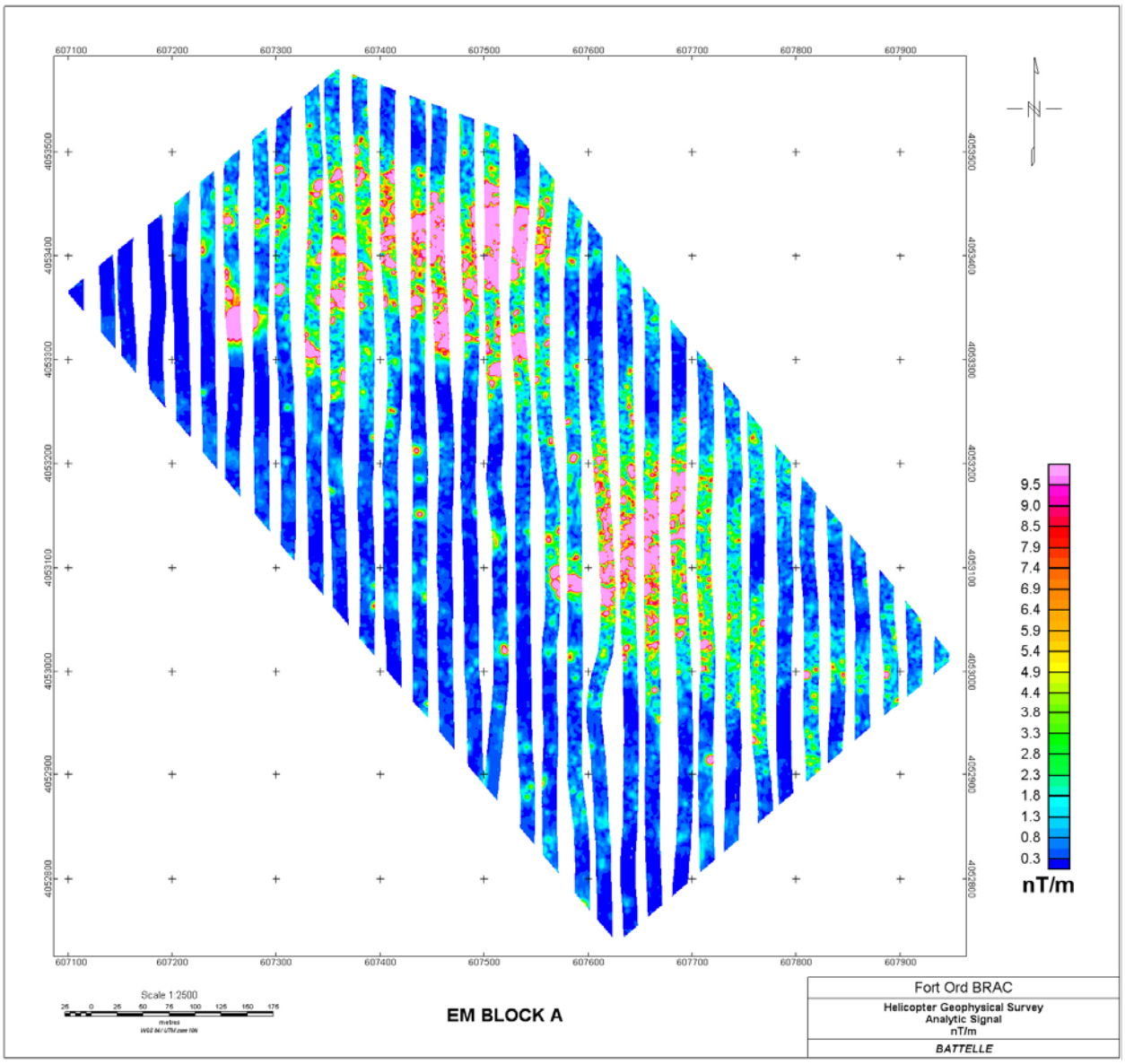

Figure B8. Analytic signal computed from total magnetic field data.

EM Block B

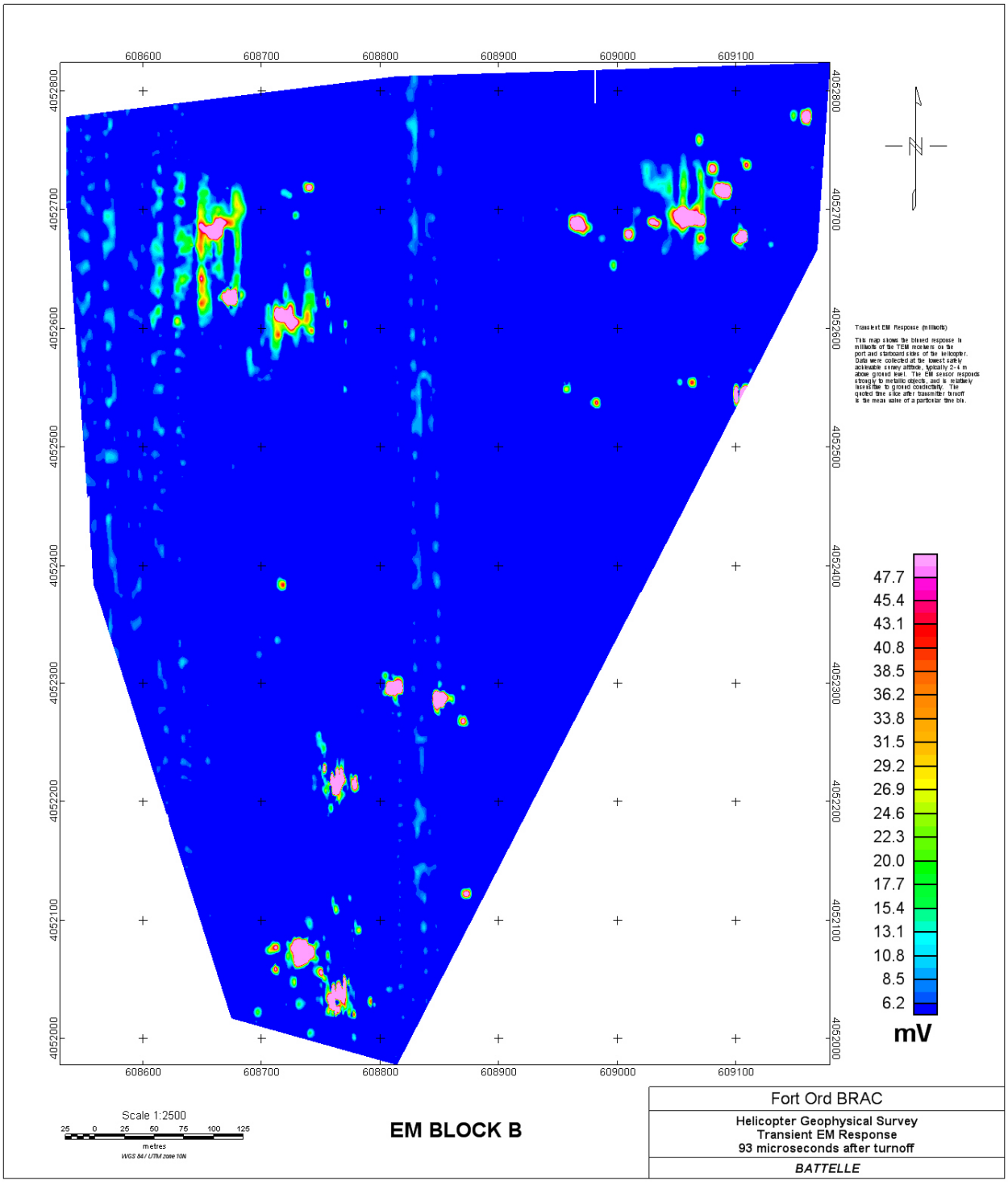

Figure B9. EM response (mV), time bin 1—93 microseconds after turnoff.

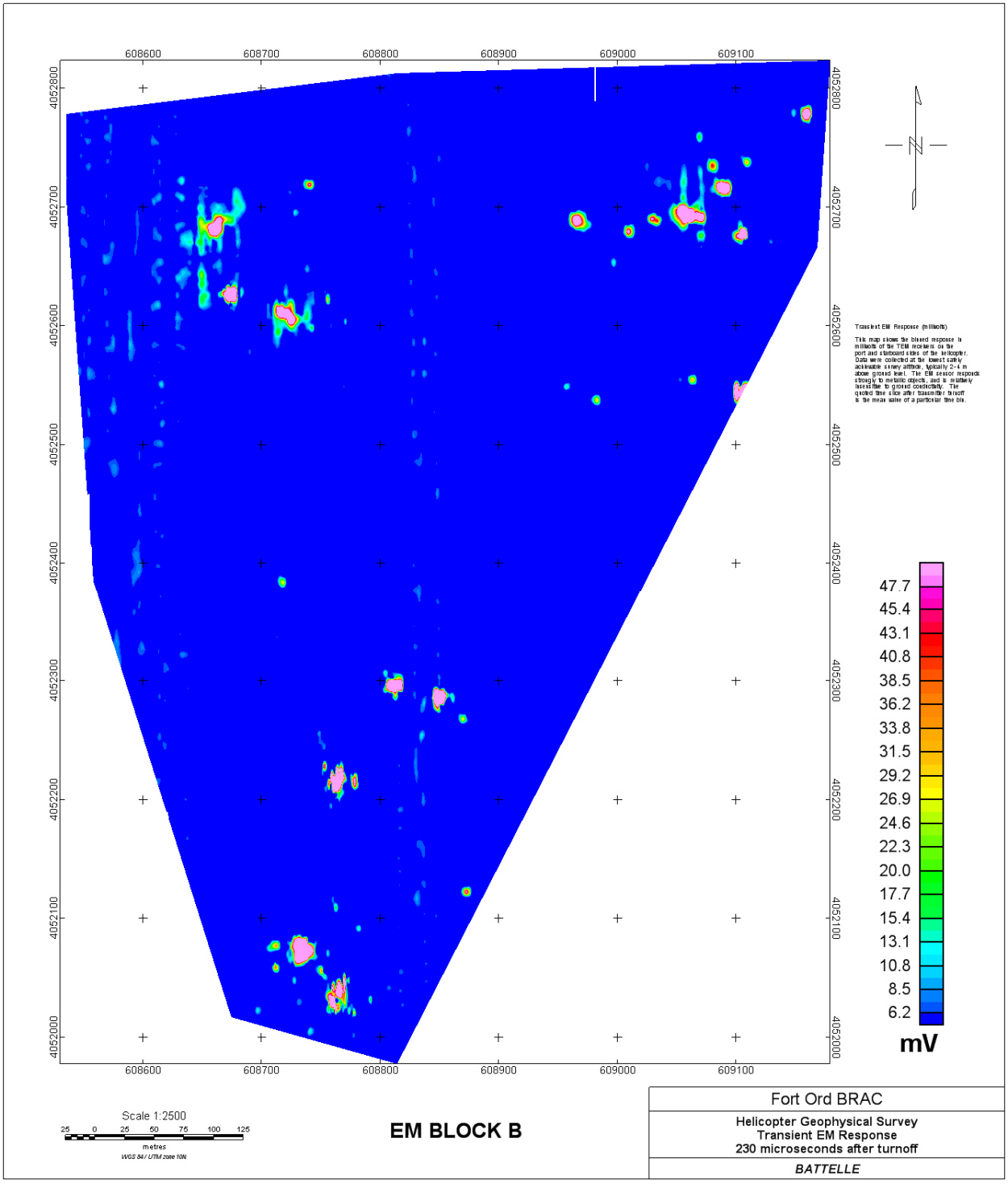

Figure B10. EM response (mV), time bin 2—230 microseconds after turnoff.

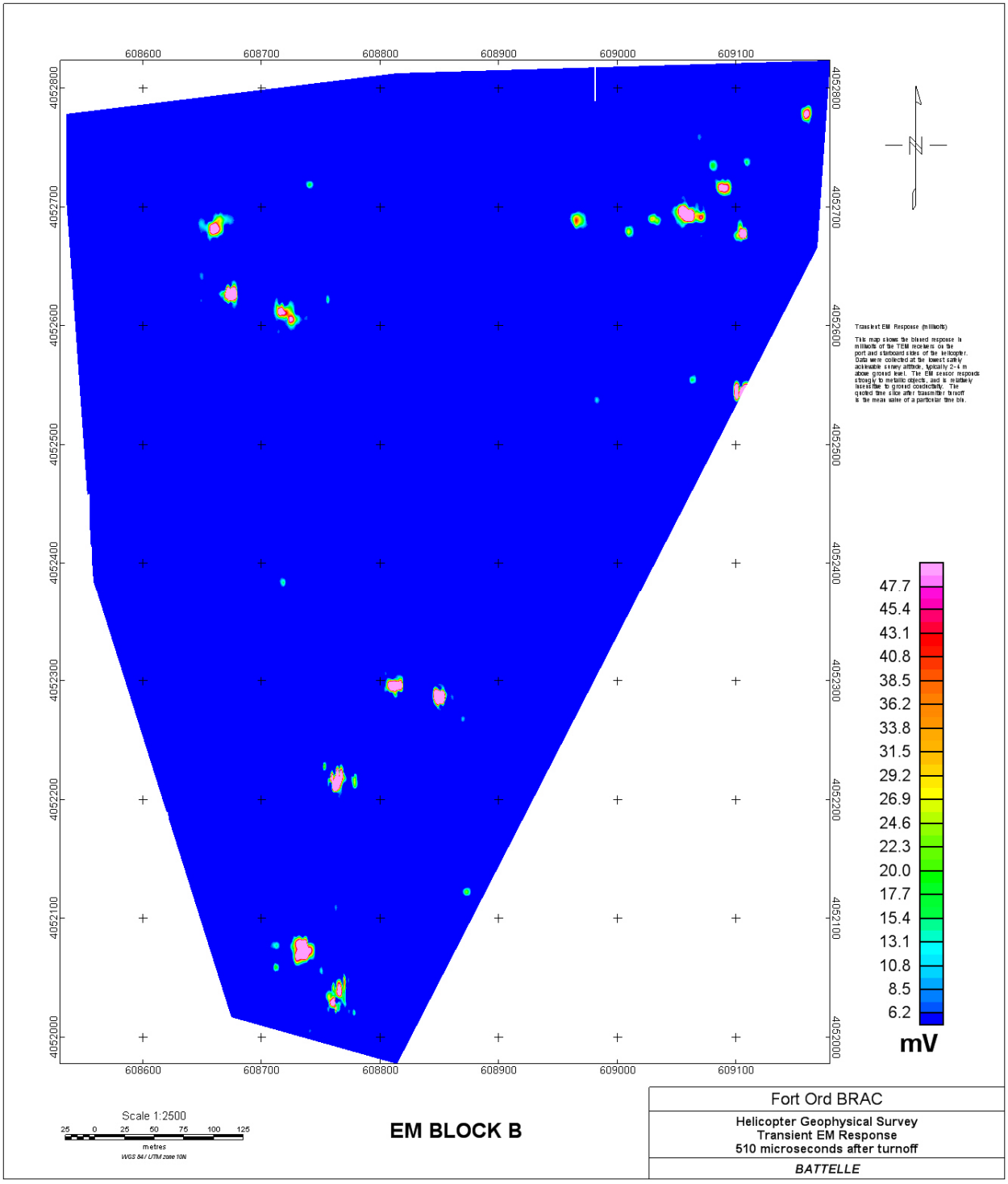

Figure B11. EM response (mV), time bin 3—510 microseconds after turnoff.

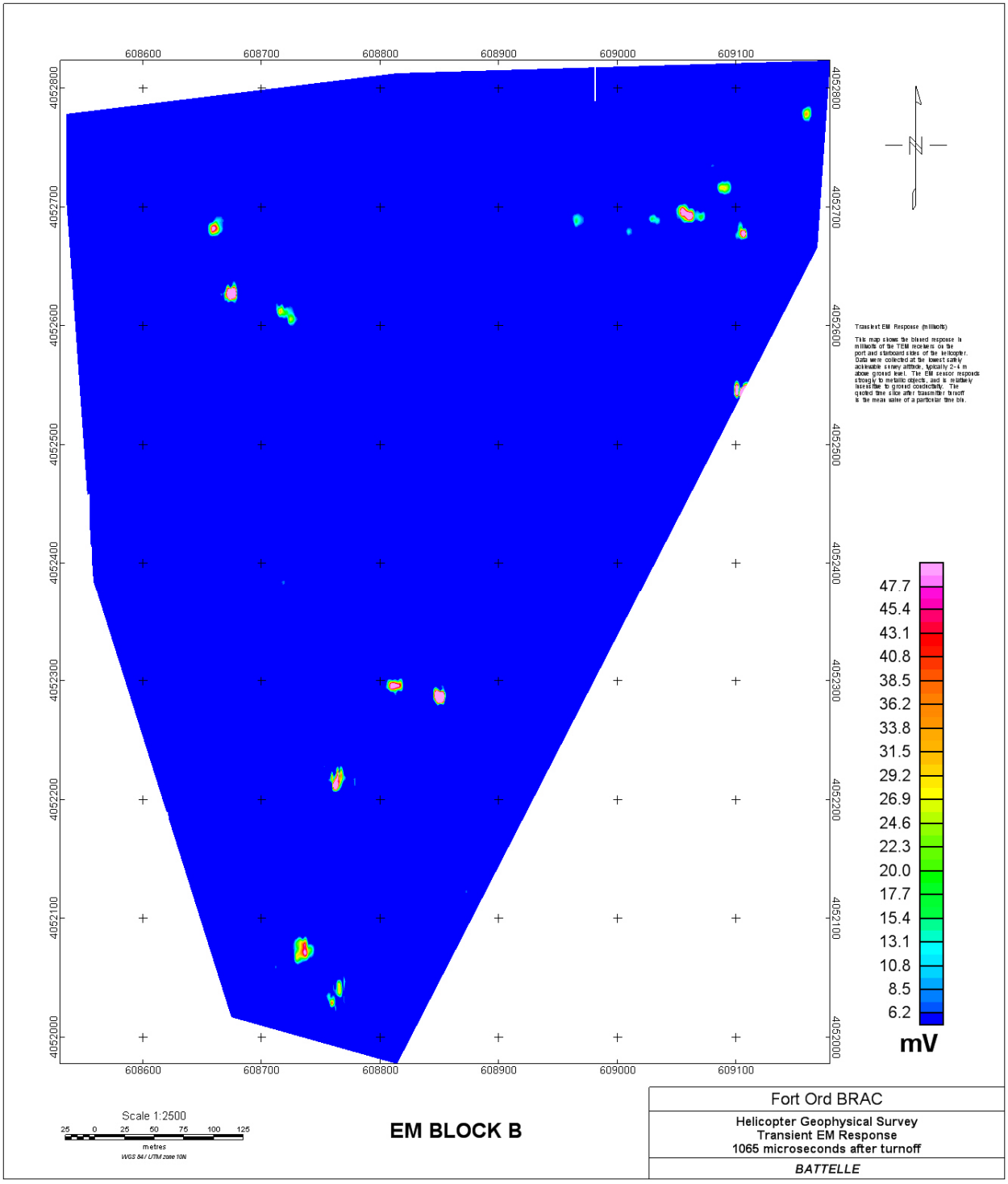

Figure B12. EM response (mV), time bin 4—1065 microseconds after turnoff.

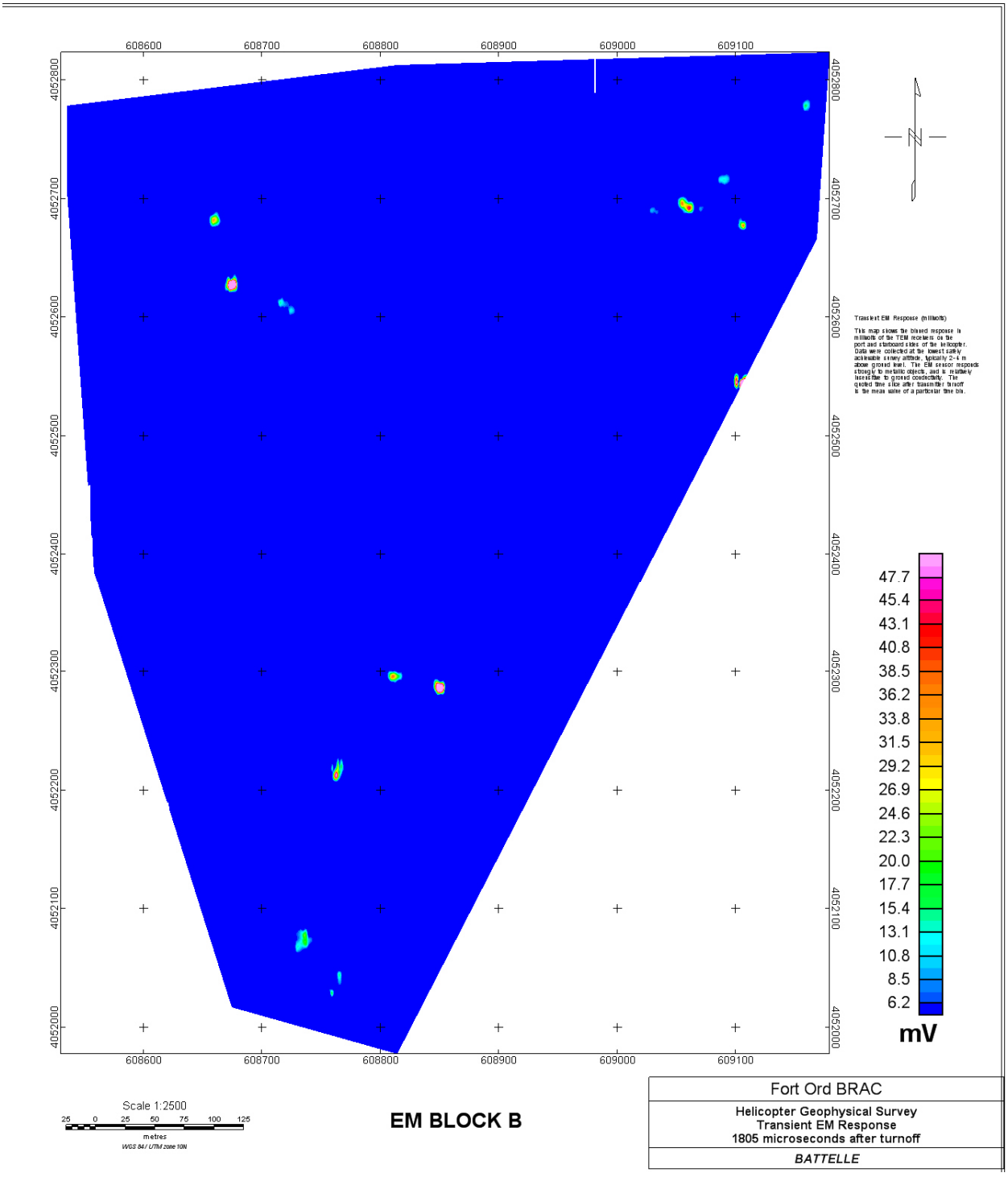

Figure B13. EM response (mV), time bin 5—1805 microseconds after turnoff.

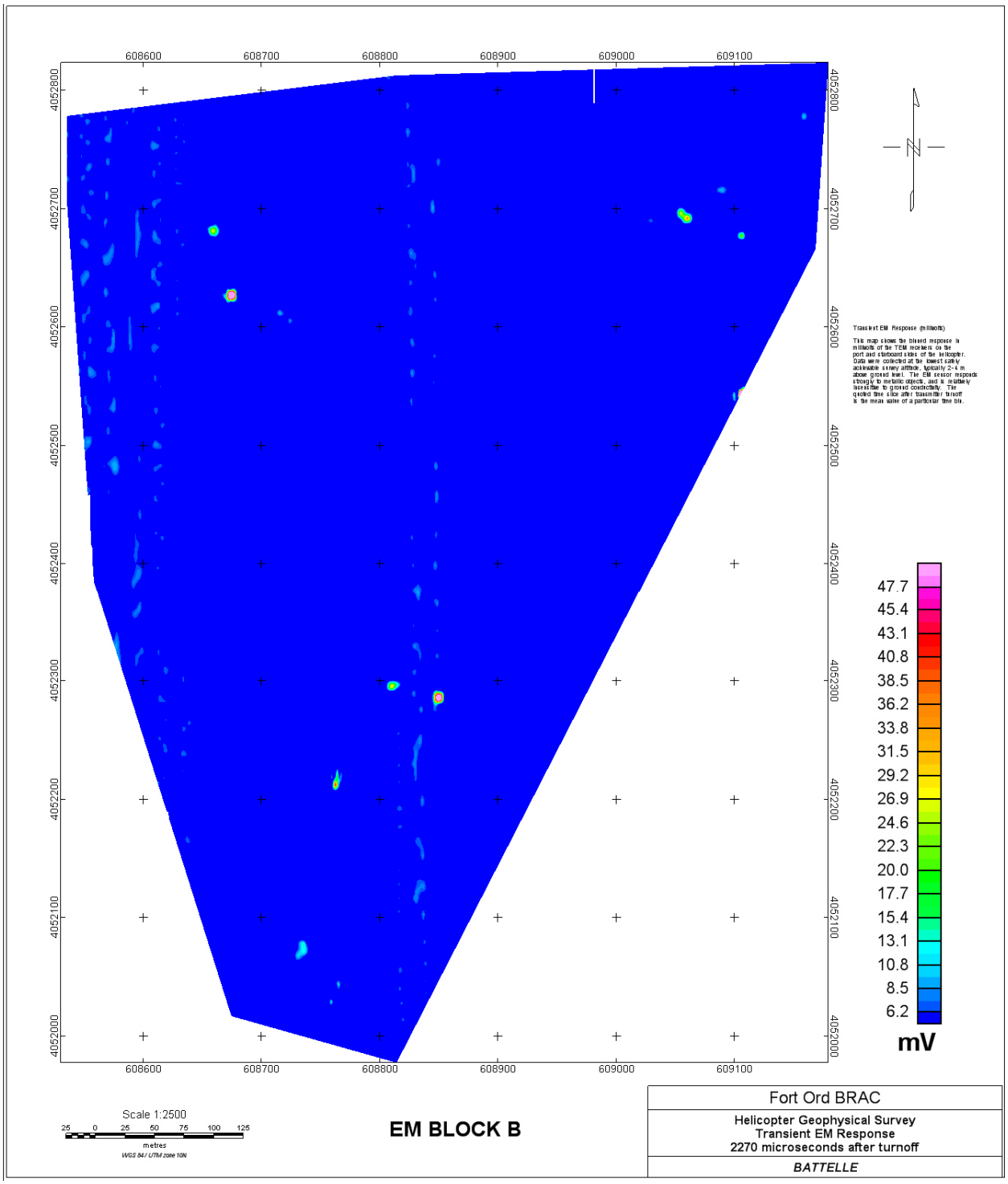

Figure B14. EM response (mV), time bin 6—2270 microseconds after turnoff.

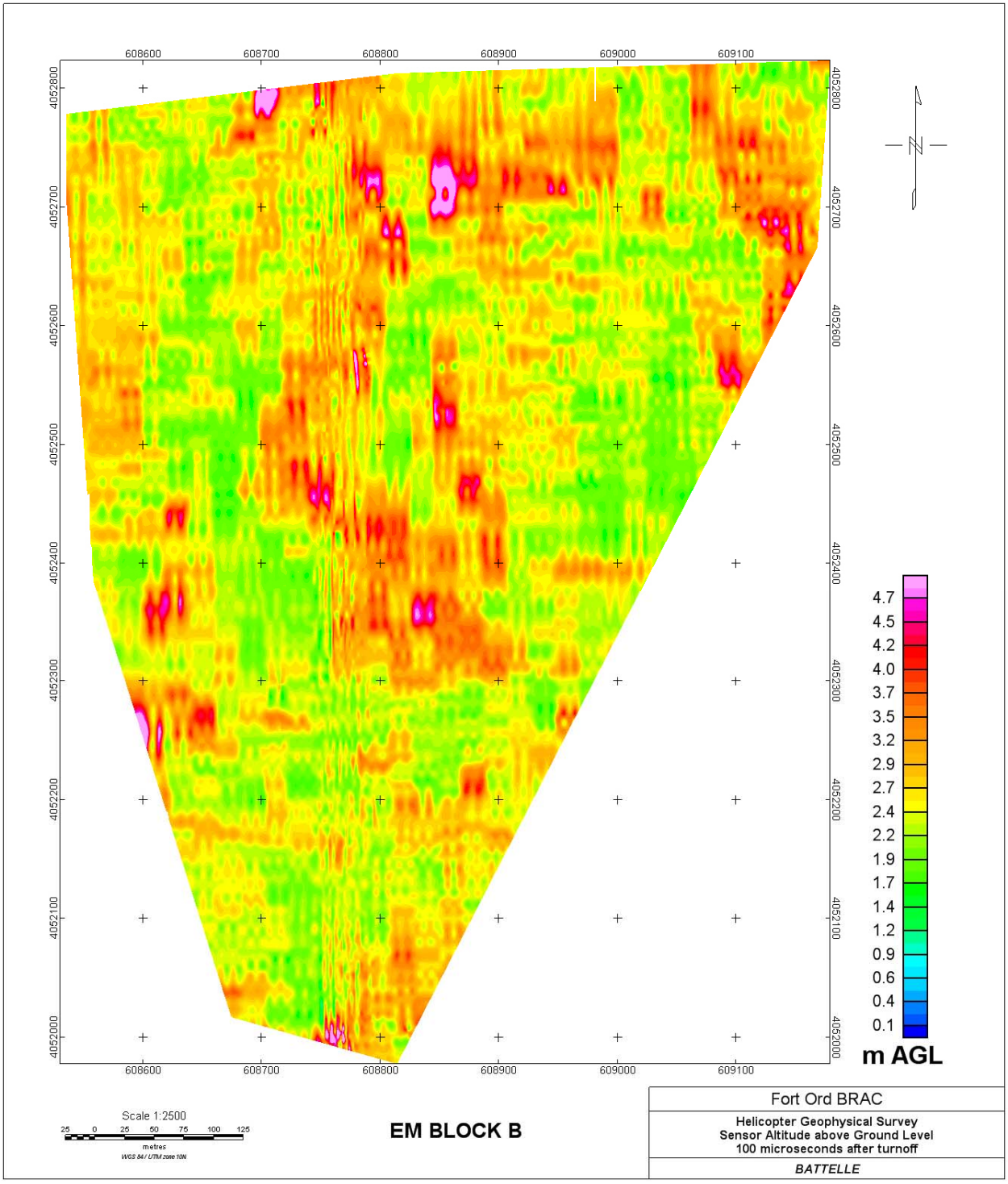

Figure B15. EM sensor altitude.

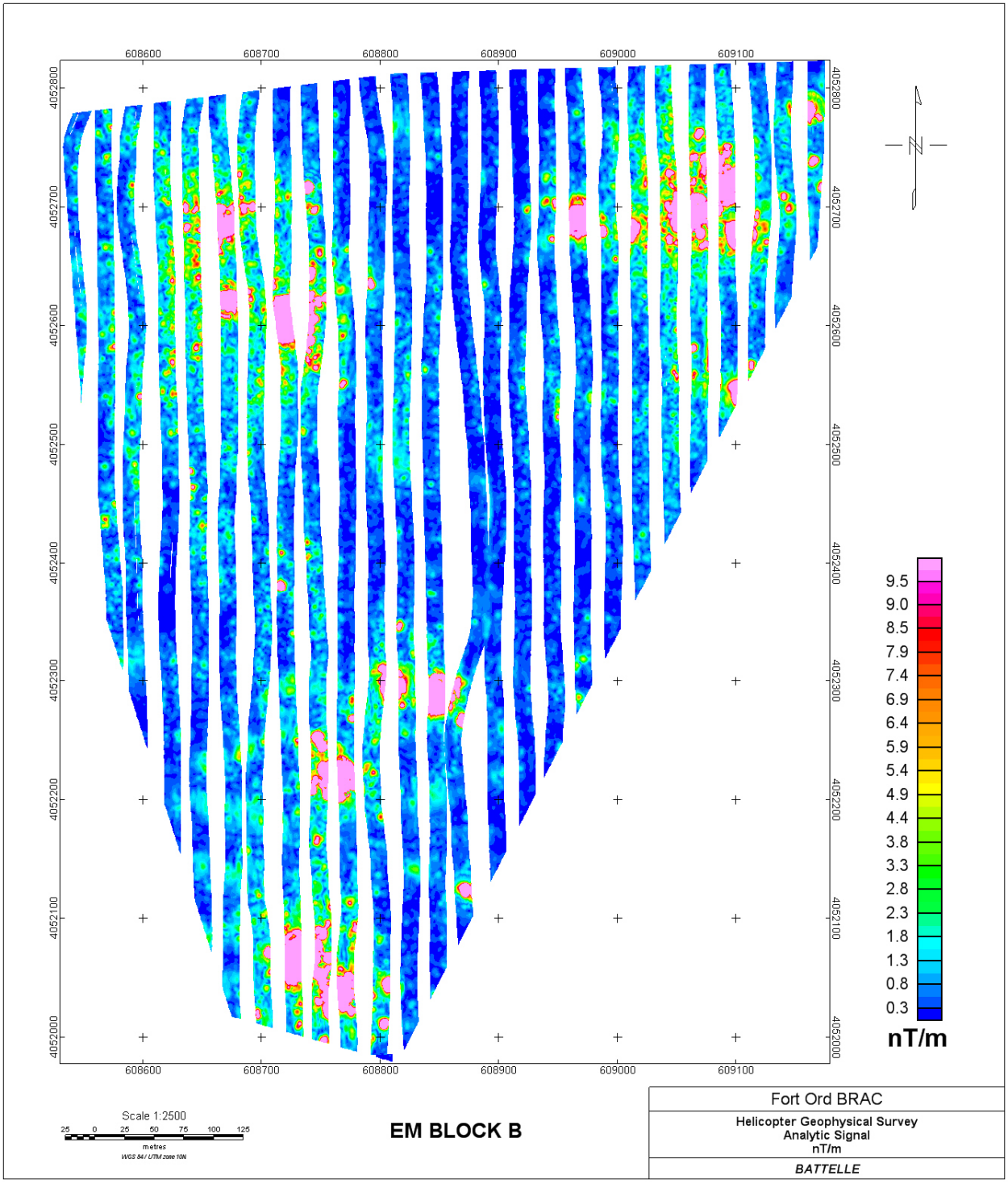

Figure B16. Analytic signal computed from total magnetic field.